DOCTORAL THESIS

An *in-situ* ATR-FTIR Spectroscopy Study of Adsorption in MFI Zeolites

A Step Towards Effective Upgrading of Biofuels

Lindsay Ohlin

LULEÅ UNIVERSITY OF TECHNOLOGY

An *in-situ* ATR-FTIR spectroscopy study of adsorption in MFI zeolites

A step towards effective upgrading of biofuels

Lindsay Ohlin

Luleå University of Technology
Department of Civil, Environmental and Natural Resources Engineering
Division of Chemical Engineering
Chemical Technology

May 2015

Printed by Luleå University of Technology, Graphic Production 2015

ISSN 1402-1544
ISBN 978-91-7583-318-7 (print)
ISBN 978-91-7583-319-4 (pdf)

Luleå 2015

www.ltu.se

Abstract

Global warming is believed to be caused by the extensive emission of greenhouse gases, for example carbon dioxide, into the atmosphere by combustion of fossil fuels, such as coal, oil and natural gas. To reduce the emission of carbon dioxide and hence avoid global warming, alternative fuels derived from renewable resources are desired. Another reason for the worldwide interest in finding alternative fuels is that the reserves of the fossil fuels are limited and the oil and gas sources will eventually run out.

Biogas and biobutanol are renewable biofuels which are interesting alternatives to fossil fuels. Biogas is produced during degradation of organic material forming a mixture of mainly methane and carbon dioxide with water as a common trace component. Biobutanol is produced from ABE (acetone, butanol and ethanol) fermentation of biomass. Purification of biogas and biobutanol is essential to increase the heat value of the fuels. Traditional purification processes are energy demanding and expensive. Therefore, other separation processes are currently sought for.

Zeolites are promising alternatives due to their great potential both as selective adsorbents and as membranes. Due to the unique pore structure, zeolites are capable of separating components based on their adsorption properties.

In the present work, single component adsorption of biogas components such as methane, carbon dioxide and water in zeolite ZSM-5 was studied as well as adsorption of water and butanol in silicalite-1 using *in-situ* ATR-FTIR spectroscopy. The method was successfully further used to study multicomponent adsorption.

For single gas adsorption experiments, recorded infrared spectra of adsorbed methane, carbon dioxide and water showed characteristic, well separated, bands for each gas. Adsorbed concentrations were determined from the recorded infrared spectra. The Langmuir model was fitted to the adsorption isotherms and the model matched the experimental data very well. The fitted Langmuir parameters obtained in the present work was in agreement with values reported in the literature.

For multicomponent adsorption experiments, the Ideal Adsorbed Solution Theory (IAST) was used to predict the adsorbed concentrations of methane, carbon dioxide and water using the single component adsorption isotherm parameters as input. In general, the IAST was shown to be a fairly good model for predicting the adsorbed concentrations of methane and carbon dioxide from binary mixtures. For the amount of adsorbed methane from mixtures including water, the IAST predicted the values fairly well. However, for mixtures containing water and carbon dioxide, the IAST could not fully describe the adsorption behavior of the two components.

The CO_2/CH_4 adsorption selectivity was determined for various gas compositions and temperatures showing a general increase in the selectivity with decreasing temperature. This indicates that the separation of carbon dioxide from biogas should be more efficient at lower temperatures. Compared to the literature, the selectivity observed in the present work is relatively high indicating that Na-ZSM-5 may be an effective membrane material for upgrading biogas. Moreover, butanol was preferentially adsorbed over water in silicalite-1, indicating that silicalite-1 may be a promising material for recovery of butanol from dilute water solutions.

Acknowledgements

First, I would like to thank my main supervisor Assoc. Prof. Mattias Grahn for his endless help and support and for giving me the great opportunity to do this research work. Secondly, I would like to thank my assistant supervisors Prof. Jonas Hedlund for his guidance and support, Dr. Danil Korelskiy for your help and discussions and Assoc. Prof. Allan Holmgren for helping me with the IR spectrometer and for our inspiring discussions.

I am also very grateful to Dr. Philippe Bazin and Prof. Frédéric Thibault-Starzyk for a great collaboration when helping me with the AGIR measurements and Assoc. Prof. Johanne Mouzon is acknowledged for helping me with the SEM pictures.

The Swedish Energy Agency is gratefully acknowledged for the financial support of this work.

I am grateful to my colleagues at the Division of Chemical Engineering for making the working days enjoyable. A special thanks to Lic. Eng. Amirfarrokh Farzaneh for our fantastic collaboration and our wonderful, inspiring and sometimes crazy discussions ☺

I would also like to thank my dear friends who make my life outside the university very enjoyable.

Till sist vill jag tacka min familj för det enorma stöd ni alltid ger. Ni är mitt allt och jag älskar er massor! ♡

List of papers

This doctoral thesis is based on the following papers

Paper I
Adsorption of CO_2, CH_4 and H_2O in zeolite ZSM-5 studied using in situ ATR-FTIR spectroscopy
Lindsay Ohlin, Philippe Bazin, Frédéric Thibault-Starzyk, Jonas Hedlund and Mattias Grahn
The Journal of Physical Chemistry C

Paper II
Detailed investigation of the binary adsorption of carbon dioxide and methane in zeolite Na-ZSM-5 studied using in situ ATR-FTIR spectroscopy
Lindsay Ohlin and Mattias Grahn
The Journal of Physical Chemistry C

Paper III
Effect of water on the adsorption of methane and carbon dioxide in zeolite Na-ZSM-5 studied using in situ ATR-FTIR spectroscopy
Lindsay Ohlin, Vladimir Berezovsky, Sven Öberg, Amirfarrokh Farzaneh, Allan Holmgren and Mattias Grahn
Submitted to The Journal of Physical Chemistry C

Paper IV
Ternary adsorption of methane, water and carbon dioxide in zeolite Na-ZSM-5 studied using in situ ATR-FTIR spectroscopy
Lindsay Ohlin, Amirfarrokh Farzaneh, Allan Holmgren, Jonas Hedlund and Mattias Grahn
Manuscript

Paper V
Adsorption of water and butanol in silicalite-1 film studied with in situ attenuated total reflectance-fourier transform infrared spectroscopy
Amirfarrokh Farzaneh, Ming Zhou, Elisaveta Potapova, Zoltán Bacsik, Lindsay Ohlin, Allan Holmgren, Jonas Hedlund, Mattias Grahn
Langmuir

The author's contribution to the papers

Paper I	lead role in experimental work and writing
Paper II	lead role in experimental work and writing
Paper III	lead role in experimental work and writing
Paper IV	lead role in writing, supervising role in experimental work
Paper V	review and discussion regarding adsorption of water

To readers of this thesis
This thesis is a summary of the research work performed in papers I-V and is divided into two parts. Part I consists of an introduction and a review of the research work and part II consists of the published papers and manuscripts where details of the research findings can be found.
The reader is encouraged to read the thesis in conjunction with the papers.

Conference contribution (related to but not included in the thesis)
Binary Adsorption of CO_2 and CH_4 in zeolite ZSM-5 studied using in situ ATR-FTIR Spectroscopy
Lindsay Ohlin and Mattias Grahn
Oral presentation at FOA 11, 11th International Conference on the Fundamentals of Adsorption in May 2013 in Baltimore, USA

Contents

Part I

"At every crossroad on the road that leads to the future, each progressive spirit is opposed by a thousand men appointed to guard the past"

-Maurice Maeterlinck

Chapter 1 Introduction

1.1 Fossil fuels

Today's society has become deeply dependent on fossil fuels such as coal, oil and natural gas. Fossil fuels were formed from organic remains of prehistoric plants and animals millions of years ago and combustion of these fuels produces greenhouse gases, for example carbon dioxide. Due to its long atmospheric lifetime, carbon dioxide is accumulated in the atmosphere and hence changes the atmospheric composition. The anthropogenic emission of greenhouse gases is believed to be the main reason for global warming.[1] Furthermore, our dependence on fossil fuels is a great risk for the future since the fuel reserves are limited and at the current and predicted rate of consumption, they will eventually run out. Hubbert[2, 3] was the first to describe what was later named "the peak oil theory", stating that the US conventional oil production would reach the peak of a great bell-shaped curve and then start to decline. Back then the theory was ignored, but it has proven itself to be quite accurate; the oil production in the USA has been declining since the 70´s, as Hubbert predicted.[4] Based on the peak oil theory, various predictions have shown that that the global oil peak production might occur before 2030.[4-7] Depending on how rapidly the fossil fuels are consumed, the reserves might be 80% depleted in 35–84 years. Regarding the current rate of consumption, the global oil reserves are believed to run out in about 40 years, assuming no new significant deposits.[7]

Due to the environmental effects and the decline in easily extracted raw oil, there is a great need for sustainable alternatives to reduce the consumption and the dependence of fossil fuels.

1.2 Biofuels

Biogas and biobutanol are examples of two renewable biofuels which are interesting sustainable alternatives to fossil fuels. Biogas is produced during anaerobic degradation of organic material where anaerobic bacteria break down the organic matter into simple organic compounds. During the degradation, a mixture of methane (60–70%), carbon dioxide (30%) and trace components (such as water) is formed.[8, 9] Biobutanol is produced from ABE (acetone, butanol and ethanol) fermentation of biomass through a two-step process. First, sugar is first converted to acetic acid and butyric acid and secondly, sugar and acids are converted to acetone, butanol and ethanol.[10] However the resulting concentration of butanol in the fermentation broth is limited to ca. 20 g/L as it is toxic to the microorganisms. Purification of biogas and biobutanol is essential to increase the heat value of the fuels. Amine absorption is a commonly used technique for the removal of carbon dioxide from gases. This process is for example sometimes used for the closely related separation of carbon dioxide from natural gas. It is possible to achieve low concentrations of carbon dioxide in the gas using amine scrubbers; however, the process is expensive and complicated.[11] Recovery of butanol by conventional distillation is energy demanding. Therefore, other separation processes are desired.

Adsorbent and membrane based processes are in general considered as energy efficient separation techniques and are consequently interesting alternatives for upgrading biofuels. Among the materials available, zeolites have received much attention in the scientific literature due to their great potential in these separations.[12-17] As the adsorption properties are crucial in both adsorbent and zeolite membrane based separations, a fundamental understanding of these properties are of outmost importance for further developing these materials.

1.3 Zeolites

Zeolites were first described by the Swedish mineralogist Axel Fredrik Cronstedt in 1756. The word zeolite originates from the Greek words *zein* and *lithos* which means boiling stones since the stones seemed to boil due to its rapid water loss upon heating.[18] A zeolite is a crystalline solid with a well-defined structure. The three dimensional structure is based on silicon, aluminum and oxygen where the silica $[SiO_4]^{4-}$ and alumina $[AlO_4]^{5-}$ tetrahedra are linked by shared oxygen atoms.[19, 20] The alumina tetrahedra gives the structure a negative charge which is balanced by a counter ion, for example H^+, Na^+ or Ba^{2+}. The counter ions are

exchangeable which gives the zeolite an ion-exchange capacity. Zeolites can be represented by a general structural formula[19, 20]

$$M_{x/n}\left[(AlO_2)_x(SiO_2)_y\right] \cdot wH_2O \quad (1)$$

where M is a cation of valence n and w is the number of water molecules. The silicon to aluminum ratio (Si/Al) is determined by the y/x ratio and is always ≥1. In synthetic zeolites, the ratio is determined by the synthesis mixture, and higher aluminum content (i.e. lower Si/Al ratio) will result in a more hydrophilic zeolite.[19] Some properties of the zeolite, such as ion exchange capacity and adsorption properties, are to a large extent determined by the Si/Al ratio.[20] For porous materials, pore size can be divided into three groups based on the classification of the International Union of Pure and Applied Chemistry (IUPAC)[21]

Micropores (pore diameter < 2 nm)
Mesopores (pore diameter between 2–50 nm)
Macropores (pore diameter > 50 nm)

The size of zeolite pores varies with the structure of the framework usually in the 0.3–1.3 nm region of the pore diameter and zeolites are thus classified as microporous materials.[19, 20] There are more than 250 zeolite frameworks known today, both natural and synthetic, and new frameworks are reported every year.[22] Each zeolite framework is represented by three capital letters. In this work, the MFI zeolite type has been used and the framework is illustrated in Figure 1. The *MFI framework* exists in two forms; *silicalite-1* and *ZSM-5*. Silicalite-1 contains no (or a very small amount of) aluminum and consequently lacks counterbalancing cations and thus ion-exchange capacity. The low amount of aluminum in silicalite-1 makes it less hydrophilic compared to ZSM-5. The three dimensional pore structure of the MFI framework contains straight channels (0.51×0.55 nm) with intersecting zigzag channels (0.54×0.56 nm).[19]

Zeolites are typically prepared at high pH (~10-11). It is well-known that zeolites prepared in the presence of hydroxide ions contain structural defects resulting in Si–OH groups at internal defect sites. These defects results in additional/different adsorption sites compared to a defect free lattice. For high silica ZSM-5 and silicalite-1, these defects will increase the hydrophilicity of the materials. The formation of silanol defects could to a large extent be avoided by an alternative zeolite synthesis using the fluoride route[23] where the synthesis is performed close to neutral pH.

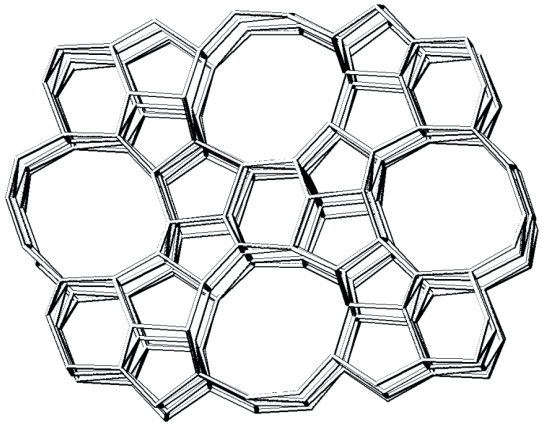

Figure 1. Skeletal model of the MFI framework viewed along the b-direction.[22]

Zeolites are commonly used as powders, for example as ion-exchangers in detergents[24] and as adsorbents or shape selective catalysts in the refining and petrochemical industries. However, zeolites can also be synthesized as films on a variety of supports for membranes applications such as gas separations as well as structured catalysts and adsorbents. Upgrading biofuels using zeolite membranes and adsorbents requires knowledge regarding adsorption separations in order to obtain efficient separation conditions and for optimizing the materials.

1.4 Sorption

Sorption is a general term describing the process in which one substance becomes incorporated into or attached to another substance. The process is divided into three categories; absorption, adsorption and ion exchange.

Absorption is a process in which particles (atoms, molecules or ions) penetrate a bulk phase (solid, liquid or gas) and where the particles are captured by the volume of the bulk phase.

Adsorption is a process where particles are attached to the surface of a bulk phase. The particles attaching are called adsorbate, and the bulk phase is called adsorbent. Adsorption may be classified as; physical adsorption (physisorption) or chemical adsorption (chemisorption). *Physisorption* involves intermolecular forces such as van der Waals attractions between the particles and the surface of

the bulk phase. *Chemisorption* involves a chemical reaction between the particles and the bulk phase where covalent bonds are formed. Adsorption is a reversible process, and the process in which the particles detach from the surface is known as *desorption*.

Ion exchange is a process in which ions are exchanged between an ion exchanger and a solution containing ions. An ion exchanger is an insoluble material, for example a zeolite, containing exchangeable ions.

1.5 Separation by adsorption

Adsorption separations are based on three mechanisms.[25] First, in the *steric mechanism*, molecules are separated due to the pore size of the adsorbent. Molecules which are larger than the pores are rejected while smaller molecules are able to enter the pore structure. Second, in the *equilibrium mechanism*, molecules are separated based on differences in affinity towards the adsorbent. Third, in the *kinetic mechanism*, molecules are separated due to their different rates of diffusion. In this work, the *equilibrium mechanism* was studied measuring how affinities of different adsorbates varied with different conditions.

1.6 Adsorption in zeolites

Zeolites are characterized by having a large surface area and hence a high adsorption capacity. A common way to describe and evaluate adsorption in zeolites is to determine the amount of adsorbed molecules as a function of concentration in the fluid or gas feed at constant temperature; an *adsorption isotherm*. For gases, the concentration in the gas feed (in this work also referred to as the gas phase) is often expressed in partial pressure. Adsorption models are frequently fitted to the experimental data for increased understanding and easier comparison to other related work. In this work, the *Langmuir model* (see Chapter 2) was fitted to the experimental data. Five general classes of adsorption isotherms exist which are characterized according to the Brunauer[26] classification shown in Figure 2. The *type I isotherm* is typical for microporous materials like zeolites; this isotherm shape is also recognized as a *Langmuir adsorption isotherm*. At lower pressure, the surface coverage increases drastically as the partial pressure of the adsorbate in the gas feed is increasing. At higher pressure, the surface coverage will level off and finally reach a saturation limit which corresponds to complete filling of the pores. This type is also typical for chemisorption where only a monolayer may form. Isotherms of *type II and III* are

common for adsorbents containing pores of various sizes in which adsorbed multilayers may form, for instance, by capillary condensation in increasingly larger pores at increasing partial pressures. Isotherms of *type IV* character are common for adsorbents in which the pore size is significantly larger compared to the diameter of the adsorbed molecule. This type of isotherm is observed when two layers of adsorbate are formed. The layers are suggested to form on a plane surface or on the porewall. Isotherms of *type V* character are quite rare and occur only if intermolecular attraction effects are significantly large.[27]

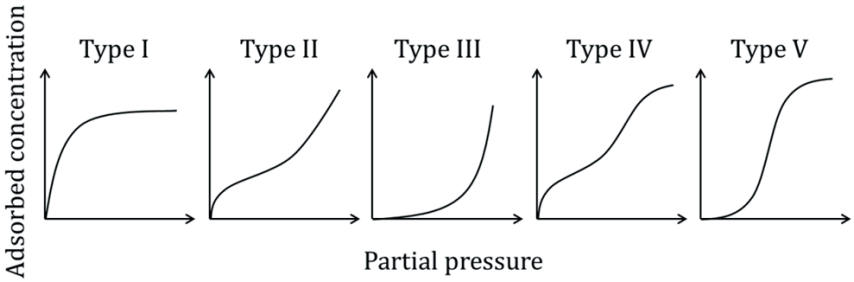

Figure 2. Adsorption isotherms according to the Brunauer classification.

Single component adsorption is commonly studied as a start when determining the adsorption properties of zeolites. Single component adsorption of methane, carbon dioxide and water in MFI zeolite has been fairly well studied in the literature, in particular carbon dioxide and methane. Adsorption of carbon dioxide in MFI is dependent on the composition of the framework where carbon dioxide is adsorbing in reasonable amounts in both silicalite-1 and high silica ZSM-5.[28-32] The adsorption is enhanced by introduction of polar sites i.e. increasing the aluminum content.[31, 33] The adsorption of methane in MFI is also dependent on the composition of the framework where methane is adsorbing stronger in low silica MFI, however the difference in adsorption strength in silicalite-1 and a in low silica ZSM-5 is much smaller for methane than for carbon dioxide.[31] Overall, carbon dioxide adsorbs stronger than methane in MFI zeolite, which is attributed to the larger quadropole moment and slightly higher polarizability of carbon dioxide compared to methane. Adsorption of water in MFI

zeolite is highly dependent on the composition as well as the presence of intracrystalline defects forming polar internal silanol groups. Water shows very low affinity for defect free silicalite-1. However, with increasing aluminum content or by introduction of internal defects the amount of adsorbed water increases. Moreover, it has been shown that water forms small clusters at the polar sites associated with aluminum or intracrystalline defects.[23, 34-36] Binary adsorption of methane and carbon dioxide in zeolites has been well studied in the literature[15, 16, 37-40] showing that carbon dioxide is preferentially adsorbed, and that the adsorption selectivity in general increases with increasing polarity of the framework. However, reports on adsorption in zeolites from binary mixtures of carbon dioxide or methane in combination with water are scarce.[41, 42]

The adsorption results summarized above have been determined using a wide range of different techniques. These methods include gravimetry,[28-31,35] volumetric measurements,[32, 42] concentration pulse methods,[16, 39, 40] zero length column[43] and infrared spectroscopy.[34, 41] Grand Canonical Monte Carlo and molecular dynamics simulations have been widely used to model adsorption.[15, 37, 38, 44-47] In this work, adsorption of methane, carbon dioxide and water in MFI zeolite was studied using ATR-FTIR spectroscopy, which will be described in the following sections.

1.7 Fourier Transform Infrared (FTIR) spectroscopy

In 1891, A. A. Michelson revolutionized the world of spectrometry by designing a two-beam interferometer. The interferometer is a main part of virtually all infrared spectrometers used today (FTIR spectrometers). The Michelson interferometer consists of two mirrors, one fixed and one movable, and a beam splitter. An infrared beam is created by a source and is guided by mirrors via the interferometer through the spectrometer onto the sample compartment and finally reaches the detector. The detected signal (also denoted interferogram) is subsequently Fourier Transformed to yield a spectrum. This calculation is the reason for the name given to this spectrometric technique (FTIR).[48] The intensity of the signal which reaches the detector depends on the absorption of the infrared beam when interacting with the sample. All molecules have a certain natural vibrational frequency and when a molecule is illuminated with infrared radiation of the same frequency as that of the molecule, the infrared radiation may be absorbed by the molecule. The molecule is only able to absorb infrared radiation of the same frequency as its natural vibrational frequency. The molecular vibration is infrared active if the dipole moment of the molecule

changes during the vibration. Hence, when a molecule is illuminated with infrared radiation of various frequencies (which is usually the case in a spectrometer) it will selectively absorb radiation with frequency matching the natural vibrational frequency of the molecule, see Figure 3. When absorbing infrared radiation, the molecule will undergo a transition from one vibrational energy state to another and the molecule will increase its own vibrational energy, hence it will vibrate with increased amplitude.[49] Two important modes of molecular vibrations used in this work are the stretching modes and bending modes. The former is characterized by changes in the bond length between the atoms in the molecule and the latter is characterized by changes in the bond angle between the atoms. When the infrared radiation is absorbed by the sample, the intensity of the signal which reaches the detector is decreased.

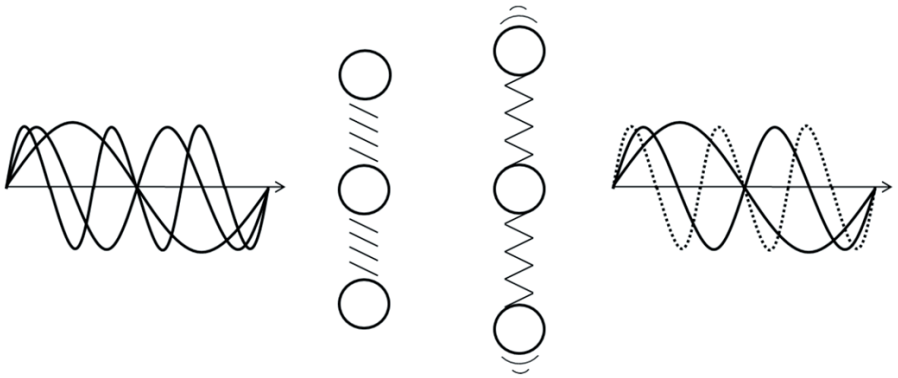

Figure 3. Schematic figure illustrating absorption of infrared radiation. Before interaction (left); infrared photons of different frequencies approach the molecule in the ground state. After interaction (right); photons of the same frequency as that of the vibration of the molecule has been absorbed and the vibrational energy of the molecule is increased.

1.8 The Attenuated Total Reflectance (ATR) technique

The attenuated total reflectance (ATR) technique is based on internal reflection where the infrared beam is totally reflected inside an ATR crystal,[50] see Figure 4. To achieve total reflection, the ATR crystal must have a higher refractive index (n_1) than the sample (n_2). Total reflection only occurs if the angle of incidence is larger than the critical angle. The angle of incidence is defined as the angle with respect to the normal and the critical angle is defined according to[50]

$$\theta_{critical} = \sin^{-1}\left(\frac{n_2}{n_1}\right) \tag{2}$$

At each point of reflection in the ATR crystal, an evanescent wave from the infrared beam is created perpendicular to the surface of the ATR crystal, see Figure 5. The electric field of the evanescent wave interacts with the sample in the vicinity of the ATR crystal where parts of the electric field may be absorbed by the sample resulting in an attenuation of the intensity of the reflected infrared beam, hence the name of the technique. The amplitude of the electric field declines exponentially with distance from the surface, z, of the ATR crystal according to

$$E = E_0 e^{-z/d_p} \tag{3}$$

where E and E_0 are the electric field after and before the exponential decline, respectively, and the penetration depth, d_p, is a measure of how far the electric field reaches from the surface of the ATR crystal.

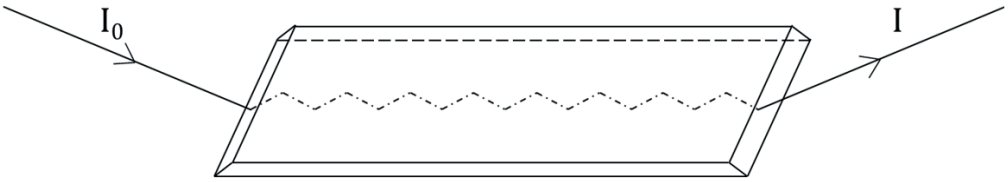

Figure 4. Schematic figure illustrating the ATR technique where the infrared beam is totally reflected several times inside the ATR crystal (in this case a trapezoidal element). I_0 and I are the intensity of the infrared beam before and after interaction with the sample, respectively.

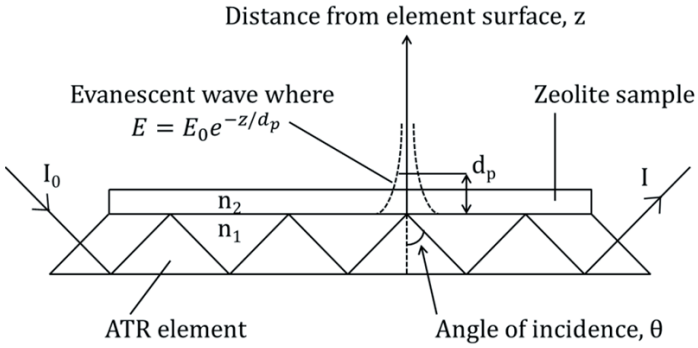

Figure 5. Schematic figure illustrating the ATR technique where the evanescent wave is penetrating the zeolite sample.

The penetration depth may be approximated by[50]

$$d_p = \frac{\lambda_1}{2\pi(sin^2\theta - n_{21}^2)^{\frac{1}{2}}} \quad (4)$$

where λ_1 is the wavelength of the infrared radiation inside the ATR crystal, θ is the angle of incidence and n_{21} is the ratio of the refractive indices (n_2/n_1).
The penetration depth is typically some hundreds of nanometers to a few micrometers, which makes ATR spectroscopy a technique ideal for studying surfaces and thin films.

1.9 Scope of the present work

The scope of the present work was to study adsorption properties of high-silica MFI zeolites using *in-situ* ATR-FTIR spectroscopy. The first step was to study the single component adsorption of methane, carbon dioxide and water in zeolite Na-ZSM-5. In the next step, the method was used to study multicomponent adsorption of the $CH_4/CO_2/H_2O$/Na-ZSM-5 system. Further, the ability of the Ideal Adsorbed Solution Theory (IAST) to predict adsorbed amounts from mixtures was assessed. Adsorption of water and butanol in silicalite-1 was also studied using ATR-FTIR spectroscopy.

Chapter 2 Theory

2.1 Concentration of the adsorbate

The well-known Beer-Lambert law describes the relationship between the absorbance observed in an infrared spectrum and the concentration of the species of interest.[51] For adsorbed concentrations in powders, the Beer-Lambert equation may be written according to Equation 5, which was used in the present work to determine the molar absorptivity, ε, for methane, carbon dioxide and water adsorbed in Na-ZSM-5

$$A = \varepsilon c l = \varepsilon \frac{n \cdot d_o}{s \cdot d_g} \tag{5}$$

where A is the integrated absorbance, c is the concentration of the adsorbate, l is the path length, n is the amount of molecules adsorbed in the powder sample (wafer), s is the surface area of the wafer, d_o is the optical path length in the wafer and d_g is the geometric thickness of the wafer. Since the optical path and the geometric thickness are most likely not identical and the optical path is almost impossible to determine, the powder was assumed to behave as an isotropic scatterer i.e. with an optical path length twice the geometrical thickness.

Since the Beer-Lambert law cannot be applied directly to the ATR technique, Tompkins[52] and Mirabella[50] developed a method to calculate the concentration of adsorbate in ATR experiments. The absorbance (for a band of interest) per reflection is given by

$$\frac{A}{N} = \frac{n_{21}E_0^2\varepsilon}{cos\theta}\int_0^{\infty} C(z)\, e^{-\frac{2z}{d_p}}dz \tag{6}$$

where A is the integrated absorbance, N is the number of reflections inside the gasket sealing in the cell, n_{21} is the ratio of the refractive indices (n_2/n_1) of the denser (ATR crystal, n_1) and the rarer (zeolite film, n_2) medium, E_0 is the amplitude of the electric field at the ATR crystal/zeolite film interface, ε is the molar absorptivity determined by Equation 5, θ is the angle of incidence which was 45° during all experiments, $C(z)$ is the concentration of the adsorbate in the zeolite film, z is distance from the surface of the ATR crystal and d_p is the penetration depth determined by Equation 4. After integration the following equation is obtained

$$\frac{A}{N} = \frac{n_{21}E_0^2 d_p C}{2cos\theta}\varepsilon\left(1 - e^{-\frac{2d_a}{d_p}}\right) \tag{7}$$

where d_a is the thickness of the zeolite film. A hypothetical thickness referred to as the "effective thickness" of the sample, d_e, must be introduced in order to apply the Beer-Lambert law to the ATR data where d_e is given by

$$d_e = \frac{n_{21}E_0^2 d_p}{2cos\theta} \tag{8}$$

d_e represents the distance required to achieve the same absorbance in a transmission experiment as in an ATR experiment. The value of d_e is dependent on the polarization direction of the infrared beam and may be estimated by

$$d_e = \frac{I_{0II}}{I_{0II} + I_{0\perp}} d_{eII} + \frac{I_{O\perp}}{I_{0II} + I_{0\perp}} d_{e\perp} \tag{9}$$

where I_{0II} and $I_{O\perp}$ are the intensity of the radiation without sample for parallel and perpendicular polarized radiation, respectively. d_{eII} is the effective thickness for parallel polarization and is determined by

$$d_{eII} = \frac{2n_{21}d_p cos\theta(2sin^2\theta - 2n_{21}^2)}{(1 - n_{21}^2)[(1 + n_{21}^2)sin^2\theta - n_{21}^2]} \tag{10}$$

$d_{e\perp}$ is the effective thickness for perpendicular polarization and is determined by

$$d_{e\perp} = \frac{2n_{21}d_p cos\theta}{1-(n_{21})^2} \tag{11}$$

By combining Equations 4–11 it was possible to determine the concentration of methane, carbon dioxide and water in the Na-ZSM-5 film as well as of water in the silicalite-1 film, assuming the same molar absorptivity for water in the two films.

2.2 Adsorption isotherms – the Langmuir model

Adsorption isotherms were retrieved from spectral data by integrating the characteristic infrared band for each of the adsorbed species. The calculated band areas were converted to concentrations using Equations 4–11 and plotted against the partial pressure, see Chapter 4. The Langmuir model is commonly used to describe adsorption in zeolites. For adsorption on one type of sites (all sites are equivalent, one molecule on each site and no interaction between molecules on adjacent sites) in the zeolite film the single site Langmuir model was used

$$q_{tot} = q_1 \frac{b_1 P}{1+b_1 P} \tag{12}$$

where q_1 is the saturation concentration of the site (mmol g^{-1}), b_1 is the Langmuir adsorption coefficient or affinity constant (Pa^{-1}) and P is the partial pressure of the species in the gas phase (Pa). For adsorption on two different sites, the dual site Langmuir model was used

$$q_{tot} = q_1 \frac{b_1 P}{1+b_1 P} + q_2 \frac{b_2 P}{1+b_2 P} \tag{13}$$

where the subscript number indicates the two sites in the zeolite film. These models were fitted to single component adsorption isotherms and will be discussed in detail later.

The heat of adsorption (enthalpy change), ΔH, was determined using the van´t Hoff equation

$$\ln b = -\frac{\Delta H}{RT} + \frac{\Delta S}{R} \tag{14}$$

where R is the gas constant (J mol^{-1} K^{-1}), T is the temperature (K) and ΔS is the entropy change (kJ/mol). By plotting $ln\, b$ against $1/T$ a straight line with the slope $-\Delta H/R$ and the y-intercept $\Delta S/R$ was obtained. Adsorption is an exothermic reaction resulting in negative ΔH values which represents the bond strength between the adsorbate and the adsorbent.

2.3 Ideal Adsorbed Solution Theory

Based on Gibbs adsorption isotherm, Myers and Prausnitz[53] proposed that the Ideal Adsorbed Solution Theory (IAST) provides a link between single and multicomponent adsorption, where multicomponent adsorption data is predicted using only single component data as input. The IAST is similar to Raoult´s law in vapor-liquid equilibrium according to

$$P_i = P_i^0(\pi_i)x_i \tag{15}$$

where π_i is the spreading pressure of component i in the adsorbed phase, x_i is the adsorbed molar fraction and P_i^0 is the pure component hypothetical pressure which yields the same spreading pressure as that of the mixture. The spreading pressures at the adsorbed equilibrium must be the same for each component in the mixture

$$\pi_i^* = \frac{\pi_i}{RT} = \int_0^{P_i^0} \frac{n_i^0(P)}{P} dP \tag{16}$$

where $i = 1,2,3 \ldots, N$ and

$$\pi_1^* = \pi_2^* = \ldots = \pi_N^* = \pi^* \tag{17}$$

where $n_i^0(P)$ is the pure component equilibrium capacity. By assuming ideal mixing at constant T and π, the total adsorbed amount is

$$\frac{1}{n_t} = \sum_{i=1}^{N} \left[\frac{x_i}{n_i^0(P_i^0)} \right] \tag{18}$$

with the constraint

$$\sum_{i=1}^{N} x_i = 1 \tag{19}$$

In the present work, the IAST was used to calculate predicted adsorbed amounts for multicomponent adsorption in the zeolite using the single component adsorption isotherm parameters as input.

2.4 Adsorption selectivity

High selectivity is required to achieve an efficient separation process using adsorption where the process is based on one component being preferably adsorbed in the zeolite compared to the other. In the present work, the adsorption selectivity, α, was determined according to[27]

$$\alpha_{i/j} = \frac{X_i/X_j}{Y_i/Y_j} \tag{20}$$

where X is the equilibrium mole fractions of components i and j in the adsorbed phase and Y is the mole fractions in the gas phase at equilibrium between the two phases.

Chapter 3 Experimental

3.1 Zeolite film synthesis

Trapezoidal ZnS crystals (Spectral systems) with dimensions of 50×20×2 mm^3 and 45° cut edges were used as ATR crystals upon which MFI zeolite films (Na-ZSM-5 with Si/Al = 130 and silicalite-1) were grown on both sides using two different seeding methods. Details of the preparation methods have been reported elsewhere[54-57] and can also be found in Paper I for Na-ZSM-5 and in Paper V for silicalite-1.

3.2 Film characterization

SEM images of the synthesized zeolite films were recorded using a FEI Magellan 400 field emission XHR-scanning electron microscope. For the Na-ZSM-5 film, X-ray diffraction data were recorded using a Siemens D5000 x-ray diffractometer running in Bragg-Brentano geometry. The Si/Al ratio and the Na/Al ratio of the zeolite film were determined using inductively coupled plasma mass spectroscopy (ICP-MS) measurements. For the silicalite-1 film, X-ray diffraction data were recorded using a PANalytical Empyrean instrument, equipped with a PIXcel[3D] detector and a Cu LFF HR X-ray tube.

3.3 Adsorption experiments

For *in-situ* ATR-FTIR adsorption measurements, the zeolite coated ATR crystal was mounted into a heatable flow cell (also referred to as an ATR cell), see Figure 6. The heatable flow cell was used to remove any pre-adsorbed species from the zeolite film prior to measurements and to perform adsorption experiments at elevated temperatures. The heating of the ATR cell as well as pre-heating of the gas feed was adjusted by programmable temperature controllers. The ATR cell was sealed with graphite gaskets to prevent gas leakage. To mount the heatable flow cell into the spectrometer, an ATR attachment from Spectratech was used. The ATR cell was connected to a gas delivery system, see Figure 7, where the gas flow was controlled by mass flow controllers (MFC). For single gas adsorption experiments of methane and carbon dioxide, the pure gas was diluted using helium to control the partial pressure of the analyzed gas before entering the ATR cell. Helium was also used as a carrier gas for the water experiments where helium was fed to two saturators connected in series filled with liquid water. The first saturator was kept at room temperature and the second was cooled using a circuit of temperature controlled glycol. The flow rate was controlled by the MFC´s in two different streams; one stream going through the saturators and the other for diluting the flow from the saturators and hence controlling the partial pressure of water. The carrier gas was not used for multicomponent adsorption experiments. The pure gases were then mixed before entering the ATR cell and for multicomponent experiments including water, one of the pure gases was fed through the saturators. To remove any adsorbed species prior to measurements, the zeolite film was dried overnight at 300 °C under a flow of helium. Thereafter, the ATR cell was mounted in the spectrometer. Prior to the adsorption measurements, a background spectrum of the dried zeolite film was recorded under a flow of helium. For each composition of the gas, infrared spectra were recorded continuously until the system reached equilibrium and changes with time could no longer be observed. The infrared spectra were recorded using a Bruker IFS 66v/S FTIR spectrometer equipped with a deuterated triglycine sulphate (DTGS) detector by co-adding 256 scans at a resolution of 4 cm^{-1}.

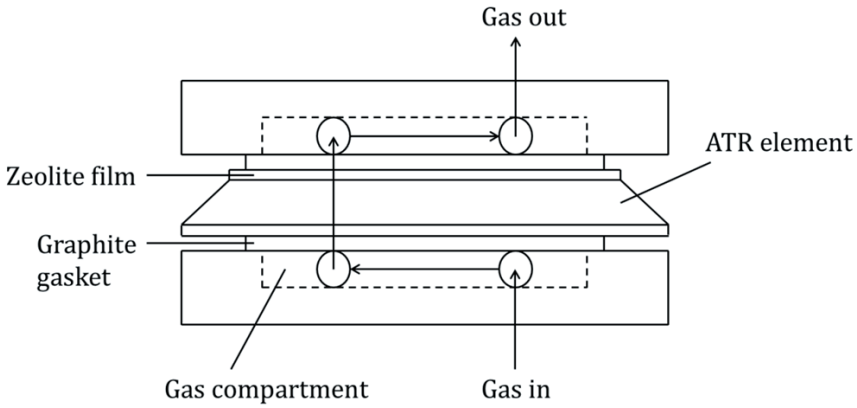

Figure 6. Schematic figure illustrating the ATR cell (seen from above) with zeolite film on both sides of the ATR element. Thermocouple and heating elements have been omitted for the sake of clarity.

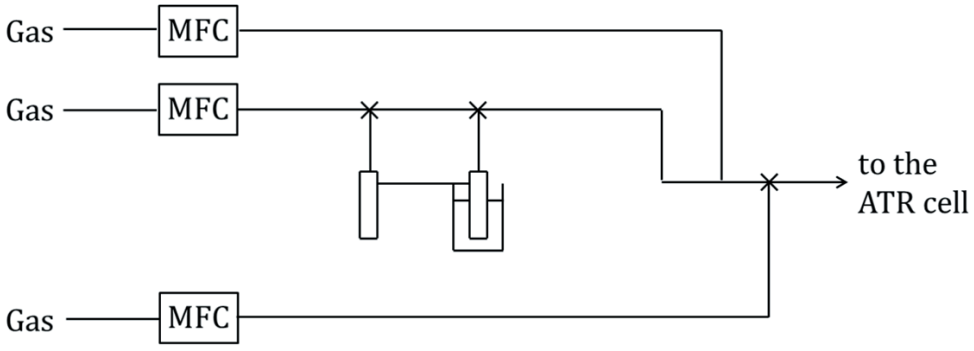

Figure 7. Schematic figure illustrating the gas delivery system.

3.4 Determining the molar absorptivities

The analysis for determining the molar absorptivity for methane, carbon dioxide and water in Na-ZSM-5 was conducted using a combination of thermogravimetry and infrared spectroscopy. Analysis by gravimetry and infrared spectroscopy (AGIR) is a recently developed technique presented by Bazin *et al*.[58] where gravimetry and IR spectroscopy are combined in the same reactor cell, see Figure 8. The balance is placed at the top of the setup and the measuring range is ±200 mg with an accuracy of 0.03 µg. The sample is attached to the balance via a suspending rod; see Figure 9, which holds the sample in the center of the IR cell perpendicular to the infrared beam. The infrared beam travels through the cell and the sample. Infrared spectra are recorded simultaneously as measurements of the mass are performed. The spectral data were collected using a Nicolet 6700 spectrometer equipped with a mercury, cadmium and tellurium (MCT) detector by co-adding 64 scans at a resolution of 4 cm^{-1}, whereas a symmetrical microbalance SETSYS-B from SETARAM was used to record the mass. The AGIR setup and the general methodology for determining molar absorptivities of species adsorbed on powders have been described in more details previously.[58]

In the present work, a 25 mg sample of zeolite ZSM-5 (Si/Al = 115) was pressed as a self-supported wafer with an area of 2 cm^2. The wafer was mounted in the AGIR setup with the measurement cell connected to a gas delivery system. Prior to measurements, the wafer was dried at 400 °C under a flow of argon. Thereafter the adsorbate was fed to the setup and infrared spectra of the adsorbed species and the mass of the sample were recorded simultaneously until equilibrium was reached. The concentration of the adsorbate in the gas was monitored by a mass spectrometer connected to the outlet of the cell. The molar absorptivity, ε, for methane, carbon dioxide and water was determined using Equation 5.

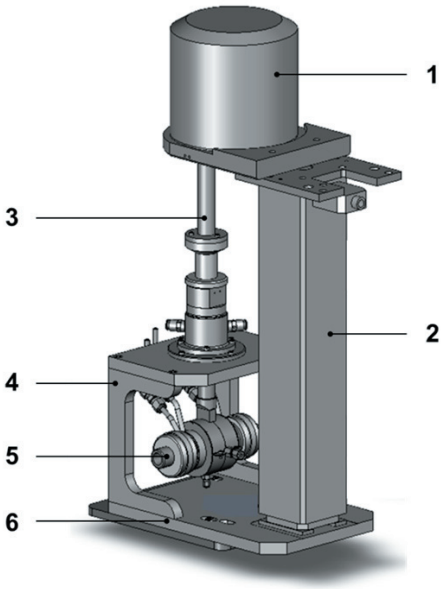

Figure 8. Schematic figure of the AGIR system[58] having the following compartments: 1. Microbalance, 2. Telescopic column, 3. Link between the balance and the IR cell, 4. Support for the IR cell, 5. IR cell, 6. Base plate.

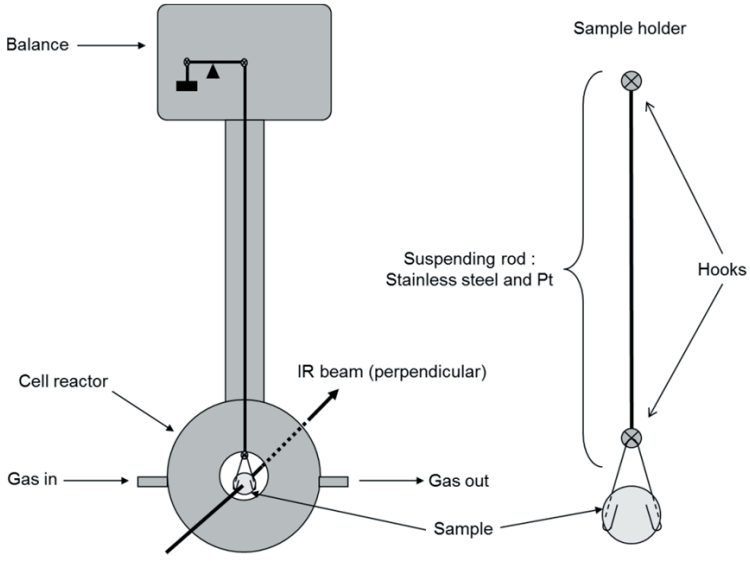

Figure 9. Schematic figure illustrating the sample holder in the AGIR system.[58]

Chapter 4 Results and discussion

4.1 Film characterization

SEM images of Na-ZSM-5 and silicalite-1 films synthesized on ZnS crystals are shown in Figures 10 and 11, respectively. The zeolite films are continuous and consist of well-intergrown crystals which form dense and homogenous films without any pinholes. The thicknesses of the Na-ZSM-5 and silicalite-1 films are approximately 550 and 750 nm, respectively.

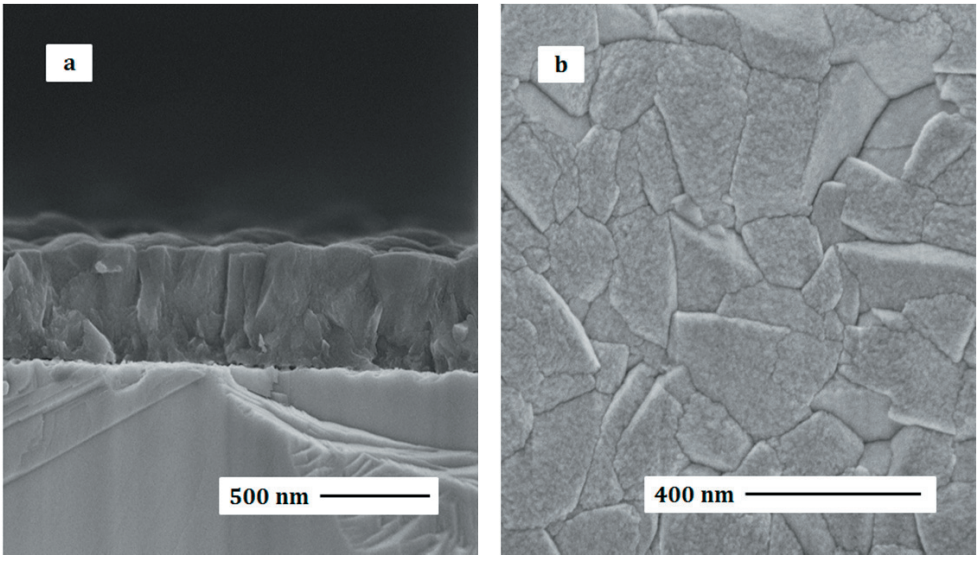

Figure 10. SEM images of the Na-ZSM-5 film synthesized on a ZnS crystal; cross section (a) and top view (b).

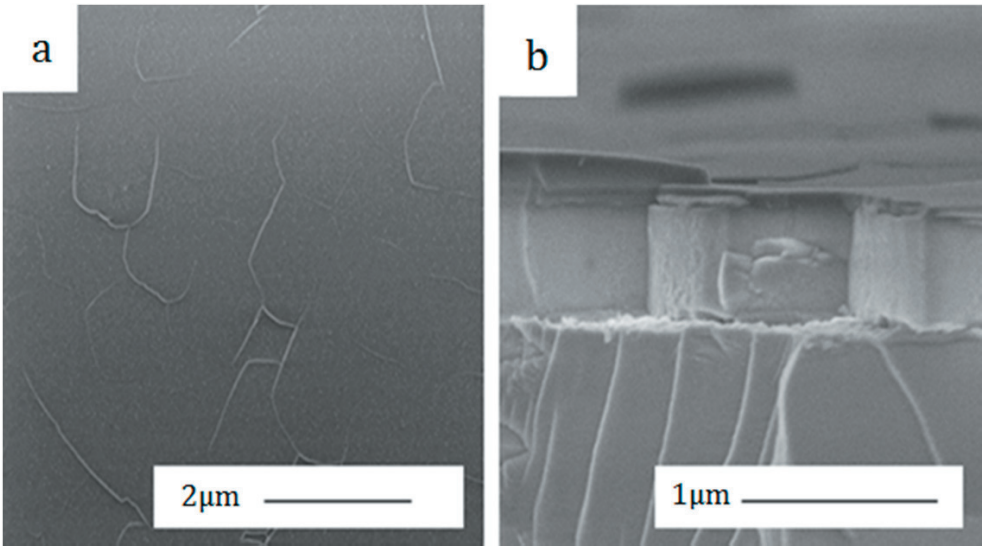

Figure 11. SEM images of the silicalite-1 film synthesized on a ZnS crystal; top view (a) and cross section (b).

The MFI phase of the zeolite films were verified by XRD and the recorded patterns are shown in Papers I and V, respectively, where more detailed information can be found.

The Si/Al and Na/Al ratios of the Na-ZSM-5 film were determined to be 130 and 1, respectively. The specific Si/Al ratio was chosen since it represents the composition of the high silica ZSM-5 membranes prepared in our group.[59, 60]

4.2 Single component adsorption experiments

Single component adsorption of methane and carbon dioxide was studied in Na-ZSM-5 (Paper I), whereas adsorption of water was studied in both Na-ZSM-5 and silicalite-1 (Papers I and V).

4.2.1 Infrared spectra

Infrared spectra of methane and carbon dioxide adsorbed in Na-ZSM-5 at 35 °C and at different partial pressures in the gas phase are presented in Figures 12 and 13, respectively. Bands in the 3020–3000 cm^{-1} region are assigned to the C-H stretching vibration[61, 62] of adsorbed methane where two bands were observed at 3015 and 3002 cm^{-1}. The asymmetric stretching vibration[41] band of carbon dioxide appeared at 2338 cm^{-1}. At lower partial pressures, two bands can be observed at 2350 and 2338 cm^{-1}, indicating that the carbon dioxide molecules are less restricted at these loadings. At higher pressures, only one band at 2338 cm^{-1} was observed, reflecting the restricted motion of the carbon dioxide molecules inside the narrow zeolite pores. The spectra of adsorbed methane and carbon dioxide at higher temperatures were of same character but weaker as expected due to reduced adsorption with increasing temperature.

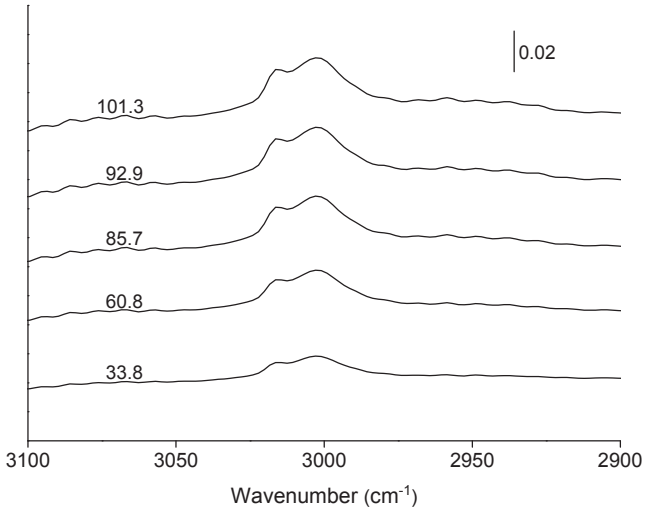

Figure 12. Infrared spectra of adsorbed methane in Na-ZSM-5 at 35 °C and various partial pressures (kPa) as indicated in the figure.

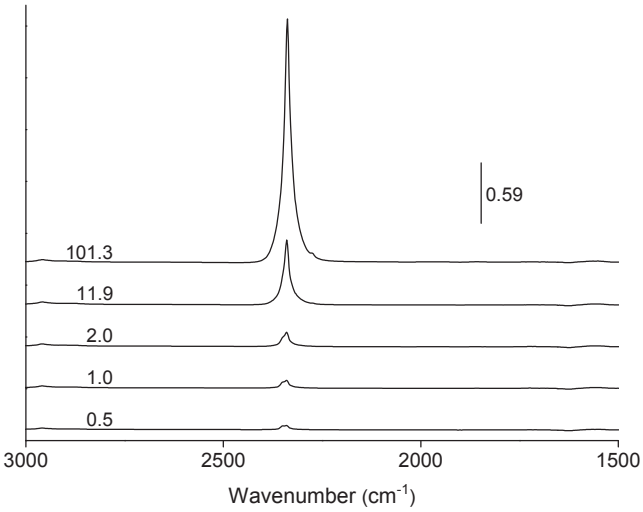

Figure 13. Infrared spectra of adsorbed carbon dioxide in Na-ZSM-5 at 35 °C and different partial pressures (kPa) as indicated in the figure.

Infrared spectra of water adsorbed in Na-ZSM-5 and silicalite-1 at 35 °C and at various partial pressures in the gas phase are presented in Figures 14 and 15, respectively. The intensity of the bands correlates well with the partial pressures showing higher absorbance at higher partial pressures. Moreover, the intensity of the bands is higher for adsorption of water in Na-ZSM-5 compared to silicalite-1 as a result of Na-ZSM-5 being more hydrophilic due to its aluminum content. The broad band in the 3700–2700 cm^{-1} region was assigned to the O-H stretching vibration (asymmetric and symmetric) of adsorbed water whereas the band at ca. 1620 cm^{-1} was assigned to the bending vibration of adsorbed water.[41, 63] The broad band is associated with hydrogen bonded water and indicates the formation of water clusters, which is in agreement with Jentys *et al*.[34] The band at ca. 1620 cm^{-1} was observed at lower wavenumber for adsorption in silicalite-1 compared to the same vibration mode for Na-ZSM-5 (ca. 1622 cm^{-1}). This indicates that the water-zeolite interactions were weaker in silicalite-1 compared to Na-ZSM-5, again due to Na-ZSM-5 being more hydrophilic compared to silicalite-1. In general, the bending vibration band is observed at a lower wavenumber compared to bulk water (ca 1650 cm^{-1}) which is a result of the stronger hydrogen bonds between water molecules compared to water-zeolite

interactions. The negative band at ca. 3730 cm^{-1} is assigned to the O-H stretching vibration of free surface silanol groups.[34] As water adsorbs on the silanol group the, silanol band is red shifted leading to a negative band at the wavenumber of the unperturbed silanol group. Similar infrared spectra of adsorbed water in ZSM-5 and 13X zeolite have been reported previously in the literature.[34, 41]

Comparing the spectra of methane, carbon dioxide and water presented in Figures 12–15 show that the characteristic bands of each component appear at different wavenumbers in the spectra. It should therefore be possible to distinguish the different adsorbed species from each other when adsorbed from multicomponent mixtures, which will be discussed later in this chapter.

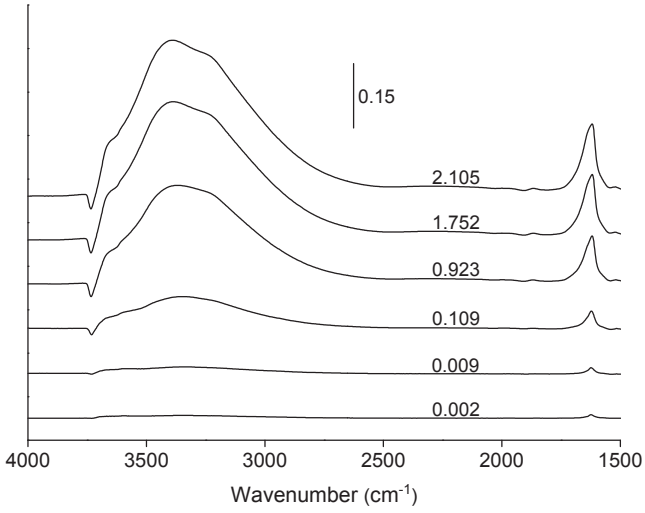

Figure 14. Infrared spectra of adsorbed water in Na-ZSM-5 at 35 °C and various partial pressures of the gas phase (kPa) as indicated in the figure.

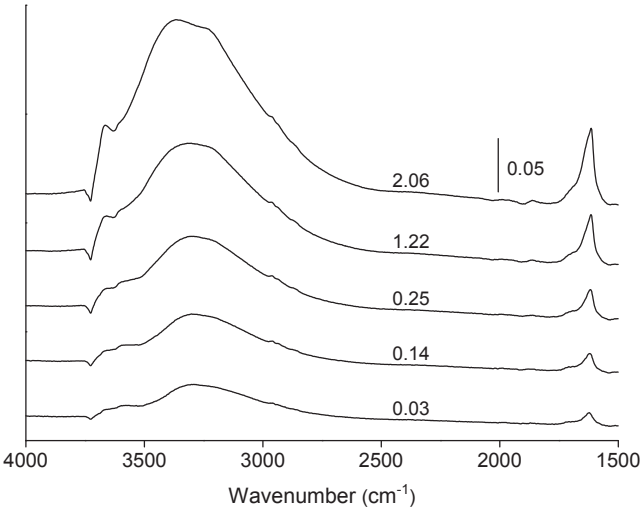

Figure 15. Infrared spectra of adsorbed water in silicalite-1 at 35 °C and various partial pressures of the gas phase (kPa) as indicated in the figure.

4.2.2 Molar absorptivity

In order to calculate the adsorbed concentrations from an ATR experiment, the molar absorptivities, ε, for the species adsorbed in the zeolite are needed. Such measurements were performed using the AGIR setup, and the data were analyzed using the Beer-Lambert law (Equation 5). The molar absorptivities for the adsorbates in Na-ZSM-5 were determined to be 0.85 cm/μmol for methane (band centered at 3002 cm^{-1}), 16.3 cm/μmol for carbon dioxide (band centered at 2340 cm^{-1}) and 0.645 cm/μmol for water (band centered at 1630 cm^{-1}). The molar absorptivity for water in silicalite-1 was assumed to be the same as for water adsorbed in Na-ZSM-5.

4.2.3 Adsorption isotherms

Data retrieved from the infrared spectra were converted to adsorbed concentrations using Equations 4–11. The adsorption isotherms for methane, carbon dioxide and water are presented in Figures 16 and 17. Curves representing the Langmuir models fitted to the experimental data are also included in the figures; the single-site Langmuir model was used for methane, and the dual-site Langmuir model for carbon dioxide and water. As can be seen, the Langmuir models fit the experimental data very well. The adsorption isotherms determined in the present work did not reach the saturation limit at the studied partial pressures for any of the components. The adsorption isotherms of methane, see Figure 16 a, show quite low loading compared to the loadings obtained for carbon dioxide and water, indicating that methane interacts weaker with Na-ZSM-5 compared to the other two components, which is agreement with the literature.[15, 16, 37, 40] It is evident that less water was adsorbed in silicalite-1 compared to Na-ZSM-5, see Figure 17, due to Na-ZSM-5 being more hydrophilic. Water did not adsorb in detectable amounts in silicalite-1 at 120 °C and hence, no isotherm could be determined at this temperature.

The fitted Langmuir adsorption coefficients (b) and the saturation concentrations (q_{sat}) for methane, carbon dioxide and water are reported in Table 1. The saturation concentration of methane in Na-ZSM-5 was determined to be 2 mmol/g in the present work using the single-site Langmuir model. The value is in agreement with values reported in literature for adsorption in MFI type zeolites, which are in the 1.9–5.4 mmol/g range.[29-31, 64-67] Regarding carbon dioxide, the saturation concentration in MFI type zeolites has been reported in the 1.2–5 mmol/g range and the value of 2.8 mmol/g determined in the present work thus agrees with values in the literature.[29-31, 33, 64-67] The two adsorption sites related to carbon dioxide are likely associated with cations and silanol groups (polar sites) with stronger interactions and sites on the pore wall with weaker interactions.[33] The saturation loading on the polar sites is significantly lower than the corresponding value for the site with weaker interaction which is reasonable due to the low aluminum content of the zeolite. In the present work, the saturation concentration of water in Na-ZSM-5 and silicalite-1 was determined to be 5.8 and 3.2 mmol/g, respectively. Reports on the saturation concentration of water in different MFI zeolites vary significantly from 0.8 to 31 mmol/g.[35, 36, 68-70] The great variation in the values is probably due to the varying Si/Al ratios and the amount of defects in the zeolites. Low Si/Al ratios will make the zeolite more hydrophilic and hence more water should be adsorbed. Crystal defects, such as the formation of silanol groups, also affect the

adsorption of water. The presence of silanol groups in the zeolite will render it more hydrophilic, and hence increase the adsorption of water. However, most literature reports are in the 0.8–4.8 mmol/g range, which is similar to the value determined in this work. As for carbon dioxide, Na-ZSM-5 and silicalite-1 probably provides the water molecules with two possible adsorption sites. The high affinity adsorption site is probably related to sites containing cations (only in Na-ZSM-5) and/or silanol groups. The low affinity adsorption site is however possibly related to the formation of water clusters.

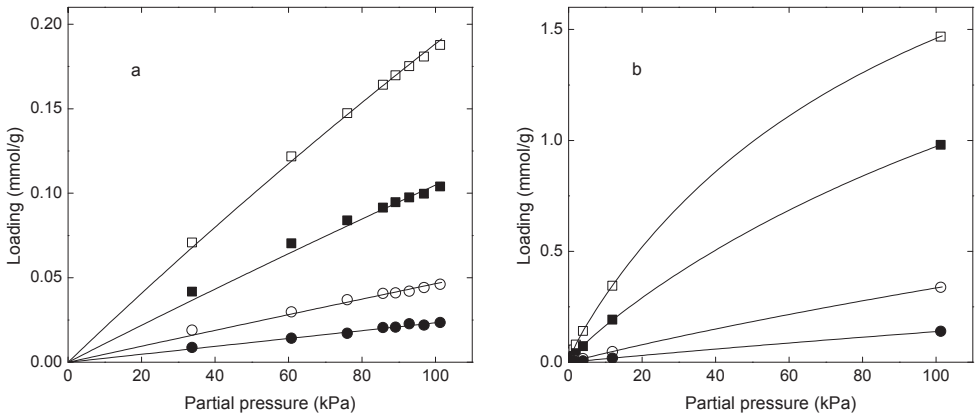

Figure 16. Adsorption isotherms for methane (a) and carbon dioxide (b) in Na-ZSM-5 at 35 °C (□), 50 °C (■), 85 °C (○) and 120 °C (●).The symbols represent the experimental data and the lines represent the Langmuir model.

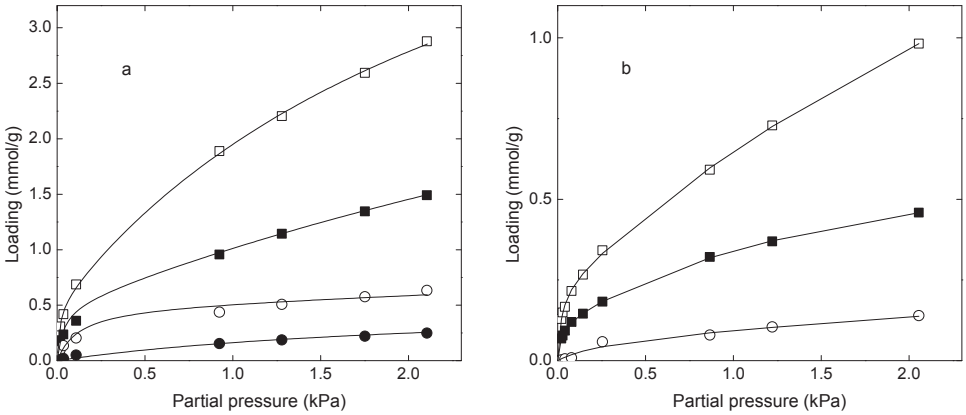

Figure 17. Adsorption isotherms for water in Na-ZSM-5 (a) and in silicalite-1 (b) at 35 °C (□), 50 °C (■), 85 °C (○) and 120 °C (●). The symbols represent the experimental data and the lines represent the Langmuir model.

4.2.4 Heat of adsorption

The heat of adsorption, ΔH, for methane, carbon dioxide and water was determined by analyzing the temperature dependency of the adsorption coefficients using the van´t Hoff equation (Equation 14). The values obtained in the present work are presented in Table 2. As for the saturation capacities, there is significant scattering in the values reported in the literature.[28-31, 33, 35, 70] However, the values obtained in the present work are within the range of previously reported data for MFI zeolites with similar Si/Al ratio and are thus in agreement with the literature. Methane has a lower isosteric heat of adsorption value compared to carbon dioxide and water, which might be expected due to its slightly lower polarizability compared to carbon dioxide and its lack of polarity.[16, 29, 40, 71] Carbon dioxide and water are therefore preferably adsorbed in Na-ZSM-5 compared to methane. For water, the isosteric heat of adsorption is of the same magnitude for both Na-ZSM-5 and silicalite-1. However, more water is adsorbed in Na-ZSM-5 due to the higher affinity of water for Na-ZSM-5 compared to silicalite-1, see Table 1.

As demonstrated above, the ATR-FTIR technique has proven to be a very successful method for studying single component adsorption in thin MFI films. The ability to use infrared spectroscopy to distinguish between different species adsorbed from a multicomponent gas mixture will be discussed next.

Table 1. Langmuir adsorption coefficients (b, Pa^{-1}) and saturation concentrations (q_{sat}, mmol/g) for methane, carbon dioxide and water.

Adsorbate	Temp. (°C)	q_1 (mmol/g)	b_1 (1/Pa)	q_2 (mmol/g)	b_2 (1/Pa)
CH_4	35	2	1.04×10^{-6}		
	50	2	5.53×10^{-7}		
	85	2	2.38×10^{-7}		
	120	2	1.18×10^{-7}		
CO_2	35	2.78	1.04×10^{-5}	0.04	6.33×10^{-4}
	50	2.78	5.03×10^{-6}	0.04	2.47×10^{-4}
	85	2.78	1.24×10^{-6}	0.04	1.83×10^{-5}
	120	2.78	4.44×10^{-7}	0.04	8.31×10^{-6}
H_2O (Na-ZSM-5)	35	5.34	3.75×10^{-4}	0.50	7.90×10^{-2}
	50	5.34	1.10×10^{-4}	0.50	2.80×10^{-2}
	85	5.34	1.10×10^{-5}	0.50	8.10×10^{-3}
	120	5.34	8.00×10^{-7}	0.50	4.63×10^{-4}
H_2O (silicalite-1)	35	2.96	1.70×10^{-4}	0.23	4.84×10^{-2}
	50	2.96	4.00×10^{-5}	0.23	1.21×10^{-2}
	85			0.23	3.43×10^{-3}

Table 2. Values of the heat of adsorption, *ΔH*, for methane, carbon dioxide and water obtained in the present work.

Adsorbate	Zeolite	Si/Al ratio	ΔH (kJ/mol)
CH_4	Na-ZSM-5	130	-23
CO_2	Na-ZSM-5	130	-37 (site 1) -54 (site 2)
H_2O	Na-ZSM-5	130	-72 (site 1) -58 (site 2)
H_2O	silicalite-1	∞	-46 (site 1) -79 (site 2)

4.3 Multicomponent adsorption experiments

In the present work, adsorption of the following multicomponent mixtures have been studied

- binary adsorption of carbon dioxide/methane (Paper II)
- binary adsorption of water/methane (Paper III)
- binary adsorption of water/carbon dioxide (Paper III)
- ternary adsorption of methane/carbon dioxide/water (Paper IV)

4.3.1 Infrared spectra

An infrared spectrum of methane and carbon dioxide adsorbed simultaneously from a binary mixture in Na-ZSM-5 at 35 °C is presented in Figure 18 while Figure 19 shows an infrared spectrum from a ternary mixture (also including water) in the same zeolite. As discussed earlier for single component adsorption, the bands at 3015 and 3003 cm^{-1} are assigned to the C-H stretching vibration of adsorbed methane and the band at 2338 cm^{-1} is assigned to asymmetric stretching vibration of carbon dioxide. In Figure 19, the broad band in the 3700–2700 cm^{-1} region and the band at ca. 1620 cm^{-1} indicate the presence of adsorbed water. The broad band is assigned to asymmetric and symmetric O-H stretching vibration and is associated with hydrogen bonded water indicating the formation of water clusters, which is in agreement with Jentys *et al*.[34] The latter band is assigned to the bending vibration of adsorbed water. Two well resolved bands appeared at 3698 cm^{-1} and 3596 cm^{-1} which were only resolved in systems containing carbon dioxide. The bands are assigned to O-H stretching vibrations located at defects (probably silanol groups) in the zeolite film, indicating that silanol groups might interact with each other before interacting with carbon dioxide molecules since these bands were not seen in the background spectra. Infrared spectra recorded for both binary and ternary mixtures at higher temperatures were similar in appearance but with lower intensities.

Thus, characteristic bands of all the adsorbed species were observed and the bands remained in the same positions as in the single component spectra, indicating that no major interaction between the species occurred.

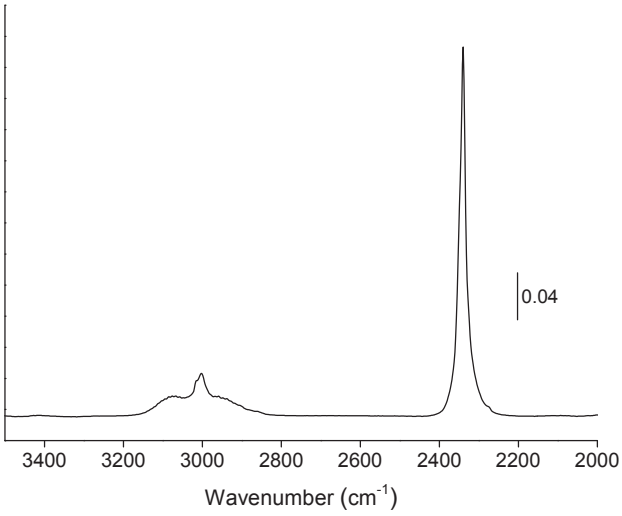

Figure 18. Infrared spectra of methane and carbon dioxide adsorbed in Na-ZSM-5 from a binary mixture at 35 °C. The partial pressure of methane and carbon dioxide was 98 and 3 kPa, respectively.

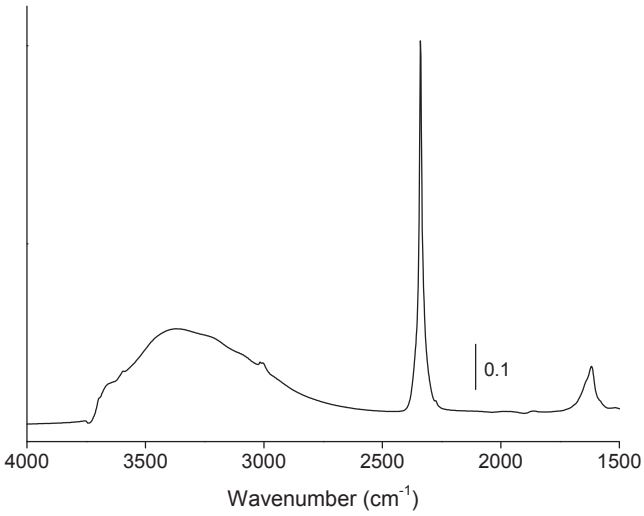

Figure 19. Infrared spectra of methane, carbon dioxide and water adsorbed in Na-ZSM-5 at 35 °C. The partial pressure of the components was 83.9, 16.8 and 0.6 kPa, respectively.

4.3.2 Adsorbed amounts

Adsorbed concentrations of methane, carbon dioxide and water were retrieved from infrared spectra using Equations 4-11. In general, for the mixtures studied in this work, the adsorbed concentrations increased with increasing partial pressure of the respective component and decreased with increasing temperature, as expected. Figure 20 shows adsorbed concentrations of methane and carbon dioxide, respectively, from both binary and ternary mixtures as a function of the mole fraction of carbon dioxide in the gas phase. At lower temperatures (35 and 50 °C), the adsorbed concentrations from ternary mixtures are lower for both methane and carbon dioxide compared to the adsorbed concentrations from binary mixtures at similar partial pressures of methane and carbon dioxide. This was due to water having a higher affinity for the zeolite than both carbon dioxide and methane. Hence, water will be preferably adsorbed leading to a decrease in the adsorbed concentrations of both methane and carbon dioxide in the ternary mixtures compared to the binary mixtures. At higher temperatures (85 and 120 °C), the absorbed concentrations are of the same magnitude for both binary and ternary mixtures indicating that neither methane nor carbon dioxide are significantly affected by the presence of water in the mixture. This could be explained by the overall lower total adsorbed concentrations at higher temperatures leading to a lower dependence on the co-adsorbed species. Further, since water has a higher isosteric heat of adsorption value compared to methane and carbon dioxide, the affinity of water is more affected by the increase in temperature than the other two components. As mentioned earlier, carbon dioxide and water are preferably adsorbed on adsorption sites related to cations or defects like silanol groups (high affinity, low capacity sites). After occupying these sites, carbon dioxide is adsorbed on the pore wall while water molecules tend to form clusters at the polar sites as the partial pressure is increased (low affinity, high capacity sites).

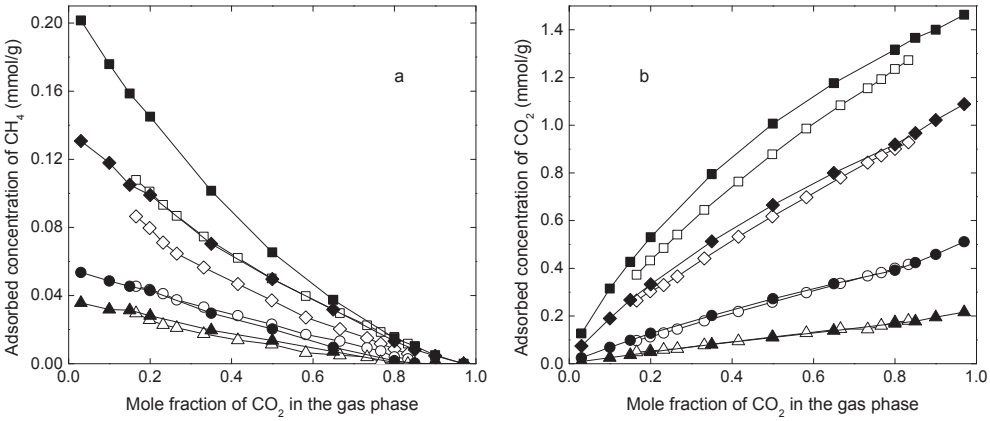

Figure 20. Adsorbed concentrations of methane (a) and carbon dioxide (b) from binary mixtures (filled markers) and ternary mixtures (open markers) at 35 °C (□,■), 50 °C (◊,♦), 85 °C (○,●) and 120 °C (Δ,▲). The lines are only a guide for the eyes.

4.3.3 The Ideal Adsorbed Solution Theory

Predicted values for multicomponent adsorption were determined through the IAST using the single component Langmuir adsorption isotherm parameters (b and q_{sat}) as input. The predicted values were compared to the experimentally determined adsorbed concentrations to assess if the IAST was an accurate model to use for the systems studied.

Figure 21 shows the adsorbed phase mole fractions of methane and carbon dioxide from binary mixtures (Paper II) as a function of the mole fraction of carbon dioxide in the gas phase. Values predicted using the IAST are also included in the figure and are in excellent agreement with the experimental data. This is in accordance with findings previously reported in the literature[15] where it has been shown that the binary adsorption of carbon dioxide and methane in zeolite MFI may accurately be predicted using the IAST. Figures 22 a and b show the adsorbed phase mole fraction of methane and carbon dioxide, respectively, from binary mixtures with water (Paper III) as a function of the mole fraction of water in the gas phase. In general, the values predicted by the IAST (lines) for methane are in reasonably good agreement with the experimental data. At 120 °C, the predicted values deviate slightly from the experimental data which could be an effect of the low amount of adsorbed methane at this temperature. The values predicted by the IAST for carbon dioxide tend to follow the same trend as the experimental data. However, the IAST cannot fully describe the adsorption

behavior of carbon dioxide and water indicating a non-ideal adsorption behavior, which is in agreement with previous reports for zeolites NaX, 5A and 13X.[41, 42] The adsorbed phase mole fractions of methane, carbon dioxide and water from ternary mixtures (Paper IV) as a function of the mole fraction of carbon dioxide in the gas phase are presented in Figures 23 a, b and c, respectively. Again, values predicted using the IAST are included in the figures. The predicted values for methane are in reasonably good agreement with the experimental data with only the highest temperature as an exception. At 120 °C, the IAST is overestimating the amount of adsorbed methane. This deviation was also noticed in binary mixtures of methane and water (Paper III) and could be an effect of the low amount of methane being adsorbed at the highest temperature. Moreover, the predicted values of carbon dioxide and water seem to be following the same trend as the experimental data, but the IAST cannot describe the adsorption behavior of the two components in ternary mixtures. This non-ideal adsorption behavior was also observed for binary mixtures of carbon dioxide and water (Paper III) and is most likely related to the adsorption behavior of water forming clusters and the inability of the dual-site Langmuir model to describe this behavior.

The IAST is a reliable model for predicting the amount adsorbed from binary methane/carbon dioxide mixtures. The non-ideal behavior of mixtures containing water may not be described by the IAST and instead more advanced models like the Real Adsorbed Solution Theory (RAST) or the Vacancy Solution Theory (VST) may be needed to accurately predict the amount of adsorbed carbon dioxide and water. In addition, a single component model accurately describing the adsorption behavior of water in high silica MFI, especially considering cluster formation, should be developed.

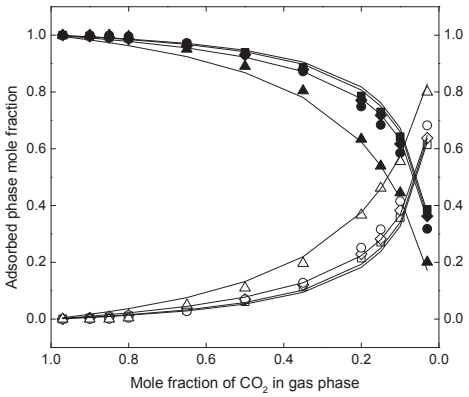

Figure 21. Adsorbed phase mole fraction as a function of carbon dioxide in the gas phase at 35 °C (□,■), 50 °C (◊,♦), 85 °C (○,●) and 120 °C (Δ,▲) using a total pressure of 101.3 kPa. The filled markers represent carbon dioxide, the open markers represent methane and the lines are representing values predicted using the IAST.

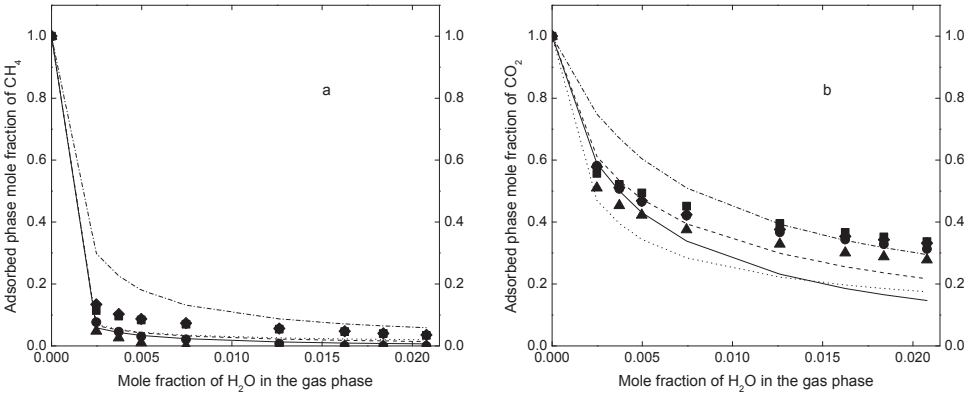

Figure 22. Adsorbed phase mole fraction of methane (a) and carbon dioxide (b) as a function of water in the gas phase at 35 °C (■,–), 50 °C (♦,---), 85 °C (●,···) and 120 °C (▲,-··) using a total pressure of 101.3 kPa. The lines represent values predicted by the IAST.

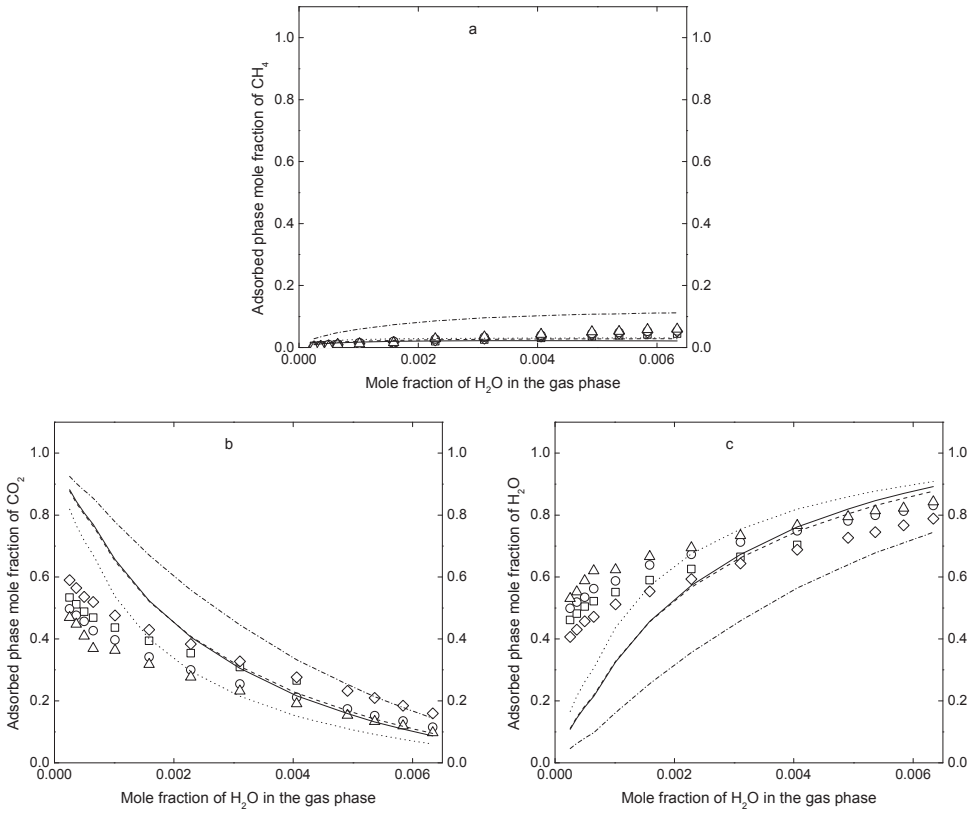

Figure 23. Adsorbed phase mole fraction of methane (a), carbon dioxide (b) and water (c) at 35°C (□,–), 50°C (◊,---), 85°C (○,···) and 120°C (Δ,-·-). The markers represent the experimental data and the lines represent values predicted using the IAST. The total pressure was 101.3 kPa.

4.3.4 Adsorption selectivity

The CO_2/CH_4 adsorption selectivity for various compositions of the gas phase at different temperatures are shown in Figures 24 a and b for both binary and ternary mixtures at low (35 and 50 °C) and high temperatures (85 and 120 °C), respectively. The introduction of water in the methane/carbon dioxide system has a larger effect at lower temperatures where the CO_2/CH_4 adsorption selectivity is slightly higher for ternary mixtures compared to the binary mixtures. This could be an effect of water having a much higher affinity at lower temperatures compared to both methane and carbon dioxide where water is preferentially adsorbed leading to a decrease in the adsorbed concentrations of both the other components, as mentioned before (see Figure 20). The adsorbed concentrations of methane and carbon dioxide were essentially unaffected by the presence of water at higher temperatures (see Figure 20) explaining the similar CO_2/CH_4 adsorption selectivity for binary and ternary mixtures at higher temperatures.

The composition of the gas phase, where the content of methane is the highest, is perhaps of greatest interest since biogas (and many natural gas sources) mainly consists of methane with a carbon dioxide content of 5–30%. The CO_2/CH_4 adsorption selectivity at 35 °C was determined to be 18.3 for a ternary mixture containing 66.6 % methane, 33.3 % carbon dioxide and 0.1 % water and 16.9 for a binary mixture of 65 % methane and 35 % carbon dioxide. The slightly higher selectivity for the ternary mixture can be explained by the higher affinity for water and carbon dioxide compared to methane where methane has difficulties competing with the other components for the adsorption sites. These CO_2/CH_4 adsorption selectivity results imply that the separation of carbon dioxide and water from methane in biogas using a ZSM-5 membrane would be more efficient at lower temperatures, in line with experimental findings.[72]

The CO_2/CH_4 selectivity for an equimolar mixture of carbon dioxide and methane is also of great interest since most of the values reported in the literature are for this gas phase composition. The CO_2/CH_4 adsorption selectivity at 35 °C was determined to be 17.6 for a ternary mixture containing 49.9 % methane, 49.9 % carbon dioxide and 0.2 % water and 15.4 for an equimolar mixture of methane and carbon dioxide. Again, the selectivity is improved when a small amount of water is present in the mixture. Table 3 shows the values obtained in the present work together with values previously reported in the literature for MFI zeolites. As literature data on adsorption selectivity are scarce, some membrane permeation selectivities are also included for comparison. In general, the

adsorption selectivity is higher compared to the permeation selectivity of membranes (it should be noted that the definition of selectivity differs between the two processes, where $\alpha_{perm}=\alpha_{ads}\times\alpha_{diff}$)[15, 73], but also the Si/Al ratio is a contributing factor. Higher aluminum content generally results in a higher selectivity towards carbon dioxide.

The relatively high selectivity values obtained in this study indicate that the separation of carbon dioxide from methane may be efficient using a high-silica Na-ZSM-5 membrane.

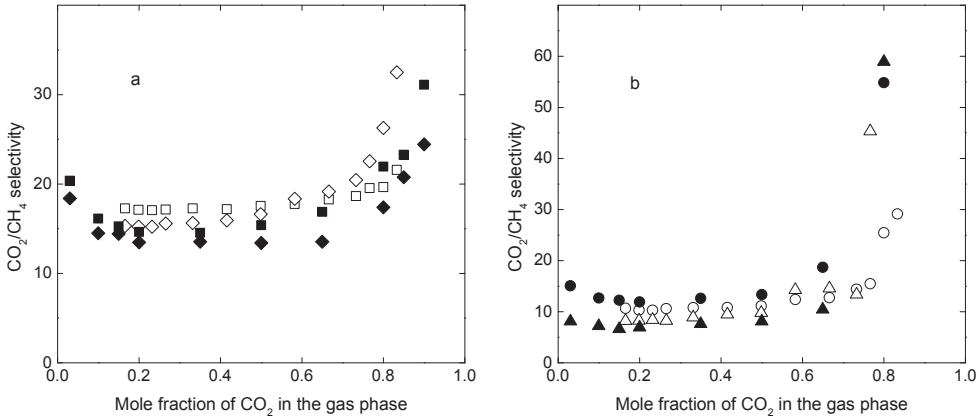

Figure 24. CO_2/CH_4 selectivity from binary (filled markers) and ternary (open markers) mixtures at a total pressure of 101.3 kPa. Figure (a) shows the selectivity at low temperatures, 35 °C (□,■) and 50 °C (◊,♦), and figure (b) shows the selectivity at high temperatures, 85 °C (○,●) and 120 °C (Δ,▲).

Table 3. CO_2/CH_4 selectivity, in an equimolar mixture, obtained in the present work presented together with values reported in the literature.

Zeolite	Si/Al ratio	Adsorbent/ membrane	Temperature (°C)	CO_2/CH_4 selectivity	Reference
Na-ZSM-5	130	adsorbent	35	15.4	Present work (binary mixture)
Na-ZSM-5	130	adsorbent	35	17.6	Present work (ternary mixture)
silicalite-1	-	adsorbent	40	7	Li and Tezel[39]
silicalite-1	-	membrane	25	2.23	Othman *et al.*[74]
Na-ZSM-5	25	membrane	25	6.28	
silicalite-1	-	membrane	r. t.	2	Poshusta *et al.*[75]
H-ZSM-5	-	membrane	r. t.	5.5	
H-ZSM-5	139	membrane	4	4.5	Sandström *et al.*[72]
MFI	-	membrane	27	2.2	Krishna and van Baten[15]

Moreover, a limited number of adsorption experiments studying binary butanol/water mixtures in silicalite-1 were carried out in Paper V. At 35 °C, a butanol/water adsorption selectivity as high as 107 was obtained, illustrating that silicalite-1 may be a promising material for recovering butanol from ABE fermentation broths, however this should system should be studied in greater detail.

Chapter 5 Conclusions

In the present work, single component adsorption of methane, carbon dioxide and water has been studied using ATR-FTIR spectroscopy and the method has successfully been further used to study multicomponent adsorption of these components.

Infrared spectra of adsorbed methane, carbon dioxide and water from single gas experiments showed distinct, non-overlapping bands for the adsorbed species, which made it possible to distinguish each adsorbed species when adsorbed from multicomponent mixtures.

From the recorded infrared spectra, the adsorbed concentrations of the studied components were determined. The Langmuir model was fitted to the adsorption data from the single component adsorption experiments and the model matched the experimental data very well. Further, the fitted Langmuir parameters obtained agreed with values previously reported in the literature.

The IAST was used to predict the adsorbed concentrations of methane, carbon dioxide and water in multicomponent mixtures using the single component adsorption isotherm parameters as input and the predicted values were compared to the experimental data. The IAST accurately predicted the amount of adsorbed methane and carbon dioxide from binary methane/carbon dioxide mixtures. For the amount of adsorbed methane from binary methane/water mixtures and ternary mixtures, the IAST predicted the values fairly well. However, for mixtures containing carbon dioxide and water (both binary and ternary mixtures), the IAST could not fully describe the adsorption behavior of the two components, indicating a non-ideal behavior. The IAST is therefore not recommended and other models, such as the Real Adsorbed Solution Theory

(RAST) or the Vacancy Solution Theory (VST), may be needed to accurately predict the amount of adsorbed carbon dioxide and water. In addition, a single component model accurately describing the adsorption behavior of water in high silica MFI, especially considering cluster formation, should be developed.

The CO_2/CH_4 selectivity was studied for various gas compositions and temperatures. In general, the selectivity was increasing with decreasing temperature indicating a more efficient separation of carbon dioxide from biogas at lower temperatures. The CO_2/CH_4 selectivity was higher for ternary mixtures compared to binary mixtures indicating that a small amount of water enhances the selectivity. The relatively high CO_2/CH_4 selectivity obtained in the present work compared to the literature indicates that the separation may be efficient using a high-silica Na-ZSM-5 membrane. It was also shown that silicalite-1 is butanol selective from butanol/water mixtures indicating that this zeolite may be efficient for recovery of butanol from dilute water mixtures.

Chapter 6 Future work

The present work has shown that ATR-FTIR spectroscopy is an efficient method to study both single and multicomponent adsorption of methane, carbon dioxide and water in MFI zeolites. The adsorption study, however, was only referring to the equilibrium mechanism. Therefore, to get a complete picture of the adsorption behavior, the kinetics should be studied as well.

For mixtures containing carbon dioxide and water, where the IAST could not fully describe the adsorption behavior, the Real Adsorbed Solution Theory or the Vacancy Solution Theory could be used. It would be interesting to compare the models to evaluate which model is more accurate when predicting the amount of adsorbed carbon dioxide and water in the zeolites. A single component model which accurately describes the adsorption behavior of water in high silica MFI, especially considering cluster formation, should be developed.

It would also be interesting to study the adsorption of methane, carbon dioxide and water in ZSM-5 exchanged with a different cation, for example barium, as well as zeolites synthesized using the fluoride route with less internal defects instead of the hydroxide route.

Furthermore, the separation of other components typically found in biogas and natural gas, such as hydrogen sulfide or heavier hydrocarbons, from methane would be interesting to study.

References

(1) Karl, T. R.; Trenberth, K. E. Modern Global Climate Change. *Science* **2003**, *302*, 1719-1723.

(2) Hubbert, M. K. Energy from Fossil Fuels. *Science* **1949**, *109*, 103-109.

(3) Hubbert, M. K. In *Nuclear energy and the fossil fuels;* American Petroleum Institute: 1956; , pp 1-40.

(4) de Almeida, P.; Silva, P. D. The Peak of Oil Production-Timings and Market Recognition. *Energy Policy* **2009**, *37*, 1267-1276.

(5) Sorrell, S.; Miller, R.; Bentley, R.; Speirs, J. Oil Futures: A Comparison of Global Supply Forecasts. *Energy Policy* **2010**, *38*, 4990-5003.

(6) Sorrell, S.; Speirs, J.; Bentley, R.; Brandt, A.; Miller, R. Global Oil Depletion: A Review of the Evidence. *Energy Policy* **2010**, *38*, 5290-5295.

(7) Aftabuzzaman, M.; Mazloumi, E. Achieving Sustainable Urban Transport Mobility in Post Peak Oil Era. *Transp. Policy* **2011**, *18*, 695-702.

(8) Brown, R. C. In *Biorenewable resources : engineering new products from agriculture;* Iowa State Press: Ames, Iowa, 2003; .

(9) Abdeshahian, P.; Dashti, M. G.; Kalil, M. S.; Yusoff, W. M. W. Production of Biofuel using Biomass as a Sustainable Biological Resource. *Biotechnology* **2010**, *9*, 274-282.

(10) Maddox, I. S.; Steiner, E.; Hirsch, S.; Wessner, S.; Gutierrez, N. A.; Gapes, J. R.; Schuster, K. C. The Cause of "Acid Crash" and "Acidogenic Fermentations" during the Batch Acetone-Butanol-Ethanol (ABE-) Fermentation Process. *J. Mol. Microbiol. Biotechnol.* **2000**, *2*, 95-100.

(11) Baker, R. W. Future Directions of Membrane Gas Separation Technology. *Ind. Eng. Chem. Res.* **2002**, *41*, 1393-1411.

(12) Kassaee, M. H.; Sholl, D. S.; Nair, S. Preparation and Gas Adsorption Characteristics of Zeolite MFI Crystals with Organic-Functionalized Interiors. *J. Phys. Chem. C* **2011**, *115*, 19640-19646.

(13) Lindmark, J.; Hedlund, J. Modification of MFI Membranes with Amine Groups for Enhanced CO(2) Selectivity. *J. Mater. Chem.* **2010**, *20*, 2219-2225.

(14) Krishna, R.; van-Baten, J. M. Segregation Effects in Adsorption of CO2-Containing Mixtures and their Consequences for Separation Selectivities in Cage-Type Zeolites. *Sep. Purif. Technol.* **2008**, *61*, 414-423.

(15) Krishna, R.; van Baten, J. M. Using Molecular Simulations for Screening of Zeolites for Separation of CO2/CH4 Mixtures. *Chem. Eng. J.* **2007**, *133*, 121-131.

(16) Harlick, P. J. E.; Tezel, F. H. Adsorption of Carbon Dioxide, Methane and Nitrogen: Pure and Binary Mixture Adsorption for ZSM-5 with SiO2/Al2O3 Ratio of 280. *Sep. Purif. Technol.* **2003**, *33*, 199-210.

(17) Garcia-Perez, E.; Parra, J. B.; Ania, C. O.; Garcia-Sanchez, A.; van-Baten, J. M.; Krishna, R.; Dubbeldam, D.; Calero, S. A Computational Study of CO2, N-2, and CH4 Adsorption in Zeolites. *Adsorption* **2007**, *13*, 469-476.

(18) Kogel, J. E. In *Industrial minerals and rocks : commodities, markets, and uses;* Society for Mining, Metallurgy, and Exploration,cop.: Littleton, Colorado, 2006; Vol. 7th ed.

(19) Satterfield, C. N. In *Heterogeneous catalysis in industrial practice;* Krieger Publ. Company: Malabar, Fla, 1996; Vol. 2nd ed.

(20) Breck, D. W. In *Zeolite molecular sieves : structure, chemistry, and use;* Krieger Publ. Company: Malabar, Fla., 1984; .

(21) Zdravkov, B. D.; Cermak, J. J.; Sefara, M.; Janku, J. Pore Classification in the Characterization of Porous Materials: A Perspective. *Cent. Eur. J. Chem.* **2007**, *5*, 385-395.

(22) International Zeolite Association (IZA) http://www.iza-online.org.

(23) Trzpit, M.; Soulard, M.; Patarin, J.; Desbiens, N.; Cailliez, F.; Boutin, A.; Demachy, I.; Fuchs, A. H. The Effect of Local Defects on Water Adsorption in Silicalite-1 Zeolite: A Joint Experimental and Molecular Simulation Study. *Langmuir* **2007**, *23*, 10131-10139.

(24) Costa, E.; de Lucas, A.; Uguina, A. M.; Ruiz, J. C. Synthesis of 4A Zeolite from Calcined Kaolins for use in Detergents. *Ind. Eng. Chem. Res.* , *27*, 1291-1296.

(25) Do, D. D. In *Adsorption analysis: equilibria and kinetics;* Imperial College Press: London, 1998; .

(26) Brunauer, S.; Deming, L. S.; Deming, W. E.; Teller, E. On a Theory of the Van Der Waals Adsorption of Gases. *J. Am. Chem. Soc.* **1940**, *62*, 1723-1732.

(27) Ruthven, D. M. In *Principles of adsorption and adsorption processes;* Wiley-Interscience publication; Wiley: New York, 1984; .

(28) Choudhary, V. R.; Mayadevi, S. Adsorption of Methane, Ethane, Ethylene, and Carbon Dioxide on Silicalite-I. *Zeolites* **1996**, *17*, 501-507.

(29) Sun, M. S.; Shah, D. B.; Xu, H. H.; Talu, O. Adsorption Equilibria of C-1 to C-4 Alkanes, CO2, and SF6 on Silicalite. *J. Phys. Chem. B* **1998**, *102*, 1466-1473.

(30) Dunne, J. A.; Mariwala, R.; Rao, M.; Sircar, S.; Gorte, R. J.; Myers, A. L. Calorimetric Heats of Adsorption and Adsorption Isotherms .1. O-2, N-2, Ar, CO2, CH4, C2H6 and SF6 on Silicalite. *Langmuir* **1996**, *12*, 5888-5895.

(31) Dunne, J. A.; Rao, M.; Sircar, S.; Gorte, R. J.; Myers, A. L. Calorimetric Heats of Adsorption and Adsorption Isotherms .2. O-2, N-2, Ar, CO2, CH4, C2H6, and SF6 on NaX, H-ZSM-5, and Na-ZSM-5 Zeolites. *Langmuir* **1996**, *12*, 5896-5904.

(32) Bao, Z.; Yu, L.; Dou, T.; Gong, Y.; Zhang, Q.; Ren, Q.; Lu, X.; Deng, S. Adsorption Equilibria of CO(2), CH(4), N(2), O(2), and Ar on High Silica Zeolites. *J. Chem. Eng. Data* **2011**, *56*, 4017-4023.

(33) Wirawan, S. K.; Creaser, D. CO2 Adsorption on Silicalite-1 and Cation Exchanged ZSM-5 Zeolites using a Step Change Response Method. *Microporous Mesoporous Mater.* **2006**, *91*, 196-205.

(34) Jentys, A.; Warecka, G.; Derewinski, M.; Lercher, J. Adsorption of Water on ZSM5 Zeolites. *J. Phys. Chem.* **1989**, *93*, 4837-4843.

(35) Olson, D. H.; Haag, W. O.; Borghard, W. S. Use of Water as a Probe of Zeolitic Properties: Interaction of Water with HZSM-5. *Microporous Mesoporous Mater.* **2000**, *35-36*, 435-446.

(36) Zhang, K.; Lively, R. P.; Noel, J. D.; Dose, M. E.; McCool, B. A.; Chance, R. R.; Koros, W. J. Adsorption of Water and Ethanol in MFI-Type Zeolites. *Langmuir* **2012**, *28*, 8664-8673.

(37) Krishna, R.; van Baten, J. M.; Garcia-Perez, E.; Calero, S. Diffusion of CH4 and CO2 in MFI, CHA and DDR Zeolites. *Chem. Phys. Lett.* **2006**, *429*, 219-224.

(38) Krishna, R.; van Baten, J. M.; Garcia-Perez, E.; Calero, S. Incorporating the Loading Dependence of the Maxwell-Stefan Diffusivity in the Modeling of CH4 and CO2 Permeation Across Zeolite Membranes. *Ind. Eng. Chem. Res.* **2007**, *46*, 2974-2986.

(39) Li, P.; Tezel, F. H. Pure and Binary Adsorption Equilibria of Methane and Carbon Dioxide on Silicalite. *Sep. Sci. Technol.* **2007**, *42*, 3131-3153.

(40) Harlick, P. J. E.; Tezel, F. H. Adsorption of Carbon Dioxide, Methane, and Nitrogen: Pure and Binary Mixture Adsorption by ZSM-5 with SiO2/Al2O3 Ratio of 30. *Sep. Sci. Technol.* **2002**, *37*, 33-60.

(41) Rege, S. U.; Yang, R. T. A Novel FTIR Method for Studying Mixed Gas Adsorption at Low Concentrations: H2O and CO2 on NaX Zeolite and Gamma-Alumina. *Chem. Eng. Sci.* **2001**, *56*, 3781-3796.

(42) Wang, Y.; LeVan, M. D. Adsorption Equilibrium of Binary Mixtures of Carbon Dioxide and Water Vapor on Zeolites 5A and 13X. *J. Chem. Eng. Data* **2010**, *55*, 3189-3195.

(43) Brandani, F.; Ruthven, D. M. The Effect of Water on the Adsorption of CO_2 and C_3H_8 on Type X Zeolites. *Ind. Eng. Chem. Res.* **2004**, *43*, 8339-8344.

(44) Krishna, R.; van Baten, J. M. Hydrogen Bonding Effects in Adsorption of Water-Alcohol Mixtures in Zeolites and the Consequences for the Characteristics of the Maxwell-Stefan Diffusivities. *Langmuir* **2010**, *26*, 10854-10867.

(45) Joos, L.; Swisher, J. A.; Smit, B. Molecular Simulation Study of the Competitive Adsorption of H_2O and CO_2 in Zeolite 13X. *Langmuir* **2013**, *29*, 15936-15942.

(46) Müller, E. A.; Hung, F. R.; Gubbins, K. E. Adsorption of Water Vapor-Methane Mixtures on Activated Carbons. *Langmuir* **2000**, *16*, 5418-5424.

(47) Ari, M. U.; Ahunbay, M. G.; Yurtsever, M.; Erdem-Senatalar, A. Molecular Dynamics Simulation of Water Diffusion in MFI-Type Zeolites. *J. Phys. Chem. B* **2009**, *113*, 8073-8079.

(48) Griffiths, P. R.; de Haseth, J. A. In *Fourier transform infrared spectrometry;* Wiley: Hoboken, 2007; Vol. 2nd ed.

(49) Colthup, N. B.; Daly, L. H.; Wiberley, S. E. In *Introduction to Infrared and Raman Spectroscopy;* Academic Press: Boston, 1990; Vol. 3rd ed.

(50) Mirabella, F. M., Ed.; In *Internal Reflection Spectroscopy : Theory and Applicatons;* Marcel Dekker, Inc.: New York, 1993; Vol. 15.

(51) Moulin, B.; Oliviero, L.; Bazin, P.; Daturi, M.; Costentin, G.; Mauge, F. How to Determine IR Molar Absorption Coefficients of Co-Adsorbed Species? Application to Methanol Adsorption for Quantification of MgO Basic Sites. *Phys. Chem. Chem. Phys.* **2011**, *13*, 10797-10807.

(52) Tompkins, H. G. The Physical Basis for Analysis of the Depth of Absorbing Species using Internal Reflection Spectroscopy. *Appl. Spectrosc.* **1974**, *28*, 335-341.

(53) Myers, A. L.; Prausnitz, J. M. Thermodynamics of Mixed-Gas Adsorption. *AIChE J.* **1965**, *11*, 121-127.

(54) Wang, Z.; Grahn, M.; Larsson, M. L.; Holmgren, A.; Sterte, J.; Hedlund, J. Zeolite Coated ATR Crystal Probes. *Sens. Actuators, B* **2006**, *115*, 685-690.

(55) Zhou, M.; Korelskiy, D.; Ye, P.; Grahn, M.; Hedlund, J. A Uniformly Oriented MFI Membrane for Improved CO2 Separation. *Angew. Chem. Int. Ed.* **2014**, *53*, 3492-3495.

(56) Zhou, M.; Grahn, M.; Zhou, H.; Holmgren, A.; Hedlund, J. The Facile Assembly of Nanocrystals by Optimizing Humidity. *Chem. Commun.* **2014**, *50*, 14261-14264.

(57) Li, X.; Peng, Y.; Wang, Z.; Yan, Y. Synthesis of Highly B-Oriented Zeolite MFI Films by Suppressing Twin Crystal Growth during the Secondary Growth. *CrystEngComm* **2011**, *13*, 3657-3660.

(58) Bazin, P.; Alenda, A.; Thibault-Starzyk, F. Interaction of Water and Ammonium in NaHY Zeolite as Detected by Combined IR and Gravimetric Analysis (AGIR). *Dalton Trans.* **2010**, *39*, 8432-8436.

(59) Hedlund, J.; Sterte, J.; Anthonis, M.; Bons, A.; Carstensen, B.; Corcoran, N.; Cox, D.; Deckman, H.; De Gijnst, W.; De Moor, P.; Lai, F.; McHenry, J.; Mortier, W.; Reinoso, J.; Peters, J. High-Flux MFI Membranes. *Microporous Mesoporous Mater.* **2002**, *52*, 179-189.

(60) Sandström, L.; Lindmark, J.; Hedlund, J. Separation of Methanol and Ethanol from Synthesis Gas using MFI Membranes. *J. Membr. Sci.* **2010**, *360*, 265-275.

(61) Scarano, D.; Bertarione, S.; Spoto, G.; Zecchina, A.; Arean, C. FTIR Spectroscopy of Hydrogen, Carbon Monoxide, and Methane Adsorbed and Co-Adsorbed on Zinc Oxide. *Thin Solid Films* **2001**, *400*, 50-55.

(62) Chen, L.; Lin, L.; Xu, Z.; Zhang, T.; Xin, Q.; Ying, P.; Li, G.; Li, C. Fourier Transform-Infrared Investigation of Adsorption of Methane and Carbon Monoxide on HZSM-5 and Mo/HZSM-5 Zeolites at Low Temperature. *J. Catal.* **1996**, *161*, 107-114.

(63) Zou, X.; Bazin, P.; Zhang, F.; Zhu, G.; Valtchev, V.; Mintova, S. Ethanol Recovery from Water using Silicalite-1 Membrane: An Operando Infrared Spectroscopic Study. *ChemPlusChem* **2012**, *77*, 437-444.

(64) Zhu, W.; Hrabanek, P.; Gora, L.; Kapteijn, F.; Moulijn, J. A. Role of Adsorption in the Permeation of CH4 and CO2 through a Silicalite-1 Membrane. *Ind. Eng. Chem. Res.* **2006**, *45*, 767-776.

(65) Rees, L. V. C.; Brückner, P.; Hampson, J. Sorption of N2, CH4 and CO2 in Silicalite-1. *Gas Sep. Purif.* **1991**, *5*, 67-75.

(66) Golden, T. C.; Sircar, S. Gas Adsorption on Silicalite. *J. Colloid Interface Sci.* **1994**, *162*, 182-188.

(67) van den Broeke, L. J. P.; Bakker, W. J. W.; Kapteijn, F.; Moulijn, J. A. Transport and Separation Properties of a Silicalite-1 Membrane - I. Operating Conditions. *Chem. Eng. Sci.* **1999**, *54*, 245-258.

(68) Krishna, R.; van Baten, J. M. Highlighting Pitfalls in the Maxwell-Stefan Modeling of Water-Alcohol Mixture Permeation Across Pervaporation Membranes. *J. Membr. Sci.* **2010**, *360*, 476-482.

(69) Puibasset, J.; Pellenq, R. J. -. Grand Canonical Monte Carlo Simulation Study of Water Adsorption in Silicalite at 300 K. *J. Phys. Chem. B* **2008**, *112*, 6390-6397.

(70) Bolis, V.; Busco, C.; Ugliengo, P. Thermodynamic Study of Water Adsorption in High-Silica Zeolites. *J. Phys. Chem. B* **2006**, *110*, 14849-14859.

(71) Mulgundmath, V. P.; Tezel, F. H.; Saatcioglu, T.; Golden, T. C. Adsorption and Separation of CO2/N2 and CO2/CH4 by 13X Zeolite. *Can. J. Chem. Eng.* **2012**, *90*, 730-738.

(72) Sandström, L.; Sjöberg, E.; Hedlund, J. Very High Flux MFI Membrane for CO(2) Separation. *J. Membr. Sci.* **2011**, *380*, 232-240.

(73) Krishna, R.; van Baten, J. M. Investigating the Influence of Diffusional Coupling on Mixture Permeation Across Porous Membranes. *J. Membr. Sci.* **2013**, *430*, 113-128.

(74) Othman, M. R.; Tan, S. C.; Bhatia, S. Separability of Carbon Dioxide from Methane using MFI Zeolite-Silica Film Deposited on Gamma-Alumina Support. *Microporous Mesoporous Mater.* **2009**, *121*, 138-144.

(75) Poshusta, J. C.; Noble, R. D.; Falconer, J. L. Temperature and Pressure Effects on CO2 and CH4 Permeation through MFI Zeolite Membranes. *J. Membr. Sci.* **1999**, *160*, 115-125.

Part II

"No amount of experimentation can ever prove me right;
a single experiment can prove me wrong"

-Albert Einstein

Paper I

Adsorption of CO_2, CH_4 and H_2O in zeolite ZSM-5 studied using in situ ATR-FTIR spectroscopy

Lindsay Ohlin, Philippe Bazin, Frédéric Thibault-Starzyk, Jonas Hedlund and Mattias Grahn

The Journal of Physical Chemistry C

THE JOURNAL OF PHYSICAL CHEMISTRY C

Article

pubs.acs.org/JPCC

Adsorption of CO_2, CH_4, and H_2O in Zeolite ZSM-5 Studied Using In Situ ATR-FTIR Spectroscopy

Lindsay Ohlin,*[,†] Philippe Bazin,[‡] Frédéric Thibault-Starzyk,[‡] Jonas Hedlund,[†] and Mattias Grahn[†]

[†]Chemical Technology, Luleå University of Technology, 971 87 Luleå, Sweden

[‡]Laboratoire Catalyse and Spectrochimie, CNRS-ENSICAEN-Université de Caen, 6 Boulevard Marechal Juin, Caen Cedex 14050, France

Supporting Information

ABSTRACT: Biogas and natural gas are interesting fuels with high H/C ratio. However, these gases frequently contain carbon dioxide and water which lowers the heat value of the gas and may induce corrosion. Therefore, the development of more efficient processes, such as membrane processes and improved adsorbents, for the separation of carbon dioxide and water from biogas and natural gas is of great importance. Zeolite ZSM-5 membranes are promising for this separation which is controlled by the adsorption and diffusion of the different species in the zeolite. Multicomponent adsorption data are therefore required for development of new membrane and adsorption processes. In the present work, the adsorption of water, carbon dioxide, and methane in a Na-ZSM-5 zeolite film at various temperatures was studied by in situ Attenuated Total Reflectance-Fourier Transform Infrared (ATR-FTIR) spectroscopy for the first time. Adsorption isotherms were retrieved from the experimental data and the Langmuir model fitted the isotherms very well. Limiting heat of adsorption was determined from the Henrýs law regime and the values determined agreed well with previously reported data. A few experiments were conducted with multicomponent mixtures and the experimentally determined amounts adsorbed were compared with values predicted by the Ideal Adsorbed Solution Theory (IAST). It was found that for the binary mixture of carbon dioxide and methane there was good agreement between the experimental values and those predicted by the IAST. However, when water was also introduced, the IAST could not fully capture the adsorption behavior of the multicomponent mixture, probably because the adsorbed phase is not ideal. These findings are in line with previous reports for adsorption in zeolites. The multicomponent adsorption behavior of this system will be further investigated in forthcoming work.

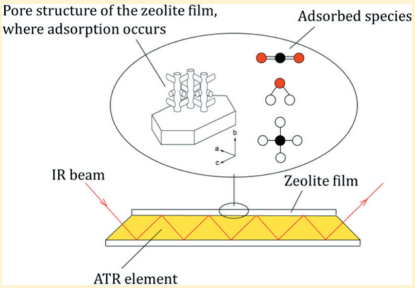

INTRODUCTION

To lower the consumption of traditional fuels derived from oil, such as gasoline and diesel, biogas and natural gas are interesting alternatives. Biogas is a renewable resource that is produced by anaerobic degradation of biomass, resulting in a mixture of carbon dioxide and methane (usually 60−70%).[1,2] In natural gas, methane is the main component (usually 80−90%) along with contaminants such as water and carbon dioxide.[3,4]

There are two main reasons for the removal of carbon dioxide and water from biogas and natural gas. First of all, from an economical aspect, there is a desire to lower the cost for the transportation of undesired gases. Second, the heat value of the gas decreases in the presence of inert species and to increase the heat value of biogas and natural gas, removal of carbon dioxide and water is desired. Adsorption or membrane based processes have been proposed as interesting alternatives for this separation. Among the different adsorbent or membrane materials available, zeolites have received much attention in the scientific literature due to its great potential.[5−8]

A zeolite is a microporous, crystalline solid with a well-defined structure of which the framework is based on silicon, aluminum, and oxygen.[9] The material is unique due to its uniform micropores which give the zeolites the characteristics of separating molecules based on their sizes,[10] shape, and polarity.[9]

Silicalite-1 and ZSM-5 are two forms of the zeolite type MFI where silicalite-1 is a pure silica analogue of ZSM-5. Silicalite-1 does not contain any aluminum, it lacks counterbalancing cations and thus ion-exchange capabilities, and it is classified as a molecular sieve rather than a zeolite. The lack of aluminum in silicalite-1 also makes it more hydrophobic compared to ZSM-5.[11]

During the last ten years, there has been a significant amount of research focusing on the usage of zeolites for carbon dioxide and methane separation by, e.g., membrane and adsorption technologies.[12−15] Recently, our group has demonstrated very effective separation of CO_2 from synthesis gas using MFI membranes.[16] Adsorption of carbon dioxide and methane in

Received: April 15, 2013
Revised: July 3, 2013
Published: July 8, 2013

   dx.doi.org/10.1021/jp4037183 | J. Phys. Chem. C 2013, 117, 16972−16982

MFI zeolites is fairly well studied whereas adsorption of water has been less investigated. Choudhary et al.[17] studied single gas adsorption of carbon dioxide and methane on silicalite-1 at 32 and 80 °C using gravimetry. The results showed that the Langmuir isotherm model fits the experimental data for carbon dioxide and the Dubinin−Polanyi equation fits for methane at 32 °C. At 80 °C, the Freundlich equation fits the experimental data for both of the analyzed gases. An isosteric heat of adsorption of −20 kJ/mol was reported for carbon dioxide and −27.5 kJ/mol for methane. Sun et al.[18] also used gravimetry to study single gas adsorption of carbon dioxide and methane in silicalite-1. The adsorption isotherms for both gases were of Type 1 in the Brunauer classification and the Virial equation was fitted to the isotherm data. The isosteric heats of adsorption for carbon dioxide and methane were reported to be approximately −28 and −20 kJ/mol, respectively. Dunne et al.[19,20] studied single gas adsorption of carbon dioxide and methane in silicalite-1, H-ZSM-5 (Si/Al = 30), and Na-ZSM-5 (Si/Al = 30) using gravimetry. The isosteric heat of adsorption of carbon dioxide was −27 kJ/mol in silicalite-1, 38 kJ/mol in H-ZSM-5, and −50 kJ/mol in Na-ZSM-5, which shows an increase in the isosteric heat of adsorption with increasing aluminum content and a rather strong dependency on the type of counterion. The choice of counterion also affects the isosteric heat of adsorption for methane, which was reported to be −21 kJ/mol in silicalite-1 and −27.3 kJ/mol in Na-ZSM-5 showing a slight increase with increasing aluminum content.

Olson et al.[21] used thermogravimetry to study single gas adsorption of water in H-ZSM-5 materials of various Si/Al ratios. The adsorption isotherms were of Freundlich type for H-ZSM-5 materials having a low Si/Al ratio and of Type 6 (according to the Brunauer classification) character for high Si/Al ratios. An isosteric heat of adsorption of water of −113 kJ/mol was reported for a Si/Al ratio of 38 and −75 kJ/mol for a Si/Al ratio of 250 showing that the isosteric heat of adsorption is increasing with increasing aluminum content. Bolis et al.[22] studied single gas adsorption of water in silicalite-1 and H-ZSM-5 using microcalorimetry. The isosteric heat of adsorption was reported to be in the range of 61−68 kJ/mol for silicalite-1 and in the −69 to −84 kJ/mol region for H-ZSM-5 (Si/Al = 3.8) showing a slightly higher value for the aluminum containing material. Our group has also studied adsorption of water and hydrocarbons in silicalite-1 films using spectroscopic ellipsometry.[23]

García-Pérez et al.[13] investigated the adsorption properties of carbon dioxide and methane in different all silica zeolites for both single and binary mixtures using molecular simulations. At the conditions studied, the adsorption of carbon dioxide was always favored but to what extent was highly dependent on zeolite structure and bulk gas consumption. Harlick et al.[14] studied the adsorption of carbon dioxide and methane in high silica H-ZSM-5 and used the IAST to predict the adsorbed loadings from binary mixtures. It was concluded that the IAST cannot fully predict the binary adsorption behavior. However, from the models tested, it gave the best fit to the experimental data. Krishna and van Baten[6] used Grand Canonical Monte Carlo and molecular dynamics simulations when studying the adsorption behavior of carbon dioxide and methane in MFI. The IAST was used to predict loadings in the mixture. It was reported that the IAST fitted the simulated data very well. Bao et al.[15] compared the adsorption of carbon dioxide and methane in ZSM-5 and silicalite-1 by volumetric measurements showing that ZSM-5 has a higher affinity for carbon dioxide than methane. Our group has previously shown that even small differences in the Si/Al ratio in MFI membranes affect the separation performance for hydrocarbon isomers.[24]

Although some data may be found in literature, experimental data on multicomponent adsorption in zeolites still remain scarce. Our group has developed a method based on ATR-FTIR spectroscopy for studies of adsorption in zeolites and reported single component adsorption of *n*-hexane and *p*-xylene in silicalite-1 films.[25,26] However, the method allows adsorbed concentrations from multicomponent mixtures to be retrieved from infrared spectra.

In this work, we use the ATR-FTIR technique to study the adsorption of water, carbon dioxide, and methane in a low alumina Na-ZSM-5 zeolite film. From the single component data we used the IAST to predict the amount adsorbed from a multicomponent mixture and the predicted values are compared to experimental data on multicomponent adsorption.

EXPERIMENTAL SECTION

Synthesis. A zeolite ZSM-5 (Si/Al = 130) film was prepared on a trapezoidal ZnS crystal (50 × 20 × 2 mm, 45° cut edges, Spectral systems) using a seeding method. This particular Si/Al ratio was chosen as it is the typical composition of the zeolite membranes produced by our group.[27,28] Details of the film preparation procedure have been given elsewhere[11] and only a short summary of the procedure is given here. Prior to synthesis, all glass and plastic ware were rinsed in a 4% HF aqueous solution. The ZnS crystal was cleaned by immersing it in acetone (VWR, 99.9%), ethanol (VWR, 99%), and distilled water while sonicating for 10 min in each solution. After cleaning, the ZnS crystal was treated with an aqueous solution of cationic polymer to render the surface positively charged. Thereafter, the crystal was immersed in a suspension of 50 nm silicalite-1 crystals for about 5 min and then rinsed in 0.1 M ammonia solution, which resulted in a monolayer of silicalite-1 seed crystals on the ZnS crystal surface. Subsequently, the ZnS crystal was kept for 48 h in a synthesis solution with a molar composition of $3TPAOH{:}0.1Al_2O_3{:}0.4NaO_2{:}25SiO_2{:}1534H_2O{:}100EtOH$. Note that the Si/Al ratio in the synthesis mixture is 125, which results in a Si/Al ratio of 130 in the film, as will be shown below. The synthesis solution was heated under reflux in an oil bath kept at 100 °C to grow the seed crystals to a continuous zeolite film. After synthesis, the sample was cooled to room temperature and rinsed with a 0.1 M ammonia solution. The sample was subsequently rinsed with distilled water and dried at 50 °C overnight. Thereafter, the film was calcined at 500 °C for 4 h with a heating and cooling rate of 0.8 deg/min to remove the template molecules from the pore system of the zeolite.[11,29]

Instrumentation. Scanning electron microscopy (SEM) images was recorded with use of a FEI Magellan 400 field emission extremely high resolution (XHR) microscope and X-ray diffraction data were recorded on a Siemens D5000 X-ray diffractometer (XRD) running in Bragg−Brentano geometry. For determining the molar absorptivities of species adsorbed in zeolite a dedicated instrument for combined analysis by gravimetry and infrared spectroscopy (AGIR) was used.[30] The infrared spectra from the AGIR measurements were recorded on a Nicolet 6700 spectrometer equipped with a mercury, cadmium, and tellurium (MCT) detector by coadding 64 scans at a resolution of 4 cm^{-1} and the mass of the zeolite wafer was recorded simultaneously by a SETSYS-B micro-balance from SETARAM. For the in situ ATR-FTIR measure-

ments, infrared spectra were recorded on a Bruker IFS 66v/S FTIR spectrometer equipped with a deuterated triglycine sulfate (DTGS) detector by coadding 256 scans at a resolution of 4 cm^{-1}.

Determination of Molar Absorptivity for Adsorbates in Zeolite. Molar absorptivities of species adsorbed in the zeolite were determined by using the AGIR setup. In this setup, a microbalance has been adapted to an infrared reactor cell facilitating simultaneous measurements of weight and infrared spectra from solid samples under gas flows and at temperatures up to 500 °C. The setup and procedure for retrieving the molar absorptivities have been described in detail elsewhere.[30] A sample of commercial zeolite powder (ZSM-5, Si/Al =115, Eka Chemicals) was pressed to a self-supported wafer with a weight of 25 mg and an area of 2 cm^2. Prior to measurements, the zeolite was dried at 400 °C under a flow of argon (AIR LIQUIDE, 99.998%) of 25 mL/min. During the adsorption measurements, infrared spectra and mass were recorded continuously until the system reached equilibrium and no changes could be observed. The molar absorbance coefficient, ε (cm/μmol), was determined using Beer−Lamberts law, which gives the relationship between the absorbance of a particular band and the amount of corresponding molecules[31] according to

$$A = \varepsilon \frac{n \cdot d_o}{s \cdot d_g} \tag{1}$$

where A (cm^{-1}) is the integrated absorbance, n (μmol) is the number of molecules adsorbed in the wafer, s (cm^2) is the surface area of the wafer, d_o (cm) is the optical path in the wafer, and d_g (cm) is the geometric thickness of the wafer. Since the optical path and the geometrical thickness are most likely not identical and since the optical path is almost impossible to determine,[32] the sample was assumed to act as an isotropic scatter, which means that the optical path is twice that of the geometrical thickness.

Adsorption Experiments. The ATR crystal was mounted in a steel flow cell connected to a gas delivery system; the system and the ATR cell have been described in detail elsewhere.[33] Prior to measurements, the zeolite film was dried overnight by heating the cell to 300 °C with use of a heating and cooling rate of 0.9 deg/min while flowing helium (AGA, 99.999%) through the cell to remove any adsorbed species from the zeolite pores. After drying, the ATR cell was mounted into the spectrometer equipped with a Specac vertical ATR attachment with a 45° angle of incidence, without disconnecting the helium flow to the cell. After mounting the cell, a background spectrum of the dried film under a flow of helium was recorded. The adsorption measurements of water (distilled water), carbon dioxide (AGA, 99.995%), and methane (AGA, 99.9995%) were performed by stepswise increasing the partial pressure of the adsorbate in the helium carrier gas with a total pressure of 1 atm. At each partial pressure, infrared spectra were recorded continuously until the system reached equilibrium.

Theory. *Concentration of the Adsorbate.* The procedure for calculations of the concentrations of the adsorbate has previously been described by Tompkins[34] and Mirabella[35] and more specifically for adsorption in zeolite films by our group.[25] The amount of absorption per reflection is given by the following equation

$$\frac{A}{N} = \frac{n_{21} {E_0}^2 \varepsilon}{\cos\theta} \int_0^\infty C(z) e^{-2z/d_p}\, dz \tag{2}$$

where A is the integrated absorbance, N is the number of reflections (20 in our case) inside the gasket sealing the cell, and n_{21} is the ratio of the refractive indices of the denser (ATR element) and the rarer (zeolite film) medium. The refractive index of the ZnS crystal is 2.25.[36] Nair and Tsapatsis[37] have reported the refractive index of empty zeolite films in the infrared region and to account for changes in the refractive index with loading, a linear model[25] was used with refractive indices[38] of water, carbon dioxide, and methane of 1.33, 1.35, and 1.3, respectively. Furthermore, E_0 is the amplitude of the electric field at the ATR element/zeolite film interface, ε is determined by eq 1 (note that according to Harrick,[39] the molar absorbance coefficient determined in a transmission experiment, ε_{AGIR}, is related to the molar absorbance coefficient in an ATR experiment, ε_{ATR}, via $\varepsilon_{ATR} = n_{21}\varepsilon_{AGIR}$), θ is the angle of incidence (45°), $C(z)$ is the concentration of the adsorbate in the zeolite, and d_p is the penetration depth. After integration over the zeolite film (it will be shown later that the contribution from the gas phase is negligible) the following equation is obtained

$$\frac{A}{N} = \frac{n_{21} {E_0}^2 d_p C}{2\cos\theta} \varepsilon \left(1 - e^{-2d_a/d_p}\right) \tag{3}$$

where d_a is the thickness of the zeolite film. The penetration depth, d_p, is given by

$$d_p = \frac{\lambda_1}{2\pi(\sin^2\theta - {n_{21}}^2)^{1/2}} \tag{4}$$

where λ_1 is the wavelength of the infrared radiation inside the ATR crystal. The "effective thickness", d_e, of the electric field is defined as

$$d_e = \frac{n_{21} {E_0}^2 d_p}{2\cos\theta} \tag{5}$$

The effective thickness is dependent on the polarization direction of the infrared radiation and was estimated by

$$d_e = \frac{I_{O\parallel}}{I_{O\parallel} + I_{O\perp}} d_{e\parallel} + \frac{I_{O\perp}}{I_{O\parallel} + I_{O\perp}} d_{e\perp} \tag{6}$$

where $I_{O\parallel}$ and $I_{O\perp}$ are the intensity of the radiation without sample for parallel and perpendicular polarized radiation respectively. In this work, the contribution from parallel and perpendicular polarized radiation was 55% and 45%, respectively. Further $d_{e\parallel}$ is the effective thickness for parallel polarization and is determined by

$$d_{e\parallel} = \frac{2 n_{21} d_p \cos\theta (2\sin^2\theta - 2{n_{21}}^2)}{(1 - {n_{21}}^2)[(1 + {n_{21}}^2)\sin^2\theta - {n_{21}}^2]} \tag{7}$$

$d_{e\perp}$ is the effective thickness for perpendicular polarization and is determined according to

$$d_{e\perp} = \frac{2 n_{21} d_p \cos\theta}{1 - (n_{21})^2} \tag{8}$$

By using the molar absorption coefficient determined from the AGIR measurements and by combining eqs 3−8, the concentration of adsorbed species in the zeolite may be calculated.

dx.doi.org/10.1021/jp4037183 | J. Phys. Chem. C 2013, 117, 16972−16982

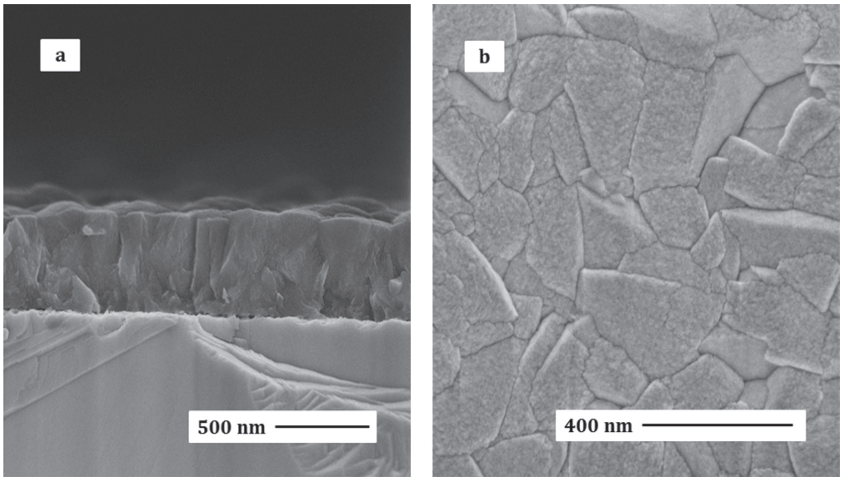

Figure 1. SEM images of the Na-ZSM-5 film synthesized on a ZnS crystal: side (a) and top view (b).

Adsorption Isotherms. Adsorption isotherms were retrieved from the spectral data by integrating the characteristic bands of the adsorbed species. For water, the bending vibration at ca. 1620 cm^{-1} was integrated, for carbon dioxide, the asymmetric stretching vibration at ca. 2350−2339 cm^{-1} was integrated, whereas for methane, the C−H stretching vibration at ca. 3015−3003 cm^{-1} was integrated. The calculated areas were subsequently converted to concentrations of the adsorbate in the zeolite film by using eqs 3−8. The single and dual site Langmuir isotherm models were used for describing the adsorption data

$$q_{tot} = q_1 \frac{b_1 P}{1 + b_1 P} \tag{9}$$

$$q_{tot} = q_1 \frac{b_1 P}{1 + b_1 P} + q_2 \frac{b_2 P}{1 + b_2 P} \tag{10}$$

where q_1 and q_2 are the saturation concentrations of the sites (mmol/g), b is the Langmuir adsorption coefficient (Pa^{-1}), and P is the partial pressure (Pa) of the adsorbate in the gas phase. The subscribed numbers represents the adsorption sites. The heat of adsorption, ΔH, were determined using the vaṅt Hoff equation

$$\ln b = -\frac{\Delta H}{RT} + \frac{\Delta S}{R} \tag{11}$$

where R is the gas constant, T is the temperature, and ΔS is the entropy change upon adsorption.

Ideal Adsorbed Solution Theory (IAST). Myers and Prausnitz[40] proposed that the IAST, based on Gibbs adsorption isotherm, provides a link between single-component and multicomponent adsorption. The IAST is similar to Raoult's law in vapor−liquid equilibrium according to

$$P_i = P_i^0(\pi_i) x_i \tag{12}$$

where P_i^0 is the pure component hypothetical pressure which yields the same spreading pressure as that of the mixture, π_i is the spreading pressure of component i in the adsorbed phase, and x_i is the adsorbed molar fraction. The reduced spreading pressures, at the equilibrium, must be the same for each component and the mixture

$$\pi_i^* = \frac{\pi_i}{RT} = \int_0^{P_i^0} \frac{n_i^0(P)}{P} \, dP \quad i = 1, 2, 3, ..., N \tag{13}$$

$$\pi_1^* = \pi_2^* = ... = \pi_N^* = \pi^* \tag{14}$$

where $n_i^0(P)$ is the pure component equilibrium capacity. By assuming ideal mixing at constant T and π, the total amount adsorbed is

$$\frac{1}{n_t} = \sum_{i=1}^{N} \left[\frac{x_i}{n_i^0(P_i^0)} \right] \tag{15}$$

with the constraint

$$\sum_{i=1}^{N} x_i = 1 \tag{16}$$

In the present work, the IAST has been used to predict the adsorbed amounts from multicomponent mixtures by using the determined single component isotherm parameters as input.

RESULTS AND DISCUSSION

Film Characterization. Representative SEM images of a zeolite coated ATR crystal are shown in Figure 1. The film is polycrystalline and continuous with a thickness of about 550 nm as shown in part a. Since the film is polycrystalline, grain boundaries are off course observed between all grains, but no defects such as cracks or pinholes are observed as shown in part b. The top surface of the film is very clean and no sediments of crystals formed in the bulk of the synthesis mixture during film growth were detected by SEM. The zeolite coated ATR crystal was also analyzed by XRD to verify the phase of the zeolite film and the pattern is shown in Figure 2. The peaks marked with an asterisk emanate from the MFI zeolite film and peaks marked with an open circle emanate from the ZnS crystal. The vertical lines represent the pattern 42−24, recorded for calcined randomly oriented ZSM-5 crystals from the ICDD database. The excellent agreement between the observed peaks and the

dx.doi.org/10.1021/jp4037183 | J. Phys. Chem. C 2013, 117, 16972−16982

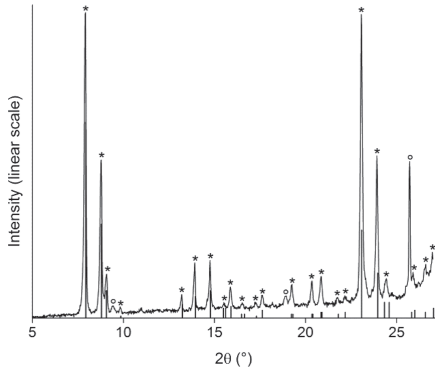

Figure 2. XRD diffractogram of the Na-ZSM-5 film synthesized on a ZnS crystal in the 2θ range 5−27° where peaks marked with an asterisk represent the zeolite film, peaks marked with an open circle represent the ZnS crystal, and the vertical lines represent the reflections in a reference pattern for ZSM-5 zeolite.

database pattern shows that the film is comprised of ZSM-5 crystals. Inductively coupled plasma mass spectroscopy (ICP-MS) measurements of the film showed that the Si/Al ratio of the crystals in the film is 130 and a Na/Al ratio of 1.

Adsorption Experiments. The molar absorbance coefficient for the adsorbates in the zeolite pores, ε, was determined from the AGIR measurements by using the Beer−Lamberts law (eq 1) to 0.645 cm/μmol for water, 16.3 cm/μmol for carbon dioxide, and 0.850 cm/μmol for methane.

Water. Figure 3 shows typical infrared spectra of water adsorbed in the ZSM-5 film at 35 °C at partial pressures in the range 0.002 to 2.105 kPa; the partial pressure in each experiment is indicated in the figure. Two main bands originating from adsorbed water appear in the spectra. The broad band in the 2800−3700 cm^{-1} region is assigned to the O−H stretching vibration of adsorbed water whereas the band at ca. 1622 cm^{-1} is assigned to the bending vibration of adsorbed water.[41] As can be expected, the spectral features assigned to water adsorbed in zeolite film increase with increasing partial pressure in the gas. The bands are typical for water in a condensed state, without any signs of gas phase rotational transitions. As the partial pressure of water is increased, there seem to be different overlapping bands in the O−H stretching region positioned at ca. 3650, 3390, and 3230 cm^{-1}. The band at 1622 cm^{-1} is observed at lower wavenumbers than for bulk water (ca. 1650 cm^{-1}) indicating that the oxygen in the water molecule is directly bound to the zeolite structure. At higher partial pressures, a shoulder appears at ca. 1640 cm^{-1}, i.e., closer to the wavenumber of bulk water. Most likely the two features correspond to isolated water molecules and clusters of adsorbed water molecules at higher partial pressures as previously shown in molecular simulations.[42−45] At the same time, a negative band appears at ca. 3730 cm^{-1} in all spectra; this band has previously been assigned to the O−H stretching vibration of silanol groups.[42] As water adsorbs on the silanol group, this band shifts to lower wavenumbers leading to a negative band at the wavenumber of the unperturbed silanol group. Infrared spectra of water adsorbed in ZSM-5 and FAU have been reported in the literature.[42,46] Jentys et al.[42] analyzed water adsorption in Na-ZSM-5 with Si/Al = 36 using transmission infrared measurements and reported several bands (2−4 depending on loading) in the 3200−3700 cm^{-1} region as well as a band at 1631 cm^{-1} in their infrared spectra in accordance with the findings in the present work. Rege and Yang[46] analyzed water adsorption in 13× zeolite at 22 °C also using transmission infrared spectroscopy. Their sample is more hydrophilic than our sample and bands were reported in the 2900−3500 cm^{-1} region and one band at 1644 cm^{-1}. The band at 1644 cm^{-1} is of similar wavenumber as for regular water indicating clusters of adsorbed water molecules. Compared to the literature it can be seen that the band assigned to the water bending vibration, which we observe at 1622 cm^{-1}, appears at a lower wavelength compared to previous reports. There are also some minor dissimilarities in the O−H stretching region between our spectra and those previously reported, which is ascribed to the low aluminum content in our sample. The relatively high aluminum content in the samples previously reported gives rise to clear bands associated with adsorption on the O−H stretching bands associated with the aluminum. Due to the low aluminum content (and the stoichiometric amounts of sodium) in our sample, we do not observe these bands. The spectra of adsorbed water recorded at 50, 85, and 120 °C were very similar in appearance as the ones shown in Figure 3 but

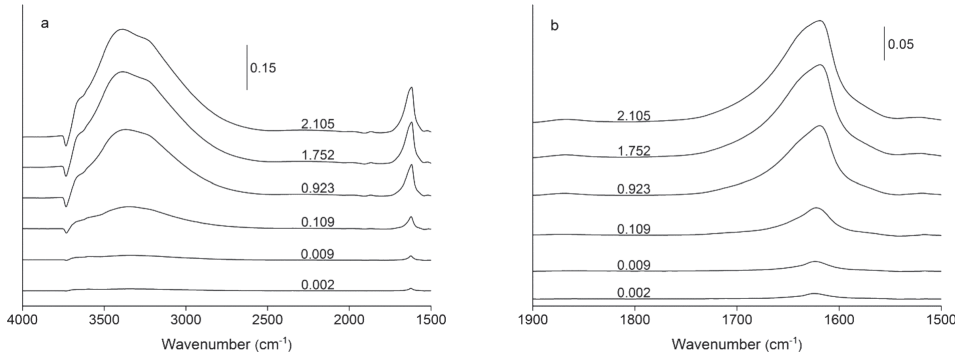

Figure 3. Infrared spectra of water adsorbed in Na-ZSM-5 at 35 °C at various partial pressures (kPa) which are indicated in the figure; the entire spectral region (a) and the O−H bending region (b).

dx.doi.org/10.1021/jp4037183 | J. Phys. Chem. C 2013, 117, 16972−16982

with lower intensity as expected from the reduced adsorption at higher temperatures.

Adsorption isotherms were retrieved from the recorded infrared spectra by calculating the loading using eqs 3−8. The adsorption isotherms (points) are presented in Figure 4

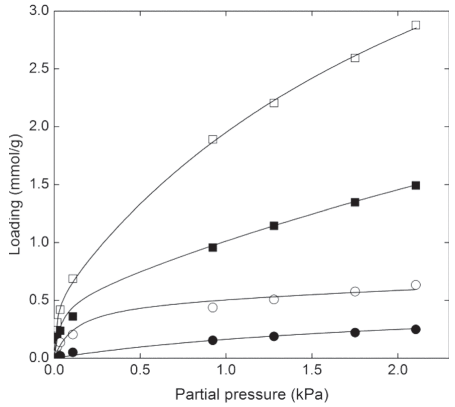

Figure 4. Adsorption isotherms for water in Na-ZSM-5 at 35 (□), 50 (■), 85 (○), and 120 °C (●). The symbols represent the experimental data and the lines represent the dual site Langmuir model fitted to the experimental data.

together with the dual site Langmuir model (curves) fitted to the data. As can be seen, the Langmuir model fits the experimental data very well. For the three lower temperatures (35, 50, and 85 °C), the isotherms show a steep increase in loading at low partial pressures, corresponding to adsorption on high energy sites. At higher partial pressures, the slopes of the isotherms level off, but saturation is not reached at any temperature at the conditions studied in the present work. The fitted dual site Langmuir model parameters, i.e., the saturation concentration (q_{sat}) and Langmuir adsorption coefficient (b), are reported in Table 1. According to the literature,[21,44,47,48] the saturation concentration of water in MFI varies significantly, and concentrations in the range 0.8 and 31 mmol/g have been reported, probably reflecting the different Si/Al ratios and the amount of defects (i.e., silanol groups) in the zeolites studied.[21,22,48] However, most values are reported in the lower part of the interval (0.8−4.8 mmol/g) and the total saturation concentration ($q_1 + q_2$) determined in the present work of 5.84 mmol/g thus agrees well with literature data. When studying the values of the Langmuir adsorption coefficient and saturating loadings obtained for the two sites it can clearly be seen that water has a higher affinity for site 2 while the saturation loading is rather small (0.50 mmol/g) compared to site 1 (5.34 mmol/g). Therefore, adsorption of water on site 2 corresponds to adsorption on a few high-energy sites, possibly related to defects in the form of silanol groups and/or to sites containing sodium ions. Site 1 on the other hand corresponds to a weaker adsorption probably on the pore wall. The adsorption isotherm of water obtained in the present work at 35 °C was compared to isotherms previously reported in the literature (see Figure 1 in the Supporting Information) showing a good agreement to previously reported data.

Table 1. Saturation Concentrations (q_{sat}, mmol/g) and Langmuir Adsorption Coefficients (b, Pa^{-1}) for Water, Carbon Dioxide, and Methane Adsorbed in Na-ZSM-5

adsorbate	temp (°C)	q_1 (mmol/g)	b_1 (1/Pa)	q_2 (mmol/g)	b_2 (1/Pa)
H_2O	35	5.34	3.75×10^{-4}	0.50	7.90×10^{-2}
	50	5.34	1.10×10^{-4}	0.50	2.80×10^{-2}
	85	5.34	1.10×10^{-5}	0.50	8.10×10^{-3}
	120	5.34	8.00×10^{-7}	0.50	4.63×10^{-4}
CO_2	35	2.78	1.04×10^{-5}	0.04	6.33×10^{-4}
	50	2.78	5.03×10^{-6}	0.04	2.47×10^{-4}
	85	2.78	1.24×10^{-6}	0.04	1.83×10^{-5}
	120	2.78	4.44×10^{-7}	0.04	8.31×10^{-6}
CH_4	35	2	1.04×10^{-6}		
	50	2	5.53×10^{-7}		
	85	2	2.38×10^{-7}		
	120	2	1.18×10^{-7}		

The heat of adsorption of water, ΔH, was determined to be −71.8 kJ/mol for the first site (R^2 = 0.9505) and −57.5 kJ/mol for the second site (R^2 = 0.9942), using the vaṅt Hoff equation (eq 11). Table 2 shows an overview of the values determined in the present work together with values previously reported in the literature. Olson et al.[21] used thermogravimetry and reported an isosteric heat of adsorption for water in H-ZSM-5 zeolite with Si/Al ratios of 38 and 250 to −113 and −75 kJ/mol, respectively. Bolis et al.[22] used microcalorimetry and reported values of the heat of adsorption in the range −69 to −84 kJ/mol for H-ZSM-5 zeolite with a Si/Al ratio of 3.8 and in the −61 to −68 kJ/mol range for silicalite-1. The Na-ZSM-5 film used in the present work had a Si/Al ratio of 130 and thus the heat of adsorption determined in the present work of −71.8 and −57.5 kJ/mol is in good agreement with previous findings for MFI zeolite with low aluminum content.

Table 2. Values of the Heat of Adsorption, ΔH, Determined in the Present Work along with Values Previously Reported in the Literature

adsorbate	zeolite	Si/Al ratio	ΔH (kJ/mol)	ref
H_2O	Na-ZSM-5	130	−72 (site 1)	this work
			−58 (site 2)	
	H-ZSM-5	38	−113	Olson et al.[21]
		250	−75	
	H-ZSM-5	3.8	−69 to −84	Bolis et al.[22]
	silicalite-1		−61 to −68	
CO_2	Na-ZSM-5	130	−37 (site 1)	This work
			−54 (site 2)	
	Na-ZSM-5	27	−30.5 (site 1)	Wirawan and Creaser[49]
			−61 (site 2)	
	silicalite-1		−20	Choudary et al.[17]
	silicalite-1		−28	Sun et al.[18]
	silicalite-1		−27	Dunne et al.[19]
	Na-ZSM-5	30	−50	Dunne et al.[20]
CH_4	Na-ZSM-5	130	−23	this work
	silicalite-1		−27.5	Choudary et al.[17]
	silicalite-1		−20	Sun et al.[18]
	silicalite-1		−21	Dunne et al.[19]
	Na-ZSM-5	30	−27.3	Dunne et al.[20]

Carbon Dioxide. Figure 5 shows infrared spectra of carbon dioxide adsorbed in Na-ZSM-5 at 35 °C at partial pressures in the range 0.5 to 101.3 kPa; the partial pressures in each

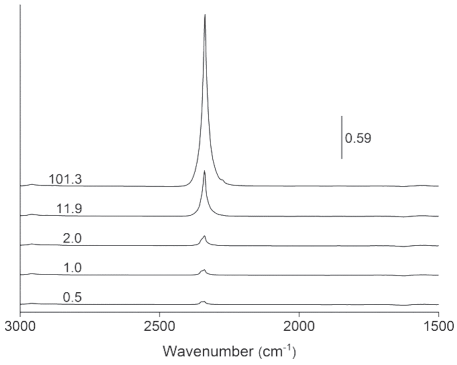

Figure 5. Infrared spectra of carbon dioxide adsorbed in Na-ZSM-5 at 35 °C at various partial pressures (kPa) which are indicated in the figure.

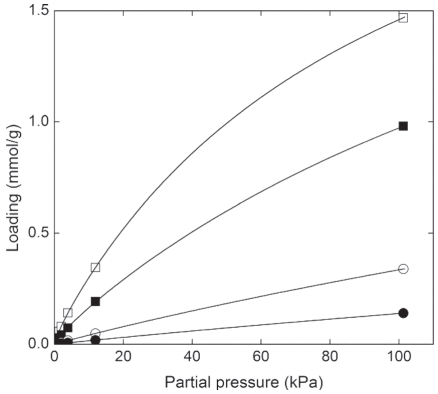

Figure 6. Adsorption isotherms for carbon dioxide in Na-ZSM-5 at 35 (□), 50 (■), 85 (○), and 120 °C (●). The symbols are representing the experimental data and the lines are representing the dual site Langmuir model fitted to the experimental data.

experiment are indicated in the figure. The most prominent band in the spectra is found at 2338 cm^{-1}. This band is assigned to the asymmetric stretching vibration of physisorbed carbon dioxide.[46] At lower partial pressures, up to 2 kPa, two bands can be observed in the spectra at 2350 and 2338 cm^{-1}, indicating that the carbon dioxide molecules are less restricted at these loadings. At higher pressures, only one band at 2338 cm^{-1} is observed, indicating that the molecules become more restricted as more carbon dioxide adsorbs in the zeolite. To rule out that the double peak originates from the gas phase outside the film, an experiment was conducted at the same conditions albeit using an uncoated ATR crystal instead. No signal from carbon dioxide (see Figure 2 in the Supporting Information) was detected when the uncoated ATR crystal was used, which shows that the two bands at 2350 and 2338 cm^{-1} originate from carbon dioxide in the film. Wirawan and Creaser[49] used in situ DRIFT spectroscopy to investigate the adsorption of carbon dioxide in silicalite-1, H-ZSM-5, Na-ZSM-5, and Ba-ZSM-5 where all ZSM-5 samples had a Si/Al ratio of 27. A band at 2354 cm^{-1} was reported for the Na-ZSM-5 sample and assigned to physisorbed carbon dioxide. Several bands in the wavenumber range of 1200−1800 cm^{-1} were also reported, indicating the presence of carbonates and bicarbonate. Rege and Yang[46] analyzed carbon dioxide adsorption on 13X zeolite at 22 °C using transmission infrared spectroscopy and reported one band at 2359 cm^{-1}. Several bands in the 1200−1700 cm^{-1} region were reported, indicating chemisorbed carbon dioxide either on the cations or in the form of carbonate or bicarbonate ions. Compared to the literature, it can be seen that the band assigned to physisorbed carbon dioxide at 2338 cm^{-1} in the present work appears at a lower wavelength than in the previous studies, however, no bands were observed in the 1200−1700 cm^{-1} region, indicating that no formation of carbonate species occurred in our study. The spectra of adsorbed carbon dioxide at 50, 85, and 120 °C were very similar but weaker as expected from the reduced adsorption at higher temperatures.

Again, adsorption isotherms were retrieved from the recorded infrared spectra and the loading was determined by using eqs 3−8. The adsorption isotherms obtained are presented as points in Figure 6 together with the dual site Langmuir model fitted to the experimental data as curves. First of all, it may be noted that saturation loading was not reached at the conditions studied and the dual site Langmuir model fit the experimental data very well, as for water. The fitted dual site Langmuir model parameters are reported in Table 1. The saturation loading obtained in the present work amounts to 2.82 mmol/g. As revealed from literature,[18−20,49−53] the saturation concentration in MFI type zeolites is scattering, ranging between 1.2 and 5 mmol/g. Hence, the value obtained in the present work is in good agreement with previous reports. A closer inspection of the Langmuir adsorption coefficient and saturation loadings obtained for the two sites reveals that the carbon dioxide has a higher affinity for site 2 and that the saturation loading of this site is rather small (0.04 mmol/g), as for water. Therefore, adsorption of carbon dioxide on this site corresponds to adsorption on a few high-energy sites, possibly related to defects in the form of silanol groups and/or to sites containing sodium ions while adsorption of carbon dioxide on site 1 corresponds to a weaker adsorption probably on the pore wall. The adsorption isotherm of carbon dioxide obtained in the present work at 35 °C was compared to isotherms previously reported in the literature (see Figure 3 in the Supporting Information) again showing a good agreement with previously reported data.

The heat of adsorption for carbon dioxide, ΔH, was determined to be −37.5 kJ/mol for site 1 (R^2 = 0.999) and −54.0 kJ/mol for site 2 (R^2 = 0.97) by using the vaṅt Hoff equation (eq 11). The values determined in the present work are presented in Table 2 together with values previously reported in the literature. Wirawan and Creaser[49] reported similar values for adsorption of carbon dioxide in Na-ZSM-5 (Si/Al = 27), viz. −30.5 kJ/mol for site 1 and −61 kJ/mol for site 2, when using a step change response method. For adsorption of carbon dioxide in silicalite-1, Choudhary et al.[17] used gravimetry and obtained an isosteric heat of adsorption of −20 kJ/mol, Sun et al.[18] used gravimetry and reported an isosteric heat of adsorption of −28 kJ/mol, whereas Dunne et al.[19] used calorimetry and obtained a heat of adsorption of −27 kJ/mol. For adsorption of carbon dioxide in Na-ZSM-5 zeolite, Si/Al = 30, Dunne et al.,[20] again using calorimetry, reported an isosteric heat of adsorption of −50 kJ/mol. The results obtained in the present work, with a sample having Si/Al =

dx.doi.org/10.1021/jp4037183 | J. Phys. Chem. C 2013, 117, 16972−16982

130, of −37.5 kJ/mol and −54.0 kJ/mol, thus lie within the range of previously reported data for the heat of adsorption of carbon dioxide in MFI zeolite.

Methane. Figure 7 shows infrared spectra of methane adsorbed in Na-ZSM-5 at 35 °C at partial pressures in the range

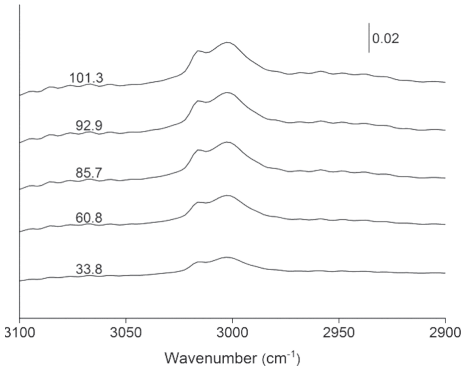

Figure 7. Infrared spectra for methane adsorbed in Na-ZSM-5 at 35 °C at various partial pressures (kPa) as indicated in the figure.

33.8 to 101.3 kPa; the partial pressures in each experiment are indicated in the figure. Bands in the 3000−3020 cm^{-1} region are assigned to the C−H stretching vibration of the adsorbed methane,[54,55] where two bands can be observed at 3015 and 3002 cm^{-1}. The spectra of adsorbed methane at 50, 85, and 120 °C were similar in appearance but weaker as expected from the reduced adsorption at higher temperatures.

The adsorption isotherms determined from the infrared spectra (points) are presented in Figure 8 together with the single site Langmuir model fitted to the experimental data (curves) and the fitted parameters are reported in Table 1. The loadings determined are quite low compared to those obtained for water and carbon dioxide showing that methane is much weaker adsorbed in the zeolite. The saturation capacity

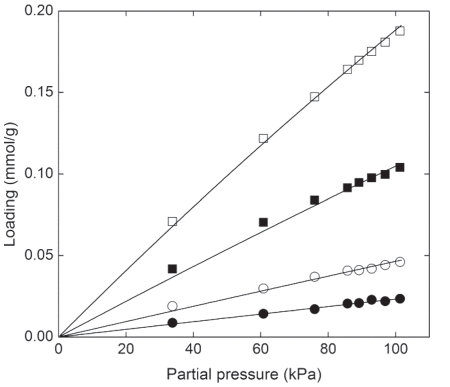

Figure 8. Adsorption isotherms for methane in Na-ZSM-5 at 35 (□), 50 (■), 85 (○), and 120 °C (●). The symbols are representing the experimental data and the lines are representing the single site Langmuir model fitted to the experimental data.

obtained in the present work of 2 mmol/g is in agreement with values reported in the literature which lie in the range of 1.9−5.4 mmol/g.[18−20,50−53] The adsorption isotherm of methane obtained in the present work at 35 °C was compared to isotherms previously reported in the literature (see Figure 4 in the Supporting Information). The amount adsorbed at a certain partial pressure was approximately a factor of two lower than previously reported data.

The heat of adsorption was determined to be −25.2 kJ/mol (R^2 = 0.9938) by using the vaŕt Hoff equation (eq 11), which is reported in Table 2 together with values previously reported in the literature. For adsorption of methane in silicalite-1, Choudhary et al.[17] used gravimetry and found an isosteric heat of adsorption of −27.5 kJ/mol, Sun et al.[18] used gravimetry and reported an isosteric heat of adsorption of −20 kJ/mol, whereas Dunne et al.[19] report a heat of adsorption of −21 kJ/mol from calorimetry measurements. For adsorption of methane in Na-ZSM-5 zeolite, Si/Al = 30, Dunne et al.[20] used calorimetry and obtained an isosteric heat of adsorption of −27.3 kJ/mol. The heat of adsorption obtained in the present work is thus in good agreement with previous findings.

By comparing the results (saturation loadings, Langmuir adsorption coefficients, and heat of adsorption) obtained for the different species, it may be concluded that water shows the greatest affinity for this zeolite followed by carbon dioxide, while methane shows the lowest affinity for the zeolite. The results presented above also clearly show that reliable single component quantitative adsorption data can be extracted from infrared spectra of the adsorbed species. A natural step is then to utilize the ability of infrared spectroscopy to discriminate between different species based on their spectral features for studying adsorption from binary and ternary mixtures.

Adsorption of Carbon Dioxide and Methane from an Equimolar Mixture. On the basis of the results from the single component adsorption data it would be expected that carbon dioxide would be preferentially adsorbed in the zeolite from a carbon dioxide/methane mixture. Figure 9a shows an infrared spectrum of carbon dioxide and methane simultaneously adsorbed in Na-ZSM-5 at 35 °C. The partial pressure of carbon dioxide and methane was 50.7 kPa. The characteristic band of physisorbed carbon dioxide appears at 2338 cm^{-1} and so do the characteristic bands of adsorbed methane at 3015 and 3003 cm^{-1}. The amount of carbon dioxide and methane adsorbed was again determined from the spectra (under the reasonable assumption that the molar absorptivity of one component is unaffected by the presence of the other species) and the results obtained were compared to concentrations predicted by the IAST, see Figure 10 (without water). There is an excellent agreement between the experimental values and those predicted by the IAST. This is in accordance with previous results for this system showing that the binary adsorption of carbon dioxide and methane on MFI can be accurately predicted with the IAST.[14,56,57]

Adsorption of Carbon Dioxide and Methane in the Presence of Water. To elucidate the effect of water on the adsorption of carbon dioxide and methane in Na-ZSM-5 at 35 °C, an experiment similar to that for the binary mixture was performed but with water also present in the gas phase. The composition of the gas phase was 50.1 kPa of carbon dioxide, 50.1 kPa of methane, and 1.1 kPa of water. Figure 9b shows an infrared spectrum recorded of the ternary mixture adsorbed in the zeolite film. Characteristic absorption bands from all species are observed in the spectrum and the bands remain in the same

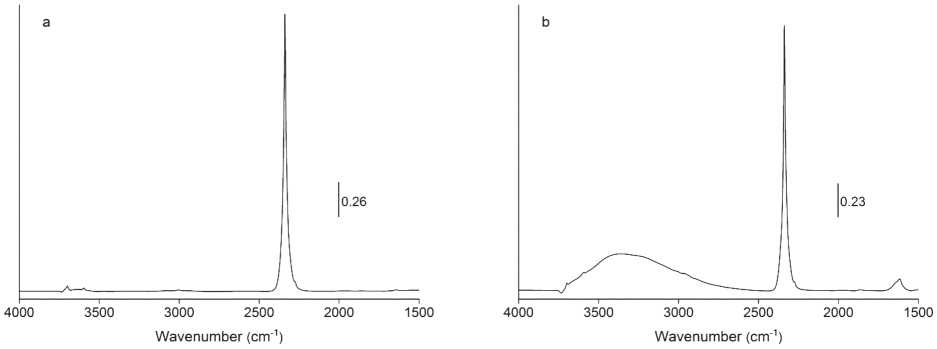

Figure 9. Infrared spectra of carbon dioxide and methane coadsorbed in Na-ZSM-5 at 35 °C: in the absence of water (a) and in the presence of water (b). When the spectrum in part a was recorded the partial pressure of carbon dioxide and methane was 50.7 kPa, whereas when spectrum b was recorded the partial pressure of carbon dioxide and methane was 50.1 kPa and the partial pressure of water was 1.1 kPa.

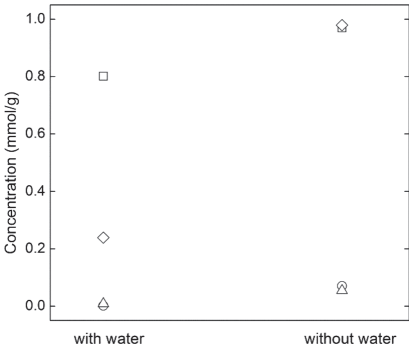

Figure 10. Amount of carbon dioxide (□) and methane (○) adsorbed in ZSM-5 at 35 °C from a gas equimolar in carbon dioxide and methane in the absence and in the presence of water in the gas phase. The partial pressure of carbon dioxide and methane was 50.7 and 50.1 kPa in the absence and presence of water, respectively, and the partial pressure of water was 1.1 kPa. The predicted amounts adsorbed calculated with the IAST for carbon dioxide (◇) and methane (△) are also shown in the figure.

positions as in the single component spectra. The band at 2338 cm^{-1}, assigned to physisorbed carbon dioxide, is slightly narrower in the presence of water, which might suggest that there is an interaction between carbon dioxide and water. The bands assigned to carbon dioxide and methane are less intense compared to the bands recorded for the binary mixture suggesting that carbon dioxide and methane are partially replaced by competitive water adsorption as could be expected from the single component data. When adding water to the mixture, the adsorbed concentration of carbon dioxide decreased by 17.5% (while the decrease in partial pressure was only 1.1%) whereas for methane, the adsorbed concentration decreased by 97.1%. The decrease in adsorbed concentration of carbon dioxide and methane in the presence of water has previously been reported in the literature.[58] For the ternary mixture, the IAST correctly predicts the amount of methane adsorbed but it severely underestimates the amount of carbon dioxide adsorbed, see Figure 10 (with water). This enhanced adsorption of carbon dioxide in zeolites in the presence of water (with respect to the value predicted by the IAST) has previously been reported for zeolites and zeolite-like materials[46,59,60] and constitutes a nonideal adsorption behavior. Snurr et al.[60] studied the multicomponent adsorption of carbon dioxide and water in MOFs. It was reported that the adsorption of carbon dioxide was enhanced in the presence of a small amount of water when using a sample loaded with 4 wt % water compared to a dry sample. When using a fully hydrated sample, the adsorption of carbon dioxide was lower, which can be explained by the pores being filled with water molecules. We speculate that a similar mechanism may be applied to our system where small amounts of water enhance the adsorption of carbon dioxide, and therefore, the IAST is not able to correctly predict the amount adsorbed carbon dioxide. However, this phenomenon will be studied in forthcoming work.

The results presented in the two last sections clearly demonstrate that the technique used in the present work may be used for studying adsorption also from multicomponent mixtures. Such data may be of great importance when developing novel zeolite adsorbent or membrane processes for carbon dioxide removal from biogas and natural gas streams. The adsorption behavior of the binary and ternary mixtures will be studied in more detail in forthcoming work.

CONCLUSIONS

In the present work, the adsorption of water, carbon dioxide, and methane in zeolite Na-ZSM-5 (Si/Al = 130) at four different temperatures was studied by using in situ ATR-FTIR spectroscopy. Quantitative adsorption isotherms were successfully extracted from the infrared spectra. Single and dual site Langmuir isotherm models were fitted to the experimental data with very good fit. The limiting heats of adsorption and saturation capacities retrieved from the Langmuir models were in very good agreement with literature data. The amount of carbon dioxide and methane adsorbed from a binary mixture was determined from infrared spectra and the experimental results from the binary mixture were in excellent agreement with values predicted by the IAST by using the single component data. When water was also introduced, the amount of adsorbed methane adsorbed could still be correctly predicted by using the IAST whereas the IAST severely underestimated the amount of carbon dioxide adsorbed. The latter finding

dx.doi.org/10.1021/jp4037183 | J. Phys. Chem. C 2013, 117, 16972−16982

indicates that water and carbon dioxide do not form an ideal adsorbed phase, in agreement with previous findings.

■ ASSOCIATED CONTENT

Supporting Information

Adsorption isotherms of water, carbon dioxide and methane at 35 °C obtained in the present work compared to isotherms previously reported in the literature and infrared spectra of carbon dioxide, with and without the zeolite film, showing that no signal from carbon dioxide was detected when using the uncoated ATR element. This material is available free of charge via the Internet at http://pubs.acs.org.

■ AUTHOR INFORMATION

Corresponding Author

*Tel: +46 920 491387. E-mail: lindsay.ohlin@ltu.se.

Notes

The authors declare no competing financial interest.

■ ACKNOWLEDGMENTS

The authors gratefully acknowledge The Swedish Energy Agency for financially supporting this work. The Knut and Alice Wallenberg foundation is acknowledged for funding of the SEM and the Kempe foundation for funding the IR spectrometer. Assoc. Professor Allan Holmgren is acknowledged for his valuable comments and Amirfarrokh Farzaneh is acknowledged for helping out in the lab.

■ REFERENCES

(1) Abdeshahian, P.; Dashti, M. G.; Kalil, M. S.; Yusoff, W. M. W. Production of Biofuel using Biomass as a Sustainable Biological Resource. *Biotechnology* **2010**, *9*, 274−282.

(2) Brown, R. C. In *Biorenewable resources: engineering new products from agriculture*; Iowa State Press: Ames, IA, 2003.

(3) Cavenati, S.; Grande, C. A.; Rodrigues, A. E. Adsorption Equilibrium of Methane, Carbon Dioxide, and Nitrogen on Zeolite 13X at High Pressures. *J. Chem. Eng. Data* **2004**, *49*, 1095−1101.

(4) Busby, R. L. In *Natural gas in nontechnical language*; Busby, R. L., Ed.; Pennwell: Tulsa, OK, 1999.

(5) Krishna, R.; van-Baten, J. M. Segregation Effects in Adsorption of CO_2-Containing Mixtures and their Consequences for Separation Selectivities in Cage-Type Zeolites. *Sep. Purif. Technol.* **2008**, *61*, 414−423.

(6) Krishna, R.; van Baten, J. M. Using Molecular Simulations for Screening of Zeolites for Separation of CO_2/CH_4 Mixtures. *Chem. Eng. J.* **2007**, *133*, 121−131.

(7) Kassaee, M. H.; Sholl, D. S.; Nair, S. Preparation and Gas Adsorption Characteristics of Zeolite MFI Crystals with Organic-Functionalized Interiors. *J. Phys. Chem. C* **2011**, *115*, 19640−19646.

(8) Lindmark, J.; Hedlund, J. Modification of MFI Membranes with Amine Groups for Enhanced CO_2 Selectivity. *J. Mater. Chem.* **2010**, *20*, 2219−2225.

(9) Tavolaro, A.; Drioli, E. Zeolite Membranes. *Adv. Mater.* **1999**, *11*, 975−996.

(10) Davis, M. E. Ordered Porous Materials for Emerging Applications. *Nature* **2002**, *417*, 813−821.

(11) Wang, Z.; Grahn, M.; Larsson, M. L.; Holmgren, A.; Sterte, J.; Hedlund, J. Zeolite Coated ATR Crystal Probes. *Sens. Actuators, B* **2006**, *115*, 685−690.

(12) Othman, M. R.; Tan, S. C.; Bhatia, S. Separability of Carbon Dioxide from Methane using MFI Zeolite-Silica Film Deposited on Gamma-Alumina Support. *Microporous Mesoporous Mater.* **2009**, *121*, 138−144.

(13) Garcia-Perez, E.; Parra, J. B.; Ania, C. O.; Garcia-Sanchez, A.; van-Baten, J. M.; Krishna, R.; Dubbeldam, D.; Calero, S. A Computational Study of CO_2, N_2, and CH_4 Adsorption in Zeolites. *Adsorption* **2007**, *13*, 469−476.

(14) Harlick, P. J. E.; Tezel, F. H. Adsorption of Carbon Dioxide, Methane and Nitrogen: Pure and Binary Mixture Adsorption for ZSM-5 with SiO_2/Al_2O_3 Ratio of 280. *Sep. Purif. Technol.* **2003**, *33*, 199−210.

(15) Bao, Z.; Yu, L.; Dou, T.; Gong, Y.; Zhang, Q.; Ren, Q.; Lu, X.; Deng, S. Adsorption Equilibria of CO_2, CH_4, N_2, O_2, and Ar on High Silica Zeolites. *J. Chem. Eng. Data* **2011**, *56*, 4017−4023.

(16) Sandström, L.; Sjöberg, E.; Hedlund, J. Very High Flux MFI Membrane for CO_2 Separation. *J. Membr. Sci.* **2011**, *380*, 232−240.

(17) Choudhary, V. R.; Mayadevi, S. Adsorption of Methane, Ethane, Ethylene, and Carbon Dioxide on Silicalite-I. *Zeolites* **1996**, *17*, 501−507.

(18) Sun, M. S.; Shah, D. B.; Xu, H. H.; Talu, O. Adsorption Equilibria of C_1 to C_4 Alkanes, CO_2, and SF_6 on Silicalite. *J. Phys. Chem. B* **1998**, *102*, 1466−1473.

(19) Dunne, J. A.; Mariwala, R.; Rao, M.; Sircar, S.; Gorte, R. J.; Myers, A. L. Calorimetric Heats of Adsorption and Adsorption Isotherms. 1. O_2, N_2, Ar, CO_2, CH_4, C_2H_6 and SF_6 on Silicalite. *Langmuir* **1996**, *12*, 5888−5895.

(20) Dunne, J. A.; Rao, M.; Sircar, S.; Gorte, R. J.; Myers, A. L. Calorimetric Heats of Adsorption and Adsorption Isotherms. 2. O_2, N_2, Ar, CO_2, CH_4, C_2H_6, and SF_6 on NaX, H-ZSM-5, and Na-ZSM-5 Zeolites. *Langmuir* **1996**, *12*, 5896−5904.

(21) Olson, D. H.; Haag, W. O.; Borghard, W. S. Use of Water as a Probe of Zeolitic Properties: Interaction of Water with HZSM-5. *Microporous Mesoporous Mater.* **2000**, *35*−*36*, 435−446.

(22) Bolis, V.; Busco, C.; Ugliengo, P. Thermodynamic Study of Water Adsorption in High-Silica Zeolites. *J. Phys. Chem. B* **2006**, *110*, 14849−14859.

(23) Bjorklund, R. B.; Hedlund, J.; Sterte, J.; Arwin, H. Vapor Adsorption in Thin Silicalite-1 Films Studied by Spectroscopic Ellipsometry. *J. Phys. Chem. B* **1998**, *102*, 2245−2250.

(24) Jareman, F.; Hedlund, J.; Sterte, J. Effects of Aluminum Content on the Separation Properties of MFI Membranes. *Sep. Purif. Technol.* **2003**, *32*, 159−163.

(25) Grahn, M.; Holmgren, A.; Hedlund, J. Adsorption of n-Hexane and p-Xylene in Thin Silicalite-1 Films Studied by FTIR/ATR Spectroscopy. *J. Phys. Chem. C* **2008**, *112*, 7717−7724.

(26) Grahn, M.; Lobanova, A.; Holmgren, A.; Hedlund, J. Orientational Analysis of Adsorbates in Molecular Sieves by FTIR/ATR Spectroscopy. *Chem. Mater.* **2008**, *20*, 6270−6276.

(27) Hedlund, J.; Sterte, J.; Anthonis, M.; Bons, A.; Carstensen, B.; Corcoran, N.; Cox, D.; Deckman, H.; De Gijnst, W.; De Moor, P.; Lai, F.; McHenry, J.; Mortier, W.; Reinoso, J.; Peters, J. High-Flux MFI Membranes. *Microporous Mesoporous Mater.* **2002**, *52*, 179−189.

(28) Sandström, L.; Lindmark, J.; Hedlund, J. Separation of Methanol and Ethanol from Synthesis Gas using MFI Membranes. *J. Membr. Sci.* **2010**, *360*, 265−275.

(29) Wang, Z.; Larsson, M. L.; Grahn, M.; Holmgren, A.; Hedlund, J. Zeolite Coated ATR Crystals for New Applications in FTIR-ATR Spectroscopy. *Chem. Commun.* **2004**, 2888−2889.

(30) Bazin, P.; Alenda, A.; Thibault-Starzyk, F. Interaction of Water and Ammonium in NaHY Zeolite as Detected by Combined IR and Gravimetric Analysis (AGIR). *Dalton Trans.* **2010**, *39*, 8432−8436.

(31) Moulin, B.; Oliviero, L.; Bazin, P.; Daturi, M.; Costentin, G.; Mauge, F. How to Determine IR Molar Absorption Coefficients of Co-Adsorbed Species? Application to Methanol Adsorption for Quantification of MgO Basic Sites. *Phys. Chem. Chem. Phys.* **2011**, *13*, 10797−10807.

(32) Morterra, C.; Magnacca, G.; Bolis, V. On the Critical use of Molar Absorption Coefficients for Adsorbed Species: The methanol/silica System. *Catal. Today* **2001**, *70*, 43−58.

(33) Grahn, M.; Wang, Z.; Lidström-Larsson, M.; Holmgren, A.; Hedlund, J.; Sterte, J. Silicalite-1 Coated ATR Elements as Sensitive Chemical Sensor Probes. *Microporous Mesoporous Mater.* **2005**, *81*, 357−363.

(34) Tompkins, H. G. The Physical Basis for Analysis of the Depth of Absorbing Species using Internal Reflection Spectroscopy. *Appl. Spectrosc.* **1974**, *28*, 335−341.
(35) Mirabella, F. M., Ed.; In *Internal Reflection Spectroscopy: Theory and Applicatons*; Marcel Dekker, Inc.,: New York, 1993, *Vol. 15*.
(36) *Guide for Infrared Spectroscopy*; Bruker Optics; Billerica, MA.
(37) Nair, S.; Tsapatsis, M. Infrared Reflectance Measurements of Zeolite Film Thickness, Refractive Index and Other Characteristics. *Microporous Mesoporous Mater.* **2003**, *58*, 81−89.
(38) Satorre, M. A.; Domingo, M.; Millan, C.; Luna, R.; Vilaplana, R.; Santonja, C. Density of CH_4, N_2 and CO_2 Ices at Different Temperatures of Deposition. *Planet. Space Sci.* **2008**, *56*, 1748−1752.
(39) Harrick, N. J. In *Internal reflection spectroscopy*; Wiley: New York, NY, 1967.
(40) Myers, A. L.; Prausnitz, J. M. Thermodynamics of Mixed-Gas Adsorption. *AIChE J.* **1965**, *11*, 121−127.
(41) Zou, X.; Bazin, P.; Zhang, F.; Zhu, G.; Valtchev, V.; Mintova, S. Ethanol Recovery from Water using Silicalite-1 Membrane: An Operando Infrared Spectroscopic Study. *ChemPlusChem* **2012**, *77*, 437−444.
(42) Jentys, A.; Warecka, G.; Derewinski, M.; Lercher, J. Adsorption of Water on ZSM5 Zeolites. *J. Phys. Chem.* **1989**, *93*, 4837−4843.
(43) Krishna, R.; van Baten, J. M. Highlighting Pitfalls in the Maxwell-Stefan Modeling of Water-Alcohol Mixture Permeation Across Pervaporation Membranes. *J. Membr. Sci.* **2010**, *360*, 476−482.
(44) Krishna, R.; van Baten, J. M. Hydrogen Bonding Effects in Adsorption of Water-Alcohol Mixtures in Zeolites and the Consequences for the Characteristics of the Maxwell-Stefan Diffusivities. *Langmuir* **2010**, *26*, 10854−10867.
(45) Krishna, R.; van Baten, J. M. Mutual Slowing-Down Effects in Mixture Diffusion in Zeolites. *J. Phys. Chem. C* **2010**, *114*, 13154−13156.
(46) Rege, S. U.; Yang, R. T. A Novel FTIR Method for Studying Mixed Gas Adsorption at Low Concentrations: H_2O and CO_2 on NaX Zeolite and Gamma-Alumina. *Chem. Eng. Sci.* **2001**, *56*, 3781−3796.
(47) Puibasset, J.; Pellenq, R. J.-M. Grand Canonical Monte Carlo Simulation Study of Water Adsorption in Silicalite at 300 K. *J. Phys. Chem. B* **2008**, *112*, 6390−6397.
(48) Zhang, K.; Lively, R. P.; Noel, J. D.; Dose, M. E.; McCool, B. A.; Chance, R. R.; Koros, W. J. Adsorption of Water and Ethanol in MFI-Type Zeolites. *Langmuir* **2012**, *28*, 8664−8673.
(49) Wirawan, S. K.; Creaser, D. CO_2 Adsorption on Silicalite-1 and Cation Exchanged ZSM-5 Zeolites using a Step Change Response Method. *Microporous Mesoporous Mater.* **2006**, *91*, 196−205.
(50) Zhu, W.; Hrabanek, P.; Gora, L.; Kapteijn, F.; Moulijn, J. A. Role of Adsorption in the Permeation of CH_4 and CO_2 through a Silicalite-1 Membrane. *Ind. Eng. Chem. Res.* **2006**, *45*, 767−776.
(51) Rees, L. V. C.; Brückner, P.; Hampson, J. Sorption of N_2, CH_4 and CO_2 in Silicalite-1. *Gas Sep. Purif.* **1991**, *5*, 67−75.
(52) Golden, T. C.; Sircar, S. Gas Adsorption on Silicalite. *J. Colloid Interface Sci.* **1994**, *162*, 182−188.
(53) van den Broeke, L. J. P.; Bakker, W. J. W.; Kapteijn, F.; Moulijn, J. A. Transport and Separation Properties of a Silicalite-1 Membrane. I. Operating Conditions. *Chem. Eng. Sci.* **1999**, *54*, 245−258.
(54) Scarano, D.; Bertarione, S.; Spoto, G.; Zecchina, A.; Arean, C. FTIR Spectroscopy of Hydrogen, Carbon Monoxide, and Methane Adsorbed and Co-Adsorbed on Zinc Oxide. *Thin Solid Films* **2001**, *400*, 50−55.
(55) Chen, L.; Lin, L.; Xu, Z.; Zhang, T.; Xin, Q.; Ying, P.; Li, G.; Li, C. Fourier Transform-Infrared Investigation of Adsorption of Methane and Carbon Monoxide on HZSM-5 and Mo/HZSM-5 Zeolites at Low Temperature. *J. Catal.* **1996**, *161*, 107−114.
(56) Heymans, N.; Alban, B.; Moreau, S.; De Weireld, G. Experimental and Theoretical Study of the Adsorption of Pure Molecules and Binary Systems Containing Methane, Carbon Monoxide, Carbon Dioxide and Nitrogen. Application to the Syngas Generation. *Chem. Eng. Sci.* **2011**, *66*, 3850−3858.
(57) Harlick, P. J. E.; Tezel, F. H. Adsorption of Carbon Dioxide, Methane, and Nitrogen: Pure and Binary Mixture Adsorption by ZSM-5 with SiO_2/Al_2O_3 Ratio of 30. *Sep. Sci. Technol.* **2002**, *37*, 33−60.
(58) Li, S.; Alvarado, G.; Noble, R. D.; Falconer, J. L. Effects of Impurities on CO_2/CH_4 Separations through SAPO-34 Membranes. *J. Membr. Sci.* **2005**, *251*, 59−66.
(59) Bertsch, L.; Habgood, H. W. An Infrared Spectroscopic Study of the Adsorption of Water and Carbon Dioxide by Linde Molecular Sieve X. *J. Phys. Chem.* **1963**, *67*, 1621−1628.
(60) Özgür Yazaydin, A.; Benin, A. I.; Faheem, S. A.; Jakubczak, P.; Low, J. J.; Willis, R. R.; Snurr, R. Q. Enhanced CO_2 Adsorption in Metal-Organic Frameworks Via Occupation of Open-Metal Sites by Coordinated Water Molecules. *Chem. Mater.* **2009**, *21*, 1425−1430.

Adsorption of CO_2, CH_4 and H_2O in zeolite ZSM-5 studied using in-situ ATR-FTIR spectroscopy

Lindsay Ohlin [a,], Philippe Bazin [b], FrédéricThibault-Starzyk [b], Jonas Hedlund [a] and Mattias Grahn [a]*

[a] Chemical Technology, Luleå University of Technology, 971 87 Luleå, Sweden

[b] Laboratoire Catalyse and Spectrochimie, CNRS-ENSICAEN-Université de Caen, 6 Boulevard Marechal Juin, Caen Cedex 14050, France

* Corresponding author. Tel: +46 920 491387; e-mail address: lindsay.ohlin@ltu.se

The adsorption isotherm of water obtained in the present work at 35 °C was compared to isotherms previously reported in the literature[1, 2] which are presented in Figure 1. Olson *et al.*[1] used thermogravimetry when studying the adsorption of water in H-ZSM-5 with Si/Al = 38 at 25 °C. To be able to compare the isotherms properly, the amounts of adsorbed water were recalculated to 35 °C using the dual site Langmuir model, the van´t Hoff equation and the adsorption enthalpy reported by the authors. Thompson *et al.*[2] used an oscillating microbalance when studying the adsorption isotherm of water in silicalite-1 at 35 °C. Figure 1 shows that there is a divergence in the water adsorption amounts in different MFI samples. However, it can clearly be seen that ZSM-5 adsorbs more water compared to silicalite-1, as may be expected due to the higher content of aluminum in ZSM-5. Our isotherm lies in between the reference isotherms as may be expected from the Si/Al ratios (130 in our work). Adsorption on internal silanol groups formed at crystallographic defects may also have contributed to the amount of water adsorbed in our work.

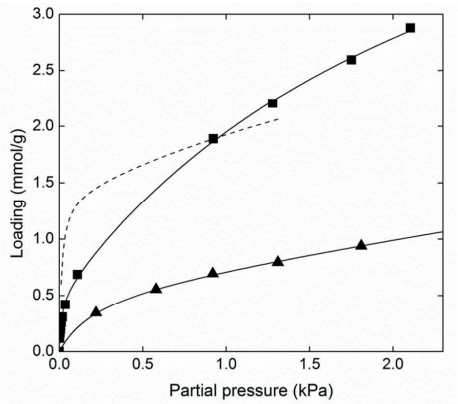

Figure 1. Adsorption isotherms for water in MFI at 35 °C obtained in the present work (■) and isotherms from Olson *et al.*[1] (---) and Thompson *et al.*[2] (▲). The isotherm from Dunne *et al.*[1] was adjusted to 35°C using the dual site Langmuir model and the van´t Hoff equation using the heat of adsorption reported by the author. The lines represent the dual site Langmuir model.

To elucidate the contribution from the gas phase on the signal recorded, spectra were recorded using an uncoated ATR element at different partial pressures of carbon dioxide (from 0.25 to 101.3 kPa). The temperature was kept at 120 °C to minimize the effect of CO_2 adsorbing on the bare ZnS element. Figure 2 show spectra recorded at 0.25 kPa with and without the zeolite film. No signal from carbon dioxide is observed in the spectrum recorded with the uncoated ATR element whereas in the spectrum recorded with the zeolite coated element the characteristic asymmetric stretching band (2350 and 2338 cm^{-1}) of carbon dioxide clearly appears. As can be seen the band shows a double peak indicating that the molecules are not that restricted at these low loadings. In the spectra recorded at higher partial pressures there was some signal of carbon dioxide in the gas phase, however this signal was ca. 80 times smaller than the signal from carbon dioxide adsorbed in the zeolite. Moreover, in the experiments where the film was used, the signal from the gas phase would be even smaller than this value because only the gas phase outside the film is then probed and because of the exponential decay of the electric field with distance from the element. In summary, these results show that the contribution from the gas phase was negligible.

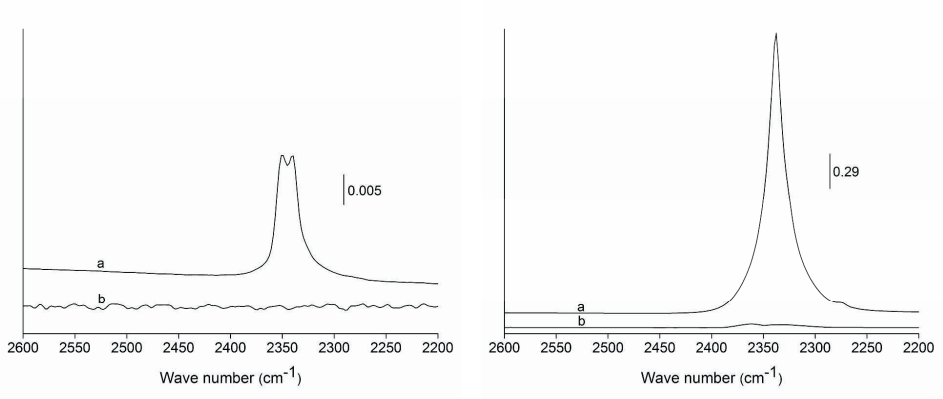

Figure 2. Infrared spectra of carbon dioxide at 0.25 kPa (right) and 101.3 kPa (left) recorded with (a) and without (b) the zeolite film.

Figure 3 shows the adsorption isotherm of carbon dioxide obtained in the present work at 35 °C together with isotherms previously reported in the literature.[3, 4] Dunne *et al.*[3, 4] used calorimetry to study the adsorption isotherms of carbon dioxide in Na-ZSM-5 (Si/Al = 30), H-ZSM-5 (Si/Al = 30) and silicalite-1 at 24.1, 23.9 and 30.6 °C, respectively. To be able to compare the isotherms properly, the amounts of adsorbed carbon dioxide reported by Dunne *et al.*[3, 4] were recalculated to 35 °C using the dual site Langmuir model, the van´t Hoff equation and their experimental data. The adsorption isotherm obtained in the present work agrees very well with the data from Dunne *et al.*[3, 4], especially with the isotherms recorded with silicalite-1 and H-ZSM-5.

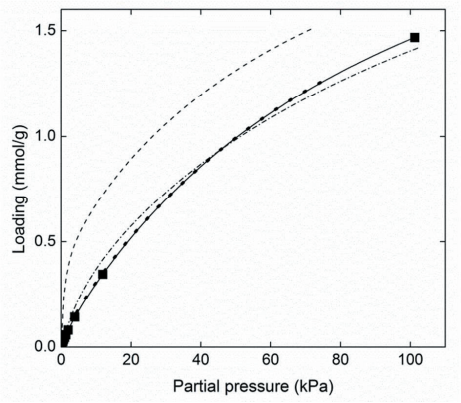

Figure 3. Adsorption isotherms for carbon dioxide in MFI at 35 °C obtained in the present work (■) and isotherms from Dunne *et al.*[3, 4] in Na-ZSM-5 (---), H-ZSM-5 (□·□) and silicalite-1 (···) adjusted to 35°C using the dual site Langmuir adsorption model and the van´t Hoff equation using the heat of adsorption reported by the authors. The lines represent the dual site Langmuir model.

Figure 4 shows the adsorption isotherm of methane obtained in the present work at 35 °C together with isotherms previously reported in the literature.[3, 4] As for carbon dioxide, Dunne et al.[3, 4] used calorimetry

to study the adsorption isotherms of methane in Na-ZSM-5 (Si/Al = 30) and silicalite-1 at 24.1 °C and 30.6 °C, respectively. Again, the amounts adsorbed were recalculated to 35 °C using the dual site Langmuir model and the van´t Hoff equation. The amount of methane adsorbed in this work is ca. a factor two lower than in previous reports.

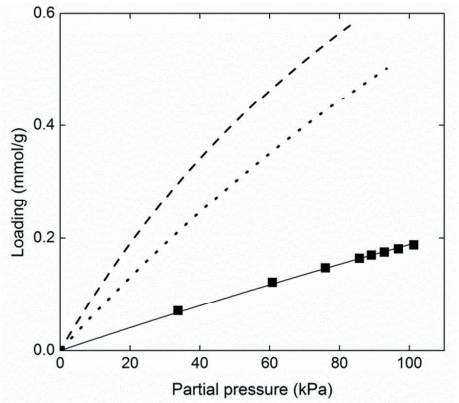

Figure 4. Adsorption isotherms for methane in MFI at 35 °C obtained in the present work (■) and isotherms from Dunne *et al.*[3, 4] in Na-ZSM-5 (---) and silicalite-1 (···) adjusted to 35°C using the dual site Langmuir adsorption model and the van´t Hoff equation using the heat of adsorption reported by the authors. The lines represent the dual site Langmuir model.

REFERENCES

(1) Olson, D. H.; Haag, W. O.; Borghard, W. S. Use of Water as a Probe of Zeolitic Properties: Interaction of Water with HZSM-5. *Microporous Mesoporous Mater.* **2000**, *35-36*, 435-446.

(2) Giaya, A.; Thompson, R. W. Single-Component Gas Phase Adsorption and Desorption Studies using a Tapered Element Oscillating Microbalance. *Microporous Mesoporous Mater.* **2002**, *55*, 265-274.

(3) Dunne, J. A.; Rao, M.; Sircar, S.; Gorte, R. J.; Myers, A. L. Calorimetric Heats of Adsorption and Adsorption Isotherms .2. O-2, N-2, Ar, CO2, CH4, C2H6, and SF6 on NaX, H-ZSM-5, and Na-ZSM-5 Zeolites. *Langmuir* **1996**, *12*, 5896-5904.

(4) Dunne, J. A.; Mariwala, R.; Rao, M.; Sircar, S.; Gorte, R. J.; Myers, A. L. Calorimetric Heats of Adsorption and Adsorption Isotherms .1. O-2, N-2, Ar, CO2, CH4, C2H6 and SF6 on Silicalite. *Langmuir* **1996**, *12*, 5888-5895.

Paper II

Detailed investigation of the binary adsorption of carbon dioxide and methane in zeolite Na-ZSM-5 studied using in situ ATR-FTIR spectroscopy

Lindsay Ohlin and Mattias Grahn

The Journal of Physical Chemistry C

THE JOURNAL OF PHYSICAL CHEMISTRY C

Article

pubs.acs.org/JPCC

Detailed Investigation of the Binary Adsorption of Carbon Dioxide and Methane in Zeolite Na-ZSM-5 Studied Using in Situ ATR-FTIR Spectroscopy

Lindsay Ohlin and Mattias Grahn*

Chemical Technology, Luleå University of Technology, 971 87 Luleå, Sweden

Supporting Information

ABSTRACT: The separation of carbon dioxide from methane is an important process when purifying biogas and natural gas. Zeolite membranes and adsorbents are among the technologies suggested for efficient separation of carbon dioxide from these gases. In the present work, the adsorption of carbon dioxide and methane from binary mixtures in a low alumina Na-ZSM-5 zeolite film at various gas compositions and temperatures was studied using in situ ATR-FTIR (attenuated total reflection Fourier transform infrared) spectroscopy. Adsorbed concentrations were successfully extracted from infrared spectra. The experimental values of the adsorbed phase mole fraction of carbon dioxide and methane were compared to values predicted using the ideal adsorbed solution theory (IAST). The values predicted with the IAST agreed very well with values determined experimentally. The CO_2/CH_4 adsorption selectivity was determined, and at 35 °C a selectivity of 15.4 was obtained for an equimolar gas mixture. At the highest (0.9) and lowest (0.03) investigated mole fractions of carbon dioxide in the gas phase, the selectivity was higher compared to the other investigated mole fractions. At 35 °C the highest observed selectivity values were 31.1 and 20.4 for the highest and the lowest adsorbed mole fraction, respectively. At compositions closest to those found in biogas and natural gas, there was a decrease in the selectivity at higher temperatures, indicating that separation of carbon dioxide from methane in biogas and natural gas may be more efficient at low temperatures.

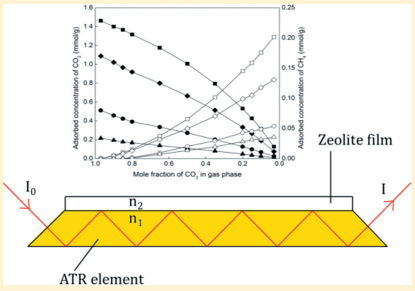

INTRODUCTION

In recent years there has been much focus toward the development of technologies for separation of carbon dioxide from methane. Amine absorption is the most commonly used technology today for the separation of carbon dioxide and methane, but the procedure is both expensive and complicated;[1] therefore more efficient separation processes are sought. Adsorption and membrane based technologies using zeolite adsorbents/membranes have been identified as attractive options.[2,3] For zeolite membranes, the membrane selectivity is usually dependent on both the adsorption selectivity and the diffusion selectivity; therefore, knowing the adsorption properties of the zeolite is of utmost importance also for membrane applications.

A large variety of zeolite and zeolite-like frameworks have been evaluated for carbon dioxide/methane separation both as membranes and as adsorbents.[4−13] The MFI framework, with the ZSM-5 and silicalite-1 zeolites, has been frequently studied both in adsorbent and, perhaps even more frequently, in membrane applications. Our group has previously reported successful separation of carbon dioxide from methane using MFI membranes.[14] The membrane was evaluated at different process conditions, and it was concluded that the MFI membranes were promising candidates for separation of carbon dioxide from, for example, biogas and natural gas. The separation of carbon dioxide and methane from binary mixtures has also been investigated using membranes with different types of MFI films, viz., silicalite-1, Na-ZSM-5, and B-ZSM-5.[15] In that study it was found that the B-ZSM-5 zeolite showed the highest separation performance, and the authors attributed this to a stronger adsorption affinity for carbon dioxide toward the B-ZSM-5 compared to silicalite-1 and Na-ZSM-5. The behavior of binary mixtures of carbon dioxide and methane in MFI zeolite membranes has also been investigated using molecular dynamic simulations and Grand Canonical Monte Carlo simulations.[16−18] According to the simulations, the selectivity toward carbon dioxide increases with increasing pressure when adsorbed from an equimolar gas mixture. The ideal adsorbed solution theory (IAST) was used to predict the adsorbed loadings for binary mixtures, and it was reported that the IAST gave an accurate estimation of the loadings.

The separation of carbon dioxide from methane by zeolite adsorbents has been studied previously, primarily on other frameworks than MFI; however, a few experimental reports on the binary adsorption of carbon dioxide and methane in MFI exist.[19−21] For example, the binary adsorption in silicalite-1 was

Received: November 8, 2013
Revised: March 6, 2014
Published: March 7, 2014

dx.doi.org/10.1021/jp4110097 | J. Phys. Chem. C 2014, 118, 6207−6213

studied experimentally using different concentration pulse methods.[19] It was reported that silicalite-1 adsorbed more carbon dioxide compared to methane according to the pure gas isotherm data and the pure gas adsorption capacity was decreasing with increasing temperature. The results were compared to predicted isotherms by a number of models such as extended Langmuir, extended dual-site Langmuir, extended Sips, ideal adsorbed solution theory, Flory–Huggins vacancy solution theory, and the statistical model. All six prediction models gave similar results and showed a big difference between the experimental and the predicted values. It was determined that none of the models could be used confidently. The separation factor was determined for various compositions of the gas phase at all temperatures showing that the experimentally determined separation factors were much higher compared to the values predicted from the models mentioned above. The binary adsorption of carbon dioxide and methane has also been studied in H-ZSM-5 adsorbents of various Si/Al ratios using concentration pulse chromatography, and the experimental values were compared to values predicted by models such as extended Langmuir, extended Nitta, ideal adsorbed solution theory, and the Flory–Huggins vacancy solution theory.[20,21] Again, none of the models predicted the values reasonably well, but the values predicted by the IAST were closest to the experimental values.

In a recent work we successfully measured single component adsorption isotherms at different temperatures and pressures for carbon dioxide, water, and methane in a low alumina Na-ZSM-5 zeolite film using in situ ATR-FTIR spectroscopy.[22] A one point (one gas composition, one temperature) adsorption experiment was also performed for an equimolar mixture of carbon dioxide and methane at 35 °C. The amount of adsorbed carbon dioxide and methane was extracted from the experimental data, and the values were compared to values predicted by the IAST. These preliminary results indicated that the IAST could correctly predict the amount of adsorbed carbon dioxide and methane in an equimolar mixture.

In the present work, we study the binary adsorption of carbon dioxide and methane in the same zeolite film as in our recent work in much greater detail, aiming at understanding the adsorption behavior of this binary mixture. The experimental data obtained were compared to values predicted by the IAST model to further investigate if the IAST is a reliable model capable of accurately predicting the values for various gas compositions and not only for an equilmolar mixture. This work builds on our previously reported adsorption data with a view to better understand the binary adsorption properties of MFI zeolite membranes in removal of carbon dioxide from biogas and natural gas.

EXPERIMENTAL SECTION

Film Preparation. The zeolite film used in the present work is the same as the zeolite film used in our previous work, and the preparation and characterization of the film has been reported in detail elsewhere.[22,23] Therefore, only a brief summary will be given here. The zeolite film (ZSM-5, Si/Al = 130, Na/Al = 1) was synthesized on an ATR element (trapezoidal ZnS crystal, 50 × 20 × 2 mm, 45° cut edges, Spectral systems). The ATR element was thoroughly cleaned before being rendered positively charged by immersing it in a solution containing a cationic polymer. Thereafter, the ATR element was immersed in a seed suspension containing 50 nm silicalite-1 seed crystals creating a monolayer of seed crystals on the surface. Subsequently, the seeded ATR element was immersed in a synthesis solution for hydrothermal synthesis at 100 °C for 48 h under reflux. After cooling down, the zeolite film was rinsed with 0.1 M ammonia solution and distilled water. The zeolite film was dried overnight and thereafter calcined at 500 °C to remove the template molecules.

The calcined film was characterized by X-ray diffraction (XRD) and scanning electron microscopy (SEM) to confirm the zeolite phase and to determine the zeolite film thickness and morphology.

Adsorption Experiments. For the adsorption experiments, the zeolite coated ATR element was mounted in a heatable flow cell connected to a gas delivery system. The zeolite film was dried at 300 °C for 4 h under a flow of helium (AGA, 99.999%) prior to measurements, and a background spectrum of the dried film was recorded under a flow of helium. For each composition of the gas mixture (carbon dioxide, AGA, 99.995%, and methane, AGA, 99.9995%), spectra were recorded continuously until equilibrium was reached. All adsorption experiments were carried out at atmospheric pressure. Details of the equipment used have been given elsewhere.[22,24] Infrared spectra were recorded on a Bruker IFS 66v/S FTIR spectrometer equipped with a deuterated triglycine sulfate (DTGS) detector by averaging 256 scans at a resolution of 4 cm^{-1}.

The ATR Technique. The ATR technique[25] is based on internal reflection where the infrared beam is totally reflected in a waveguide (ATR element), see Figure 1. An electromagnetic

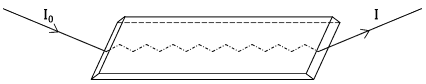

Figure 1. Schematic figure illustrating the ATR technique where the infrared beam is totally reflected inside a trapezoidal ATR element.

field originating from the infrared beam may interact with the sample in the vicinity of the waveguide, where some of the energy may be absorbed by the sample. The amplitude of the electromagnetic field will attenuate exponentially with distance from the element surface, making the ATR technique very useful for studying surfaces and thin films. The penetration depth of the electromagnetic field, d_p, is a rough measure of the distance outside the waveguide that is probed (typically a couple of hundreds of nm to a few μm) and can be determined by[26]

$$d_p = \frac{\lambda_1}{2\pi(\sin^2\theta - {n_{21}}^2)^{1/2}} \quad (1)$$

where λ_1 is the wavelength of the infrared radiation inside the ATR crystal, θ is the angle of incidence, and n_{21} is the ratio of the refractive indices of the zeolite film and the ATR element. The refractive index of ZnS is 2.25, whereas for the zeolite film the refractive index varies with loading.[27] To account for the change in refractive index with loading, a linear model[28] was assumed; however, as the refractive indices[29] of carbon dioxide and methane are quite similar to that of the zeolite film, the net effect was small under the conditions studied in the present work.

Theory. To calculate the adsorbed concentrations from infrared spectra, the Lambert–Beers law used for transmission experiments is not directly applicable to the ATR technique due

dx.doi.org/10.1021/jp4110097 | J. Phys. Chem. C 2014, 118, 6207–6213

to the exponential decay of the electric field. However, Tompkins[30] and Mirabella[25] have derived expressions for determining adsorbed concentrations from ATR experiments. The procedure and details for calculating the adsorbed concentrations in the zeolite films have been described in detail in our previous work[22] and are provided in the Supporting Information.

The IAST[31] was used to predict the adsorbed concentrations of carbon dioxide and methane in binary mixtures, and the values were compared to the experimental data. Details of the calculations used for the IAST have been described in our previous work[22] and are also included in the Supporting Information.

The CO_2/CH_4 adsorption selectivity[32] was determined as

$$\alpha_{CO_2/CH_4} = \frac{X_{CO_2}/X_{CH_4}}{Y_{CO_2}/Y_{CH_4}} \quad (2)$$

where X is the mole fraction in the adsorbed phase and Y is the mole fraction of the gas phase at equilibrium.

RESULTS AND DISCUSSION

Film Characterization. The zeolite film was characterized in detail in our previous work.[22] In brief, XRD data confirmed that the films consisted of randomly oriented zeolite ZSM-5 crystals. The SEM analysis showed that the films consisted of well-intergrown crystals forming a dense and homogeneous film without any sediment and with a film thickness of about 550 nm. Both the SEM images and the XRD patterns were very similar to those in previous reports on zeolite coated ATR elements.[23,28] The Si/Al ratio was determined to 130 by ICP-MS, and this particular Si/Al ratio was chosen as it is representative of the composition of the low-alumina ZSM-5 membranes prepared in our group.[33]

Adsorption Experiments. An infrared spectrum of carbon dioxide and methane adsorbed simultaneously in Na-ZSM-5 at 35 °C and a total pressure of 1 atm is shown in Figure 2. The partial pressures of carbon dioxide and methane in the gas phase were 3 and 98.3 kPa, respectively. The characteristic band of adsorbed carbon dioxide appears at 2338 cm^{-1} and is assigned to the asymmetric stretching vibration of physisorbed carbon dioxide.[34] The characteristic band of methane appears in the 3000−3030 cm^{-1} region with two peaks at 3015 cm^{-1} and 3003 cm^{-1} and is assigned to the C−H stretching vibrations.[35,36] The absorption bands assigned to carbon dioxide and methane are well separated in the spectrum and may therefore be used to monitor the change in adsorbed loading with changing partial pressure of the gases. Infrared spectra recorded at higher temperatures (50, 85, and 120 °C) were very similar in appearance but with less intensity of the bands, as expected due to the reduced adsorption at higher temperatures. In our previous work we performed experiments with an uncoated ATR element to assess the contribution from the gas phase on the measurements.[22] It was concluded that, at the conditions used in that work, as well as in the present work, the signal originating from the gas phase was negligible compared to the strong signal emanating from the adsorbed phase.

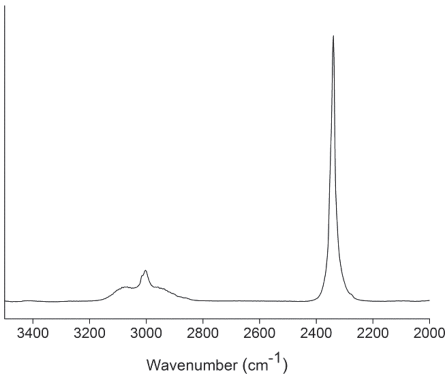

Figure 2. Infrared spectrum of carbon dioxide and methane adsorbed in Na-ZSM-5 film at 35 °C and a total pressure of 1 atm for a binary mixture of carbon dioxide and methane with a mole fraction of carbon dioxide in the gas phase of 0.03.

Figures 3a and 3b show the infrared spectra of adsorbed carbon dioxide and methane at various binary gas phase compositions as well as reference spectra recorded from single component adsorption for each gas. First of all, it is evident that the intensity of the absorption bands increases when the partial pressure of the gas increases, indicating an increased adsorption at higher partial pressures in the gas phase, as may be expected. Moreover, when comparing the bands in the spectra recorded with one adsorbed component to those recorded for adsorption from the binary mixture, the band positions and shapes are the same, indicating that there is no strong interaction between carbon dioxide and methane when adsorbed from the binary mixture.

The adsorbed concentrations were extracted from the IR spectra using the calculations presented in the Supporting Information and were plotted as a function of the mole fraction of carbon dioxide in the gas phase, see Figure 4. The amount adsorbed increases with increasing mole fraction in the gas phase and with decreasing temperature, as expected. Moreover, carbon dioxide is preferentially adsorbed compared to methane with adsorbed concentrations of carbon dioxide being almost 1 order of magnitude larger than that for methane at the same mole fraction in the gas phase. The preferential adsorption of carbon dioxide over methane is consistent with the larger Langmuir adsorption coefficients and heat of adsorption observed for carbon dioxide than for methane[16,19,21,22] (see Table 1 in the Supporting Information).

Comparison between Measured Adsorbed Concentrations and Those Predicted by the Ideal Adsorbed Solution Theory (IAST). The IAST was used to predict the amount adsorbed from binary mixtures using the Langmuir parameters (q_{sat} and b) determined in our previous work, see Table 1 in the Supporting Information. Figure 5 shows the adsorbed phase mole fractions of carbon dioxide and methane predicted by the IAST (solid lines) compared to the experimental data (markers) obtained in this work. As can be seen, the values predicted by the IAST agree very well with the experimental values. This is in accordance with findings previously reported by Krishna and van Baten,[16] but in contrast to the findings reported by Tezel and co-workers.[19−21] It can be seen that the curves for the three lowest temperatures are quite similar but the trend is that the adsorbed mole fraction of carbon dioxide is decreasing with increasing temperature. This trend is even clearer when including also the highest temperature, which shows a significantly lower adsorbed mole fraction of carbon dioxide compared to the lower temperatures.

dx.doi.org/10.1021/jp4110097 | J. Phys. Chem. C 2014, 118, 6207−6213

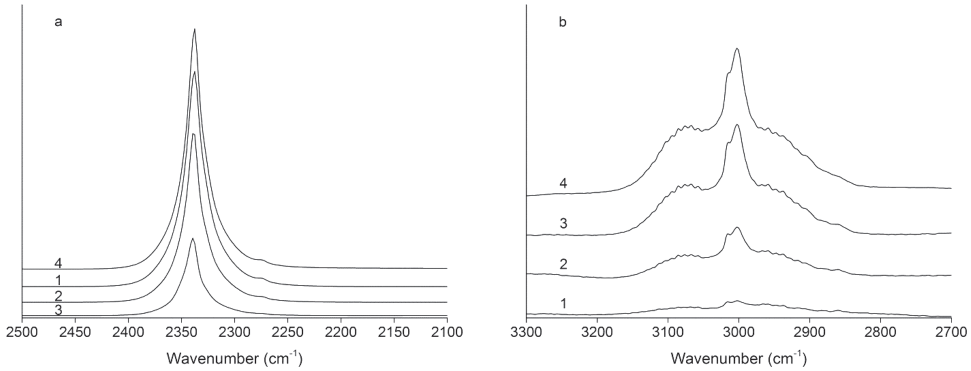

Figure 3. Infrared spectra of carbon dioxide (a) and methane (b) adsorbed in Na-ZSM-5 film at 35 °C for binary mixtures containing various mole fractions of carbon dioxide in the gas phase: 0.85 (1), 0.50 (2), 0.15 (3), and single gas[22] (4). The total pressure was 101.3 kPa.

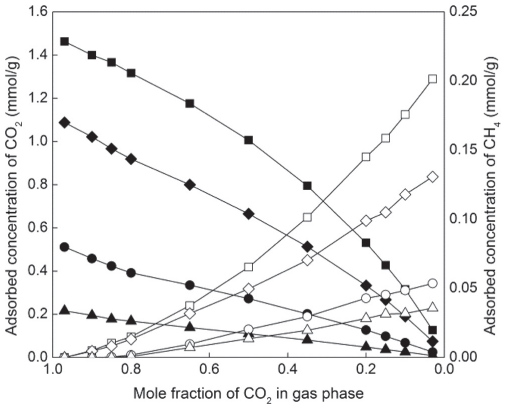

Figure 4. Adsorbed concentrations of carbon dioxide and methane as a function of the mole fraction of carbon dioxide in the gas phase at 35 °C (□), 50 °C (◇), 85 °C (○), and 120 °C (Δ). The filled symbols represent carbon dioxide, and the open symbols represent methane. Lines are only guides for the eyes.

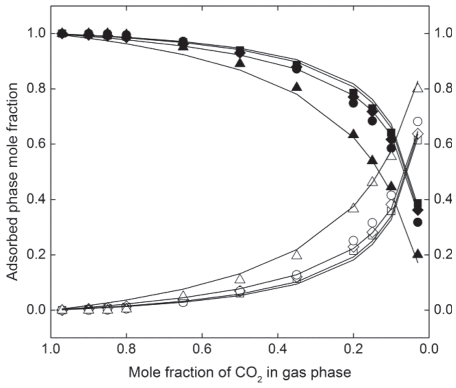

Figure 5. Experimentally determined adsorbed phase mole fraction as a function of the gas phase composition at 35 °C (□), 50 °C (◇), 85 °C (○), and 120 °C (Δ) compared to values predicted by the IAST. The filled symbols represent carbon dioxide, the open symbols represent methane, and the lines represent values predicted using the IAST. The total pressure was 101.3 kPa.

Since biogas and natural gas mainly consist of methane, the region with lower mole fraction of carbon dioxide is of special interest. For example, at a mole fraction of 0.2 of carbon dioxide in the gas phase, the corresponding mole fraction of carbon dioxide in the adsorbed phase is approximately 0.8 at 35 °C, indicating that, at a CO_2/CH_4 ratio in the gas phase typical for natural gas, the zeolite is selective toward carbon dioxide. At 120 °C and the same composition in the gas phase (a mole fraction of carbon dioxide of 0.2), the composition of the adsorbed phase is about 65% of carbon dioxide and 35% of methane, showing that the zeolite is less selective toward carbon dioxide at higher temperatures as may also be expected from the higher adsorption enthalpies for carbon dioxide than for methane.

As shown in the present work, the IAST provides a good estimation of the total amount of adsorbed gas in the zeolite film and can thus be satisfactorily used for predicting binary adsorption of carbon dioxide and methane in this low aluminum MFI zeolite.

Selectivity. The CO_2/CH_4 adsorption selectivity as a function of the mole fraction of carbon dioxide in the gas phase is presented in Figure 6a. At 35 °C the CO_2/CH_4 adsorption selectivity increases at the highest (0.9) and lowest (0.03) mole fractions of carbon dioxide in the gas phase with the highest selectivity values of 31.1 and 20.4, respectively. The same trend, with higher selectivities at the highest and lowest gas phase concentrations, is also observed at 50 °C. At 85 and 120 °C, however, the selectivity could not be determined for all mole fractions as the adsorption of methane was sometimes too low to be determined from the spectra, in particular at the higher temperatures and low methane content in the gas phase. Nevertheless, it can still be seen that the CO_2/CH_4 adsorption selectivity increases at the highest (0.65) and the lowest (0.03) mole fractions of carbon dioxide in the gas phase also at 85 and 120 °C. The CO_2/CH_4 adsorption selectivity predicted using the IAST as a function of the mole fraction of carbon dioxide in the gas phase is also presented in Figure 6a. As can be seen, the experimental data and the values predicted using the IAST lie in

dx.doi.org/10.1021/jp4110097 | J. Phys. Chem. C 2014, 118, 6207−6213

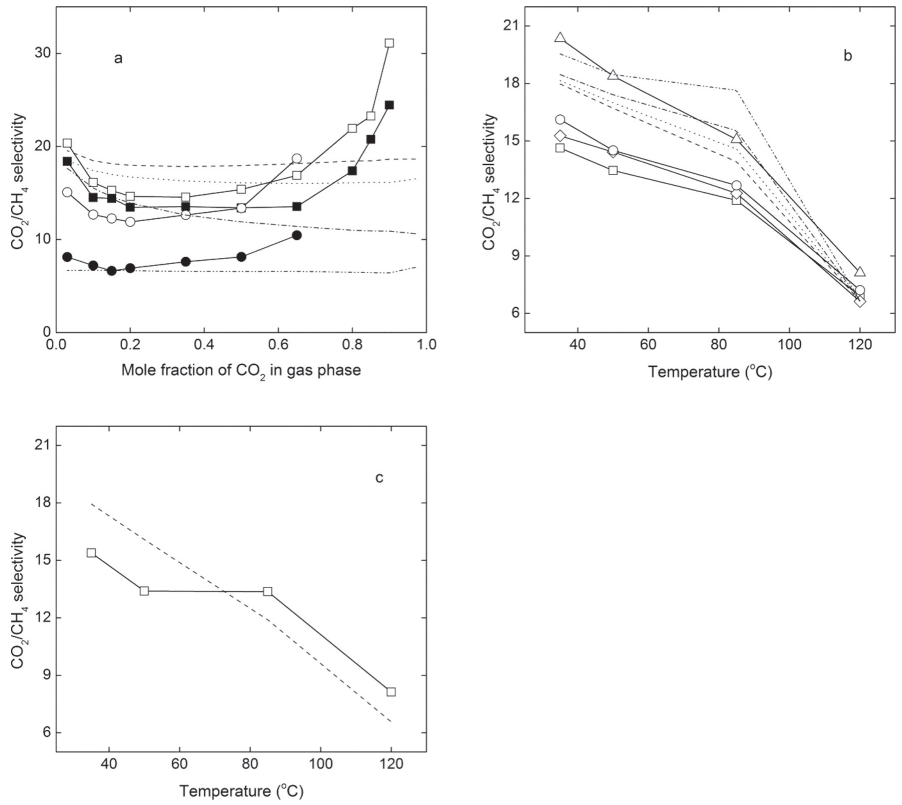

Figure 6. (a) Experimenlly determined CO_2/CH_4 selectivities at 35 °C (□), 50 °C (■), 85 °C (○), and 120 °C (●) compared to selectivity values predicted by the IAST at 35 °C (- - -), 50 °C (···), 85 °C (−•−), and 120 °C (−••−). (b) Experimentally determined CO_2/CH_4 selectivity as a function of temperature for various mole fractions of carbon dioxide in the gas phase indicated in the figure, 0.20 (□), 0.15 (◇), 0.10 (○), and 0.03 (Δ), along with selectivity values predicted by the IAST, 0.20 (- - -), 0.15 (···), 0.10 (−•−), and 0.03 (−••−). (c) Experimentally determined CO_2/CH_4 selectivity (□) as a function of temperature in an equimolar mixture of carbon dioxide and methane compared to selectivity values predicted by the IAST (- - -). The total pressure was always 101.3 kPa, and the solid lines are only guides for the eyes.

the same range but the values do not fit very well. Both the experimental data and the predicted values show an increase in the CO_2/CH_4 adsorption selectivity at lower mole fraction of carbon dioxide in the gas phase. At low content of carbon dioxide in the gas phase, the carbon dioxide will primarily be adsorbed on the high affinity sites (site 2 in Table 1 in the Supporting Information). There are only a few of these sites as evidenced by the relatively low saturation loading of 0.04 mmol/g compared to a total saturation capacity of 2.82 mmol/g. These high affinity sites likely correspond to polar sites associated with the sodium cations or silanol groups. As carbon dioxide is quadropolar and also has a higher polarizability than methane,[2,3] the adsorption selectivity should be higher for these sites than for sites not involving sodium cations or polar silanol groups. Indeed, other groups[2,15] have previously reported increasing adsorption selectivities of carbon dioxide over methane with increasing aluminum content and thus increasing polarity. The predicted values are a bit higher compared to the experimental data at 35, 50, and 85 °C, indicating that the IAST predicts a higher amount of adsorbed carbon dioxide at those temperatures than what is actually adsorbed in the zeolite film. According to the experimental data, the CO_2/CH_4 adsorption selectivity increases again also at higher mole fraction of carbon dioxide in the gas phase. This is probably the result of the low amount of adsorbed methane in the zeolite film which seemingly yields higher selectivities. The predicted CO_2/CH_4 adsorption selectivity values only show a slight increase at higher mole fraction of carbon dioxide in the gas phase (if any increase at all), indicating that the IAST cannot fully predict the CO_2/CH_4 adsorption selectivity when the amount of adsorbed methane in the zeolite film becomes too low.

Since methane is the main component in biogas and natural gas, with a content of 70−90%, the CO_2/CH_4 adsorption selectivity in this region is especially interesting, and we will therefore investigate this region more closely. Figure 6b shows the selectivity as a function of temperature for the four gas compositions with the highest methane content. All gas compositions show the same trend with the highest selectivity at the lowest temperature, reflecting the greater heat of adsorption (in absolute terms) of carbon dioxide compared to methane (see Table 1 in the Supporting Information), as discussed before. The CO_2/CH_4 adsorption selectivity

dx.doi.org/10.1021/jp4110097 | J. Phys. Chem. C 2014, 118, 6207−6213

predicted using the IAST as a function of temperature is also included in Figure 6b. In general, the predicted values are slightly higher compared to the experimental data, which, again, indicate that the IAST predicts a higher amount of adsorbed carbon dioxide than what is actually adsorbed in the zeolite film. The higher selectivities at low temperatures indicate that the separation of carbon dioxide from methane in biogas and natural gas may be more efficient at lower temperatures.

Selectivities from equimolar gas mixtures are commonly reported in the literature, and therefore we highlight this data as well. Figure 6c shows the CO_2/CH_4 adsorption selectivity when adsorbed from an equimolar gas mixture at different temperatures. Again, the highest selectivity of 15.4 was obtained at the lowest investigated temperature, and, in accordance with the results for the gas mixtures with low carbon dioxide content, the CO_2/CH_4 adsorption selectivity decreases with increasing temperature. The CO_2/CH_4 adsorption selectivity predicted using the IAST is also presented in Figure 6c, showing the same trend as the experimental data: decreasing with increasing temperature. The adsorption of carbon dioxide and methane in silicalite-1 has previously been studied by Li and Tezel.[19] When adsorbed from an equimolar mixture at 40 °C, the separation factor was reported to be 7. This value is a bit lower than the selectivity reported in the present work, which could be due at least partly to the temperature difference. The lower selectivity value could also be affected by the difference in Si/Al ratio as carbon dioxide in general adsorbs more strongly in the polar zeolites than in the hydrophobic pure silica analogue.[2] Moreover, different amounts of intracrystalline defects in the zeolite used in the work reported by Li and Tezel and in our work may also have affected the result. Intracrystalline defects create polar silanol groups which present different adsorption sites than the pore walls of zeolites without any defects. Krishna et al.[16] studied the separation of carbon dioxide from methane in a variety of zeolites using grand canonical Monte Carlo and molecular dynamics simulation techniques. It was reported that the CO_2/CH_4 sorption selectivity in MFI zeolite increased with increasing total loading: from 2 to 20 when the total loading increased from 0 to 6 mol/kg. A selectivity of 2.2 for silicalite-1 and 13 for Na-ZSM-5 with Si/Al = 23 at 27 °C and a pressure of 0.1 MPa has been reported by Krishna and van Baten.[2]

Compared to the literature, the relatively high selectivity values obtained in this study indicate that the separation of carbon dioxide from methane in biogas and natural gas may be efficient using membranes prepared from MFI zeolite. The presence of other components frequently encountered in biogas and natural gas such as water, hydrogen sulfide, and heavier hydrocarbons and how they affect the separation are also of great interest. The effect of some of these components on the adsorption of carbon dioxide and methane in MFI will be studied in forthcoming work.

CONCLUSIONS

The binary adsorption of carbon dioxide and methane in a low alumina Na-ZSM-5 zeolite film at various gas compositions and temperatures was studied using in situ ATR-FTIR spectroscopy. Adsorbed concentrations were retrieved from infrared spectra, and the values obtained were compared to values predicted using the ideal adsorbed solution theory. The predicted values were in good agreement with the experimental values showing that the IAST can be used for predicting adsorbed phase concentrations for various compositions of binary mixtures of carbon dioxide and methane in low alumina Na-ZSM-5. The CO_2/CH_4 adsorption selectivity determined showed an increase at the highest and lowest mole fractions of carbon dioxide in the gas phase at all studied temperatures. At 35 °C the highest selectivity values were 31.1 for the highest mole fraction (0.9) and 20.4 for the lowest mole fraction of carbon dioxide (0.03). The highest selectivity value observed for an equimolar mixture was 15.4 at 35 °C. The observed selectivity generally decreased with increasing temperature, indicating a more efficient separation of carbon dioxide from methane at lower temperatures. The relatively high selectivity values obtained in this study indicate that the separation of carbon dioxide and methane in biogas and natural gas may be efficient at low temperatures using a membrane prepared from the studied zeolite.

ASSOCIATED CONTENT

Supporting Information

Theory behind the calculation of the adsorbed concentrations from infrared spectra and the ideal adsorbed solution theory (IAST). Parameters of the dual site Langmuir model. This material is available free of charge via the Internet at http://pubs.acs.org.

AUTHOR INFORMATION

Corresponding Author

*Tel: +46 920 491928. E-mail: mattias.grahn@ltu.se.

Notes

The authors declare no competing financial interest.

ACKNOWLEDGMENTS

The financial support from The Swedish Energy Agency and the Swedish Research Council under Grant 621-2011-4060 is gratefully acknowledged. The Kempe foundation is acknowledged for funding of the spectroscopy lab. Linda Sandström is acknowledged for valuable discussions.

REFERENCES

(1) Baker, R. W. Future Directions of Membrane Gas Separation Technology. *Ind. Eng. Chem. Res.* **2002**, *41*, 1393−1411.
(2) Krishna, R.; van Baten, J. M. In Silico Screening of Zeolite Membranes for CO_2 Capture. *J. Membr. Sci.* **2010**, *360*, 323−333.
(3) D'Alessandro, D. M.; Smit, B.; Long, J. R. Carbon Dioxide Capture: Prospects for New Materials. *Angew. Chem., Int. Ed.* **2010**, *49*, 6058−6082.
(4) Li, S.; Falconer, J. L.; Noble, R. D. SAPO-34 Membranes for CO_2/CH_4 Separation. *J. Membr. Sci.* **2004**, *241*, 121−135.
(5) Mulgundmath, V. P.; Tezel, F. H.; Saatcioglu, T.; Golden, T. C. Adsorption and Separation of CO_2/N_2 and CO_2/CH_4 by 13X Zeolite. *Can. J. Chem. Eng.* **2012**, *90*, 730−738.
(6) Buss, E. Gravimetric Measurements of Binary Gas-Adsorption Equilibria of Methane-Carbon Dioxide Mixtures on Activated Carbon. *Gas Sep. Purif.* **1995**, *9*, 189−197.
(7) Tagliabue, M.; Rizzo, C.; Onorati, N. B.; Gambarotta, E. F.; Carati, A.; Bazzano, F. Regenerability of Zeolites as Adsorbents for Natural Gas Sweetening: A Case-Study. *Fuel* **2012**, *93*, 238−244.
(8) Xu, X.; Zhao, X.; Sun, L.; Liu, X. Adsorption Separation of Carbon Dioxide, Methane, and Nitrogen on H Beta and Na-Exchanged Beta-Zeolite. *J. Nat. Gas Chem.* **2008**, *17*, 391−396.
(9) Li, S.; Alvarado, G.; Noble, R. D.; Falconer, J. L. Effects of Impurities on CO_2/CH_4 Separations through SAPO-34 Membranes. *J. Membr. Sci.* **2005**, *251*, 59−66.
(10) Tomita, T.; Nakayama, K.; Sakai, H. Gas Separation Characteristics of DDR Type Zeolite Membrane. *Microporous Mesoporous Mater.* **2004**, *68*, 71−75.

(11) Poshusta, J. C.; Tuan, V. A.; Pape, E. A.; Noble, R. D.; Falconer, J. L. Separation of Light Gas Mixtures using SAPO-34 Membranes. *AIChE J.* **2000**, *46*, 779−789.
(12) Krishna, R.; Long, J. R. Screening Metal-Organic Frameworks by Analysis of Transient Breakthrough of Gas Mixtures in a Fixed Bed Adsorber. *J. Phys. Chem. C* **2011**, *115*, 12941−12950.
(13) Krishna, R.; van Baten, J. M. Investigating the Potential of MgMOF-74 Membranes for CO_2 Capture. *J. Membr. Sci.* **2011**, *377*, 249−260.
(14) Sandström, L.; Sjöberg, E.; Hedlund, J. Very High Flux MFI Membrane for CO_2 Separation. *J. Membr. Sci.* **2011**, *380*, 232−240.
(15) Othman, M. R.; Tan, S. C.; Bhatia, S. Separability of Carbon Dioxide from Methane using MFI Zeolite-Silica Film Deposited on Gamma-Alumina Support. *Microporous Mesoporous Mater.* **2009**, *121*, 138−144.
(16) Krishna, R.; van Baten, J. M. Using Molecular Simulations for Screening of Zeolites for Separation of CO_2/CH_4 Mixtures. *Chem. Eng. J.* **2007**, *133*, 121−131.
(17) Krishna, R.; van Baten, J. M.; Garcia-Perez, E.; Calero, S. Diffusion of CH_4 and CO_2 in MFI, CHA and DDR Zeolites. *Chem. Phys. Lett.* **2006**, *429*, 219−224.
(18) Krishna, R.; van Baten, J. M.; Garcia-Perez, E.; Calero, S. Incorporating the Loading Dependence of the Maxwell-Stefan Diffusivity in the Modeling of CH_4 and CO_2 Permeation Across Zeolite Membranes. *Ind. Eng. Chem. Res.* **2007**, *46*, 2974−2986.
(19) Li, P.; Tezel, F. H. Pure and Binary Adsorption Equilibria of Methane and Carbon Dioxide on Silicalite. *Sep. Sci. Technol.* **2007**, *42*, 3131−3153.
(20) Harlick, P. J. E.; Tezel, F. H. Adsorption of Carbon Dioxide, Methane, and Nitrogen: Pure and Binary Mixture Adsorption by ZSM-5 with SiO_2/Al_2O_3 Ratio of 30. *Sep. Sci. Technol.* **2002**, *37*, 33−60.
(21) Harlick, P. J. E.; Tezel, F. H. Adsorption of Carbon Dioxide, Methane and Nitrogen: Pure and Binary Mixture Adsorption for ZSM-5 with SiO_2/Al_2O_3 Ratio of 280. *Sep. Purif. Technol.* **2003**, *33*, 199−210.
(22) Ohlin, L.; Bazin, P.; Thibault-Starzyk, F.; Hedlund, J.; Grahn, M. Adsorption of CO_2, CH_4 and H_2O in zeolite ZSM-5 Zeolite Studied using in-situ ATR-FTIR Spectroscopy. *J. Phys. Chem. C* **2013**, *117*, 16972−16982.
(23) Wang, Z.; Grahn, M.; Larsson, M. L.; Holmgren, A.; Sterte, J.; Hedlund, J. Zeolite Coated ATR Crystal Probes. *Sens. Actuators, B* **2006**, *115*, 685−690.
(24) Grahn, M.; Wang, Z.; Lidström-Larsson, M.; Holmgren, A.; Hedlund, J.; Sterte, J.; Silicalite-1 Coated, A. T. R. Elements as Sensitive Chemical Sensor Probes. *Microporous Mesoporous Mater.* **2005**, *81*, 357−363.
(25) Mirabella, F. M., Ed. In *Internal Reflection Spectroscopy: Theory and Applicatons*; Marcel Dekker, Inc.: New York, 1993; Vol. *15*.
(26) Harrick, N. J. In *Internal Reflection Spectroscopy*; Wiley: New York, 1967.
(27) Nair, S.; Tsapatsis, M. Infrared Reflectance Measurements of Zeolite Film Thickness, Refractive Index and Other Characteristics. *Microporous Mesoporous Mater.* **2003**, *58*, 81−89.
(28) Grahn, M.; Holmgren, A.; Hedlund, J. Adsorption of n-Hexane and p-Xylene in Thin Silicalite-1 Films Studied by FTIR/ATR Spectroscopy. *J. Phys. Chem. C* **2008**, *112*, 7717−7724.
(29) Satorre, M. A.; Domingo, M.; Millan, C.; Luna, R.; Vilaplana, R.; Santonja, C. Density of CH_4, N_2 and CO_2 Ices at Different Temperatures of Deposition. *Planet. Space Sci.* **2008**, *56*, 1748−1752.
(30) Tompkins, H. G. The Physical Basis for Analysis of the Depth of Absorbing Species using Internal Reflection Spectroscopy. *Appl. Spectrosc.* **1974**, *28*, 335−341.
(31) Myers, A. L.; Prausnitz, J. M. Thermodynamics of Mixed-Gas Adsorption. *AIChE J.* **1965**, *11*, 121−127.
(32) Ruthven, D. M. In *Principles of Adsorption and Adsorption Processes*; Wiley-Interscience publication; Wiley: New York, 1984.
(33) Sandström, L.; Lindmark, J.; Hedlund, J. Separation of Methanol and Ethanol from Synthesis Gas using MFI Membranes. *J. Membr. Sci.* **2010**, *360*, 265−275.
(34) Rege, S. U.; Yang, R. T. A Novel FTIR Method for Studying Mixed Gas Adsorption at Low Concentrations: H_2O and CO_2 on NaX Zeolite and Gamma-Alumina. *Chem. Eng. Sci.* **2001**, *56*, 3781−3796.
(35) Scarano, D.; Bertarione, S.; Spoto, G.; Zecchina, A.; Arean, C. FTIR Spectroscopy of Hydrogen, Carbon Monoxide, and Methane Adsorbed and Co-Adsorbed on Zinc Oxide. *Thin Solid Films* **2001**, *400*, 50−55.
(36) Chen, L.; Lin, L.; Xu, Z.; Zhang, T.; Xin, Q.; Ying, P.; Li, G.; Li, C. Fourier Transform-Infrared Investigation of Adsorption of Methane and Carbon Monoxide on HZSM-5 and Mo/HZSM-5 Zeolites at Low Temperature. *J. Catal.* **1996**, *161*, 107−114.

Detailed Investigation of the Binary Adsorption of Carbon dioxide and Methane in Zeolite Na-ZSM-5 Studied Using *in-situ* ATR-FTIR Spectroscopy

*Lindsay Ohlin and Mattias Grahn**

Chemical Technology, Luleå University of Technology, 971 87 Luleå, Sweden

* Corresponding author. Tel: +46 920 491928; e-mail address: mattias.grahn@ltu.se

Calculating adsorbed concentrations from spectra recorded with the ATR-FTIR sampling technique

In a transmission experiment the spectral intensity (absorbance) is directly related to the concentration in the sample via the well-known Lambert-Beers law

$$A = \varepsilon c l \tag{1}$$

where A is the integrated absorbance, ε is the molar absorptivity, c is the concentration and l is the path length of the light beam in the sample (i.e. the thickness of the sample). To convert the spectral intensities in the spectra to adsorbed concentrations the molar absorptivity, ε, of the species adsorbed in ZSM-5 is needed. These were determined by a combined gravimetric and infrared set-up, AGIR, and the procedure for obtaining the molar absorptivities by this set-up has been described in detail elsewhere.[1, 2] The molar absorptivities for carbon dioxide (band at 2340 cm^{-1}) and methane (band at 3002 cm^{-1}) adsorbed in ZSM-5 were determined to 16.3 cm/µmol and 0.85 cm/µmol, respectively.[3]

The Lambert-Beers law is not directly applicable to the ATR technique because of the exponential decline of the electric field with distance from the ATR element/sample interface, which has to be accounted for. The procedure for determining adsorbed concentrations was derived by Tompkins[4] and Mirabella[5]. In an ATR experiment, the concentration of the adsorbed specie in the film is related to the absorbance band in the spectrum via

$$\frac{A}{N} = \frac{n_{21} E_0^2 \varepsilon}{\cos\theta} \int_0^\infty C(z) e^{-\frac{2z}{d_p}} dz \tag{2}$$

where A is the integrated absorbance of the band of interest, N is the number of reflections in the ATR-element (20 in our case), E_0 is the amplitude of the electric field at the ATR element/zeolite film interface, C(z) is the concentration of the adsorbate in the zeolite as a function of distance from the ATR element/zeolite film interface (assumed homogenous i.e. not varying with distance at equilibrium) and d_p is the penetration depth given by equation 1 in the main article. After integration the following equation is obtained

$$\frac{A}{N} = \frac{n_{21} E_0^2 d_p C}{2\cos\theta} \varepsilon \left(1 - e^{-\frac{2d_a}{d_p}}\right) \tag{3}$$

where d_a is the thickness of the zeolite film. In our previous work we have shown that the contribution from the gas phase is negligible and therefore it is sufficient to just integrate over the film thickness.[3] Further, the "effective thickness", d_e, of the electric field is given by[5, 6]

$$d_e = \frac{n_{21} E_0^2 d_p}{2\cos\theta} \tag{4}$$

The effective thickness is dependent on the polarization direction and may be estimated by[5]

$$d_e = \frac{I_{OII}}{I_{OII} + I_{O\perp}} d_{eII} + \frac{I_{O\perp}}{I_{OII} + I_{O\perp}} d_{e\perp} \tag{5}$$

where I_{0II} and $I_{0\perp}$ are the intensity of the radiation without sample for parallel and perpendicular polarized radiation (in the present work the contribution was 55% and 45% from the parallel and perpendicular polarization, respectively). Further, d_{eII} is the effective thickness for parallel polarization and is determined by

$$d_{eII} = \frac{2n_{21} d_p \cos\theta \, (2sin^2\theta - 2n_{21}^2)}{(1 - n_{21}^2)[(1 + n_{21}^2)sin^2\theta - n_{21}^2]} \tag{6}$$

and $d_{e\perp}$ is the effective thickness for perpendicular polarization and is determined by

$$d_{e\perp} = \frac{2n_{21} d_p \cos\theta}{1 - (n_{21})^2} \tag{7}$$

By combining equations 1-7 and equation 1 in the main article it is thus possible to calculate the adsorbed concentrations from infrared spectra recorded in an ATR experiment.

The Ideal Adsorbed Solution Theory (IAST)

The IAST developed by Myers and Prausnitz[7] provides a straightforward way of predicting binary adsorption from single component adsorption data. The IAST was used in the present work to estimate the adsorption equilibrium of gas mixtures based on the single gas adsorption isotherms determined in our previous work.[3] The equilibrium between the gas phase and the adsorbed can be expressed by

$$P_i = P_i^0(\pi_i) x_i \tag{8}$$

where P_i^0 is the pure component hypothetical pressure which yields the same spreading pressure as that of the mixture, π_i is the spreading pressure of component i in the adsorbed phase and x_i is the molar fraction. The reduced spreading pressures, at the adsorbed equilibrium, must be the same for each component and the mixture

$$\pi_i^* = \frac{\pi_i}{RT} = \int_0^{P_i^0} \frac{n_i^0(P)}{P} dP \qquad i = 1, 2, 3 \ldots, N \tag{9}$$

$$\pi_1^* = \pi_2^* = \cdots = \pi_N^* = \pi^* \tag{10}$$

where $n_i^0(P)$ is the pure component equilibrium capacity. By assuming ideal mixing at constant T and π, the total amount adsorbed is

$$\frac{1}{n_t} = \sum_{i=1}^{N} \left[\frac{x_i}{n_i^0(P_i^0)} \right] \tag{11}$$

with the constrain

$$\sum_{i=1}^{N} x_i = 1 \tag{12}$$

The IAST need parameters from single component adsorption isotherms as input. Table 1 shows the parameters of the dual site Langmuir model fitted to the experimental data from our previous work.[3]

Table 1. Saturation concentrations (q_{sat}, mmol/g), Langmuir adsorption coefficients (b, Pa^{-1}) and heat of adsorption (ΔH, kJ/mol) for carbon dioxide and methane adsorbed in Na-ZSM-5.[3]

Adsorbate	Temperature (°C)	q_1 (mmol/g)	b_1 (1/Pa)	q_2 (mmol/g)	b_2 (1/Pa)	ΔH (kJ/mol)
CO_2	35	2.78	$1.04 \cdot 10^{-5}$	0.04	$6.33 \cdot 10^{-4}$	-37 (site 1)
	50	2.78	$5.03 \cdot 10^{-6}$	0.04	$2.47 \cdot 10^{-4}$	-54 (site 2)
	85	2.78	$1.24 \cdot 10^{-6}$	0.04	$1.83 \cdot 10^{-5}$	
	120	2.78	$4.44 \cdot 10^{-7}$	0.04	$8.31 \cdot 10^{-6}$	
CH_4	35	2	$1.04 \cdot 10^{-6}$	-	-	-23
	50	2	$5.53 \cdot 10^{-7}$	-	-	
	85	2	$2.38 \cdot 10^{-7}$	-	-	
	120	2	$1.18 \cdot 10^{-7}$	-	-	

References

(1) Bazin, P.; Alenda, A.; Thibault-Starzyk, F. Interaction of Water and Ammonium in NaHY Zeolite as Detected by Combined IR and Gravimetric Analysis (AGIR). *Dalton Trans.* **2010**, *39*, 8432-8436.

(2) Moulin, B.; Oliviero, L.; Bazin, P.; Daturi, M.; Costentin, G.; Mauge, F. How to Determine IR Molar Absorption Coefficients of Co-Adsorbed Species? Application to Methanol Adsorption for Quantification of MgO Basic Sites. *Phys. Chem. Chem. Phys.* **2011**, *13*, 10797-10807.

(3) Ohlin, L.; Bazin, P.; Thibault-Starzyk, F.; Hedlund, J.; Grahn, M. Adsorption of CO_2, CH_4 and H_2O in zeolite ZSM-5 Zeolite Studied using in-situ ATR-FTIR Spectroscopy. *J. Phys. Chem. C* **2013**, *117*, 16972-16982.

(4) Tompkins, H. G. The Physical Basis for Analysis of the Depth of Absorbing Species using Internal Reflection Spectroscopy. *Appl. Spectrosc.* **1974**, *28*, 335-341.

(5) Mirabella, F. M., Ed.; In *Internal Reflection Spectroscopy : Theory and Applicatons;* Marcel Dekker, Inc.: New York, 1993; Vol. 15.

(6) Harrick, N. J. In *Internal reflection spectroscopy;* Wiley: New York, 1967; .

(7) Myers A.L.; Prausnitz J.M. Thermodynamics of Mixed-Gas Adsorption. *AIChE J.* **1965**, *11*, 121-127.

Paper III

Effect of water on the adsorption of methane and carbon dioxide in zeolite Na-ZSM-5 studied using in situ ATR-FTIR spectroscopy

Lindsay Ohlin, Vladimir Berezovsky, Sven Öberg, Amirfarrokh Farzaneh, Allan Holmgren and Mattias Grahn

Submitted to The Journal of Physical Chemistry C

Effect of Water on the Adsorption of Methane and Carbon dioxide in Zeolite Na-ZSM-5 Studied Using in situ ATR-FTIR Spectroscopy

Lindsay Ohlin[a], *Vladimir Berezovsky*[b], *Sven Öberg*[b], *Amirfarrokh Farzaneh*[a], *Allan Holmgren*[a] *and Mattias Grahn*[a]*

[a] Chemical Technology, Department of Civil, Environmental and Natural Resources Engineering, Luleå University of Technology, 971 87 Luleå, Sweden

[b] Applied physics, Department of Engineering Sciences and Mathematics, Luleå University of Technology, 971 87 Luleå, Sweden

* Corresponding author. Tel: +46 920 491928; e-mail address: mattias.grahn@ltu.se

ABSTRACT

Methane is the main component in biogas and natural gas along with contaminants such as water and carbon dioxide. Separation of methane from these contaminants is therefore an important step in the upgrading process. Zeolite adsorbents and zeolite membranes have great potential to be cost efficient candidates for upgrading biogas and natural gas, and in both of these applications knowing the nature of the competitive adsorption is of great importance to further develop the properties of the zeolite materials. The binary adsorption of methane and carbon dioxide in zeolites has been studied to some extent, but the influence of water has been much less studied. In the present work, in-situ ATR (Attenuated Total Reflection) - FTIR (Fourier Transform Infrared) spectroscopy was used to study the adsorption of water/methane and water/carbon dioxide from binary mixtures in a high silica Na-ZSM-5 zeolite film at various gas compositions and temperatures. Adsorbed concentrations for all species were determined from the recorded IR spectra, and the experimental values were compared to values predicted using the Ideal Adsorbed Solution Theory (IAST). At lower temperatures (35, 50 and 85 ºC), the IAST was able to predict the binary adsorption of water and methane, whereas the values predicted by the IAST deviated from the experimental data at the highest temperature (120 ºC). For the binary adsorption of water and carbon dioxide, the IAST could not predict the adsorption values accurately. This discrepancy was assigned to the particular adsorption behavior of water in high silica MFI forming clusters at hydrophilic sites. However, the predicted values did follow the same trend as the experimental values. The adsorption selectivity was determined, and it was found that the H_2O/CH_4 adsorption selectivity was decreasing with increasing water content in the gas phase at low temperatures, whereas the selectivity was increasing at higher temperatures.

The H_2O/CO_2 adsorption selectivity was increasing with increasing water content at all temperatures.

Keywords: water, carbon dioxide, methane, binary adsorption, ZSM-5, IAST, ATR-FTIR spectroscopy

INTRODUCTION

Biogas and natural gas are fuels with high H/C ratio which are interesting alternatives to fossil fuels derived from crude oil such as diesel and gasoline. Methane is usually the main component (60-95%), but the gases also contain contaminants such as water and carbon dioxide.[1-4] The presence of contaminants lowers the heat value and the separation of these compounds from methane is therefore of great importance. A commonly used technique for removal of carbon dioxide is amine absorption, this technique is efficient for obtaining low levels of carbon dioxide in the gas but expensive and energy demanding.[5] Therefore, other more energy efficient separation techniques are sought for. Adsorbent and membrane based processes are interesting alternatives, where zeolite adsorbents and membranes have shown great potential in the literature.[6-8] However, to accurately evaluate and further develop these materials, knowledge of the adsorption and mass transfer characteristics of the materials are pivotal. In particular, data on multicomponent adsorption is desirable as these are closer to practical applications.

The binary adsorption of methane and carbon dioxide in zeolites has been fairly well studied in the literature,[9-13] whereas the co-adsorption of water with carbon dioxide or methane has been much less studied. For binary adsorption of water and carbon dioxide, there is some FTIR data available in the literature, whilst data of binary adsorption of water and methane is scarce. Rege and Yang[14] studied single and mixed gas adsorption of water and carbon dioxide in zeolite NaX and γ-alumina using FTIR spectroscopy. The experimental data from binary mixtures of water and carbon dioxide was compared with two model predictions; the Doong-Yang (DY) and the IAST. The values predicted from both models were quite similar, especially for high concentration of the adsorbates and the models were able to predict the loading of water reasonably well in both NaX zeolite and γ-alumina. However, none of the models predicted the

loading of carbon dioxide very well, especially at low partial pressures. This was expected since both the DY and the IAST models assume ideality of the gases, and hence the lateral interactions between water and carbon dioxide were neglected. However, DY was marginally the better model since the predicted values for this model appeared to be closer to the experimental values. Brandani and Ruthven[15] used the zero length column (ZLC) method to study the effect of water on the adsorption of carbon dioxide in different types of X zeolites. The authors reported that the adsorption of carbon dioxide was inhibited in the presence of water. Wang and LeVan[16] studied adsorption of binary mixtures of water and carbon dioxide in zeolites 5A and 13X using a volumetric apparatus. They also reported that the adsorption of carbon dioxide was inhibited in the presence of water for both zeolites. Furthermore, the IAST was used to predict component loadings from binary adsorption showing that the predictions were close to the experimental data for low water loadings. However, the deviation between the predictions and the experimental data increased with increasing water loadings indicating a non-ideal system. Joos *et al.*[17] used Grand Canonical Monte Carlo (GCMC) simulations to study the competitive adsorption of water and carbon dioxide in zeolite 13X. Molecular simulations were performed for pure gas adsorption as well as binary mixtures. The authors concluded that for binary mixtures, water was the dominant adsorbed specie reducing the amount of available adsorption sites for carbon dioxide. The amount of adsorbed water was close to the loading obtained for the pure component whereas the adsorbed loading of carbon dioxide decreased compared to the case with pure component adsorption.

Several groups have reported the formation of water clusters when adsorbed in MFI zeolite.[18-23] Jentys *et al.*[18] studied the adsorption of water in H-ZSM-5 and alkali metal exchanged ZSM-5, all having a Si/Al ratio of 36, using transmission absorption infrared spectroscopy. It was

reported that the largest fraction of water molecules was adsorbed on the cations, and the concentration of adsorbed water was decreasing with increasing atomic number of the cation. For Na-ZSM-5, several water molecules were adsorbed on each cation without lateral interactions at lower equilibrium pressures (10^{-3} mbar). While increasing the pressure to 10^{-2} mbar, infrared bands appeared which were assigned to asymmetric adsorption of the first layer of water molecules around the cation. Continuing to increase the pressure (10^{-1} mbar) resulted in the formation of water clusters, where bands of OH-stretching vibrations associated with hydrogen-bonded perturbed water (inside the cluster), and unperturbed water (at the boundary of the cluster) appeared in the IR spectra. The interaction of water with the oxygen atoms in the zeolite structure was found to be negligible. Ari *et al.*[19] studied molecular dynamics simulations of water diffusion in MFI zeolites and reported formation of water clusters due to strong ion-dipole interactions when water molecules were located in the vicinity of the cation. Krishna and van Baten[20] used GCMC simulations to study adsorption and diffusion of polar molecules such as water and alcohols. It was reported that cluster formation of water occurred in MFI due to hydrogen bonding.

To the best of our knowledge, no data on the co-adsorption of water and methane in zeolite MFI has been reported in the open literature thus far. However, Müller *et al.*[24] studied the adsorption of water vapor and methane on activated carbons using grand canonical Monte Carlo simulations. For graphitic carbons, almost no adsorption of water occurred at moderate pressures while condensation of water in the pores occurred at higher pressures. Introducing oxygenated sites on the carbon surface enabled the formation of H-bonds between the water molecules and the surface sites. It was shown that the adsorption of water increased with the increasing density of surface sites leading to a reduction in the capacity of the carbon to adsorb methane. It was also

shown that the selectivity for methane was decreasing with the increasing density of surface sites.

We have previously studied adsorption of hydrocarbons in zeolite and single component adsorption of carbon dioxide, water and methane as well as the binary adsorption of carbon dioxide/methane mixtures in high silica Na-ZSM-5 using in-situ ATR-FTIR spectroscopy.[25-28] In the present paper, we extend our work by studying adsorption from binary mixtures of water/methane and water/carbon dioxide adsorbed in a high silica Na-ZSM-5 zeolite film. To the best of our knowledge, this is the first report on the binary adsorption of carbon dioxide/water and methane/water in high silica zeolite Na-ZSM-5.

EXPERIMENTAL

Synthesis and characterization

The zeolite Na-ZSM-5 film (Si/Al = 130) used in this work was grown on both sides of a trapezoidal ZnS crystal (Spectral systems, 50 x 20 x 2 mm, 45° cut edges) using a seeding method. The synthesis procedure and characterization have been described in detail elsewhere[27, 29], and only a short summary of the method is presented here. The cleaned ZnS crystal was immersed into a cationic polymer solution to render the surface positively charged. After rinsing with ammonia solution, the ZnS crystal was immersed in a seed suspension to create a monolayer of Silicalite-1 seed crystals on the surface. Thereafter, the seeded ZnS crystal was kept in a synthesis solution at 100 °C for 48 h under reflux to grow the seed crystals into a continuous zeolite film. After synthesis, the zeolite film was rinsed with ammonia solution and distilled water and then dried overnight. The zeolite film was thereafter calcined at 500 °C to remove the template molecules from the pore system.

X-ray diffraction (XRD) and scanning electron microscopy (SEM) were used to verify the zeolite phase formed and to determine the morphology and thickness of the film.

Adsorption experiments

A heatable flow cell connected to a gas delivery system was used to perform the adsorption experiments. The setup used to perform for the adsorption experiments have previously been described elsewhere.[27, 30] Prior to measurements, the zeolite film was dried by heating the cell to 300 °C under a flow of helium (AGA, 99.999%) in order to remove any adsorbed species. The cell was thereafter mounted into the infrared spectrometer, and a background spectrum was recorded under a flow of helium at the experimental temperature of interest. The binary adsorption experiments of water (distilled water)/methane (AGA, 99.9995%) and water/carbon

dioxide (AGA, 99.995%) were performed by stepwise increasing the partial pressure of one of the adsorbate while decreasing the partial pressure of the other adsorbate using a total pressure of 1 atm. For each composition of the gas mixture, spectra were recorded continuously until equilibrium was reached.

A Bruker IFS 66v/S FTIR spectrometer equipped with a deuterated triglycine sulphate (DTGS) detector was used to collect the infrared spectra. Spectra were recorded by averaging 256 scans at a resolution of 4 cm^{-1}.

Theory

The Lambert-Beers law is commonly used to calculate the concentrations from infrared spectra in transmission experiments. However, due to the exponential decay of the electric field, the Lambert-Beers law is not directly applicable to the ATR technique. Tompkins[31] and Mirabella[32] have derived expressions for determining adsorbed concentrations from ATR experiments. The following equation was used to determine the adsorbed concentrations in the zeolite film

$$\frac{A}{N} = \frac{n_{21} E_0^2 d_p C}{2\cos\theta} \varepsilon \left(1 - e^{-2d_a/d_p}\right) \qquad (1)$$

where A is the integrated absorbance, N is the number of reflections inside the ATR element (20 in this work), n_{21} is the ratio of the refractive indices of the denser (ATR element) and the rarer (zeolite film) medium, E_0 is the amplitude of the electric field at the ATR element/zeolite film interface, d_p is the penetration depth, C is the concentration of the adsorbate in the zeolite, θ is the angle of incidence (45º), ε is the molar absorptivity and d_a is the thickness of the zeolite film. Details of how to calculate the adsorbed concentrations in the zeolite film have been described in detail in our previous work.[27] To assess whether water interacting with carbon dioxide via a hydrogen bond would affect the molar absorptivity used in equation 1, and thus the adsorbed concentrations, a limited number of DFT (Density Functional Theory) calculations

were performed on free molecules (outside a zeolite lattice) of carbon dioxide and water and a hydrogen bonded complex. DFT calculations were executed using the Perdew-Burke-Ernzerhof (PBE) functional[33], and the dispersion corrections was included using the DFT-D2 method of Grimme[34, 35]. The calculations were performed with plane waves and ultrasoft pseudopotentials using Quantum Espresso (QE) version 5.0.2.[36] All pseudopotentials were taken from the QE pseudopotential library.[37] The kinetic energy cutoff was 47 Ry and the density cutoff 330 Ry for all calculations. Infrared spectra were calculated from the energy minimized structures and the intensities of the resulting peaks were used for estimating the effect on the molar absorptivities for water and carbon dioxide.

Myers and Prausnitz[38] proposed that the Ideal Adsorbed Solution Theory (IAST), based on Gibb´s adsorption isotherm, provides a link between single component and multicomponent adsorption. In this work, the IAST was used to predict the adsorbed concentrations of water, methane and carbon dioxide in binary mixtures (water/methane and water/carbon dioxide), and the values predicted by the IAST were compared to experimentally determined adsorbed concentrations. Furthermore, the adsorption selectivity[39] was determined by

$$\alpha_{i/j} = \frac{X_i / X_j}{Y_i / Y_j} \qquad (2)$$

where X_i and X_j are the equilibrium mole fractions of the components i and j in the adsorbed phase and Y_i and Y_i are the corresponding mole fractions in the gas phase.

RESULTS AND DISCUSSION

Film characterization

The zeolite film used in this work was characterized in detail in our previous work,[27] and only a short summary is given here. The zeolite film was confirmed by XRD data to consist of randomly oriented ZSM-5 crystals, and from the SEM analysis it was concluded that the zeolite film consist of well-intergrown crystals forming a continuous film with a thickness of about 550 nm. Both the XRD patterns and the SEM images were very similar to previous reports on zeolite coated ATR elements.[25, 29] The Si/Al ratio of the zeolite was determined to 130 by ICP-MS, and this particular Si/Al ratio was chosen as it represents the composition of the high silica ZSM-5 membranes studied for CO_2 separation in our research group.[40]

Adsorption experiments

Figure 1 shows infrared spectra of water and methane adsorbed from binary mixtures of varying compositions in the zeolite at 35 °C and a total pressure of 1 atm. Adsorbed water appeared in the spectra as a broad band with overlapping hydrogen bonding features in the 3750-2500 cm^{-1} range assigned to H-O-H asymmetric and symmetric stretching vibrations and a narrow band at ca. 1617 cm^{-1} with a shoulder at 1633 cm^{-1} assigned to O-H bending vibration.[41] The half-width of the latter band was considerably larger (62 cm^{-1}) than the infrared band at 1617 cm^{-1} (20 cm^{-1}). It is well known that the bending vibration of water shifts to higher wavenumber, whilst the stretching vibrations shift to lower wavenumber with increasing strength of the hydrogen bond, and simultaneously the half-width of the bands increase. Both the stretching vibrations and the bending vibration of water therefore show hydrogen bonded water. Assuming that the water molecules firstly occupies sodium sites in the Na-ZSM-5 structure through ion-dipole interaction, additional water molecules should be hydrogen bonded indicating the

formation of water clusters at high partial pressures of water, which is in agreement with the work of Jentys *et al.*[18] Alternatively, water may first also adsorb on polar silanol groups at intracrystaline defects, followed by water cluster formation at higher partial pressures. The C-H stretching vibrations of methane appeared as two bands at 3016 cm^{-1} and 3005 cm^{-1}.[42, 43] As expected, the intensity of the bands assigned to the water adsorbed in the zeolite is increasing with increasing partial pressure of water in the gas phase, and at the same time, the intensity of the bands assigned to adsorbed methane is decreasing. Spectra were of similar appearance but of lower intensity for co-adsorbed water and methane recorded at higher temperatures (50, 85 and 120 ºC). The adsorbed concentrations of water and methane were retrieved from the recorded infrared spectra using equation 1. The retrieved adsorbed concentrations were plotted as a function of the mole fraction of water in the gas phase, see Figure 2. The amount of adsorbed water is increasing with increasing mole fraction of water in the gas phase, whereas the amount of adsorbed methane is decreasing, as expected, and the adsorbed concentrations of both species are decreasing with increasing temperature. Water is preferentially adsorbed relative to methane and the adsorbed concentration of water is 2.48 mmol/g at the highest mole fraction of water in the gas phase at 35 ºC whilst the adsorbed concentration of methane is merely 0.087 mmol/g, although the partial pressure of methane is 47 times higher than that of water. At the lowest partial pressure of water (250 Pa) in the gas phase, where the partial pressure of methane is about 400 times higher, the adsorbed concentrations of water and methane are 0.015 mmol/g and 0.16 mmol/g, respectively. The preferential adsorption of water is consistent with the more negative heat of adsorption and larger Langmuir adsorption coefficient values for water compared to methane in high silica ZSM-5.[27] The adsorbed concentrations of water and methane from binary mixtures have been compared to the adsorbed concentrations from single gas experiments from

our previous work, see Table 1 in the supporting information. The amount of adsorbed water in the zeolite was slightly lower for the binary mixtures compared to the single gas experiments.[27] However, the amount of adsorbed methane was significantly lower viz. roughly half the concentration compared to the single gas experiment. This indicates a competitive adsorption between water and methane where methane is almost entirely suppressed by water, which is in agreement with the thermodynamic data, as mentioned earlier.

Figure 3 shows infrared spectra of water and carbon dioxide of various gas compositions adsorbed simultaneously in Na-ZSM-5 zeolite at 35 °C and, again, a total pressure of 1 atm. The bands assigned to adsorbed water are similar to the bands in Figure 1. The asymmetric stretching vibration of physisorbed carbon dioxide[14] appeared as a narrow band at 2338 cm^{-1}. The intensity of the bands increased with increasing partial pressure of each gas, as expected. The spectra of co-adsorbed water and carbon dioxide recorded at 50, 85 and 120 °C were similar in appearance although the intensity decreased with increasing temperature. However, in the spectrum of the adsorbed carbon dioxide, two well resolved bands appeared at 3698 cm^{-1} and 3596 cm^{-1}. These bands persist also upon increasing the partial pressure of water, although the intensity of the bands had decreased by about 15 % at the highest water concentration. The two bands were not resolved at any partial pressure of water in the H_2O/CH_4 system (Fig. 1). Thus it appears as if these absorption bands, caused by OH stretching vibrations, are mainly influenced by adsorbed CO_2 molecules. The wavenumber position of the bands indicate that the O-H functions are related to defects in the zeolite film and probably weakly hydrogen bonded to other O-H functions in the defect before they are allowed to interact with carbon dioxide molecules. The bands used for determining the adsorbed concentrations of water (1617 cm^{-1}) and carbon dioxide (2338 cm^{-1}), see equation 1, are well separated in the spectra. Figure 4 shows the retrieved

adsorbed concentrations plotted against the mole fraction of water in the gas phase. With increasing amount of water in the gas phase, the adsorbed amount of water in the zeolite increased whereas the amount of adsorbed carbon dioxide decreased, and as expected, the adsorbed concentrations of both species are decreasing with increasing temperature. For the highest mole fraction of water (0.02%, ca. 2 kPa) in the gas phase at 35 ºC, the adsorbed concentration of water and carbon dioxide was 2.13 mmol/g and 1.08 mmol/g, respectively, showing that water is preferentially adsorbed in the zeolite although the partial pressure of carbon dioxide is 47 times higher than that of water. Again, this is in agreement with the more negative heat of adsorption and the higher Langmuir adsorption coefficient values for water compared to carbon dioxide reported in our previous work.[27] However, the presence of water had a lesser effect on the amount of adsorbed carbon dioxide compared to methane, which can be seen upon comparison of Figures 2 and 4. The amount of adsorbed methane decreased much faster compared to carbon dioxide when the mole fraction of water in the gas phase is increased. The small decrease in the adsorbed concentration of carbon dioxide when water is co-adsorbed compared to when no water is present is striking. At 35°C and the highest partial pressure of water in the gas, the decrease in adsorbed concentration is ca 0.18 mmol/g (about 14 %) whereas the difference in adsorbed water is as high as 2.13 mmol/g. This indicates that the water to a large extent adsorbs on different sites than carbon dioxide. We suggest that this is due to formation of water clusters on the hydrophilic sites (sites associated to sodium/aluminum and internal silanol groups) in the zeolite, with little adsorption of water in the defect free parts of the framework, in accordance with previous findings.[18-23] On the contrary, carbon dioxide also adsorbs significantly on sites not associated with sodium/aluminum or lattice defects, i.e. the pore wall.[44] Thus, there seem to be some competition between water and carbon dioxide for the

hydrophilic sites with water being the stronger competitor, whereas most of the carbon dioxide adsorbs at sites of more hydrophobic character in defect free and aluminum free parts of the pore system.

To assess whether carbon dioxide interacting with water affected the molar absorptivity, ε, (and thus the adsorbed concentration) in equation 1, DFT calculations were performed. Simulated infrared spectra of free water and carbon dioxide molecules were compared to simulated infrared spectra of a water molecule interacting with a carbon dioxide molecule. For carbon dioxide, the ratio (interacting/free) for the asymmetric stretching vibration (same as used for quantification above) was ca. 0.87 whereas the corresponding ratio for water (bending vibration) was ca. 1.53, see supporting information. These numbers are fairly close to unity, and considering the results discussed above (i.e. that most of the carbon dioxide adsorbs on other sites than water), we conclude that the overall effect of water interacting with carbon dioxide on the adsorbed concentration of the two species will be small and was therefore neglected.

Experimentally determined values in comparison with values predicted by the Ideal Adsorbed Solution Theory (IAST)

Langmuir parameters (q_{sat} and b) for single component adsorption determined in our previous work[27] were used to predict the amount adsorbed from binary mixtures of water/methane and water/carbon dioxide. The adsorbed mole fractions of water and methane predicted by the IAST (solid lines) were compared to the experimental data (markers) obtained in this work and are presented in Figure 5a and b, respectively. The values predicted by the IAST agree very well with the experimental data at 35, 50 and 85 ºC. Values predicted by the IAST deviate slightly from the experimental values at 120 ^{o}C, which could be an effect of the low amount of adsorbed

methane at this temperature. Overall, the IAST seems to accurately predict the binary adsorption of water and methane at lower temperatures. However, at higher temperatures the IAST should be used with caution. Figure 6a and b show the mole fractions of the adsorbed water and carbon dioxide, respectively, predicted by the IAST (solid lines) and the experimental data (markers) as a function of the mole fraction of water in the gas phase. The values predicted by the IAST follows the same trend as the values determined experimentally. However, the IAST cannot fully capture the binary adsorption of water and carbon dioxide indicating a non-ideal adsorption behavior which is in line with previous reports.[14, 16] According to Rege and Yang,[14] the DY and IAST models were able to predict the loading of water reasonable well, but not the loading of carbon dioxide, due to the assumed ideality of the gases by the models. Wang and LeVan[16] showed that the IAST was able to predict the amount of adsorbed carbon dioxide fairly well at low water loadings and temperatures. However, at increasing water loadings and temperatures, there was a large deviation indicating a non-ideal system. Figure 6b shows that the deviation of the values predicted by the IAST from the experimental values is increasing with increasing water content in the gas phase. At 35, 50 and 85 ºC, the IAST is underestimating the amount of adsorbed carbon dioxide, but overestimates at the highest temperature. The discrepancy between the experimentally determined concentrations and those predicted by the IAST is again ascribed to the particular adsorption behaviors of water in MFI, where water is forming clusters at hydrophilic sites while carbon dioxide adsorbs throughout the whole pore system. The IAST is therefore not an optimal model for the prediction of the amount of adsorbed water and carbon dioxide from binary mixtures. The use of other, more sophisticated models, for predicting the binary adsorption from water/carbon dioxide mixtures in MFI zeolites is recommended. Rege and Yang[14] considered DY to be a more accurate model compared to the IAST since the

predicted values for this model appeared to be closer to the experimental values, as mentioned earlier. Furthermore, Wang and LeVan[16] reported the viral excess mixing coefficient (VEMC) model to have strong improvement over the IAST model. In addition, better models for describing adsorption with associated formation of clusters should be developed and possibly used in conjunction with the IAST to predict mixture adsorption of cluster forming species.

Selectivity

Figure 7 shows the H_2O/CH_4 adsorption selectivity as a function of the mole fraction of water in the gas phase at four different temperatures. At 35 and 50 ºC, the H_2O/CH_4 adsorption selectivity decreased with increasing water content in the gas phase, which is believed to be an effect of the formation of water clusters mentioned earlier. Furthermore, at lower water content in the gas phase a larger fraction of the water molecules will be adsorbed due to the strong affinity of water for the zeolite, and hence the H_2O/CH_4 adsorption selectivity will reach a higher value. When the water content in the gas phase is increasing, the fraction of the water molecules which will be adsorbed will decrease due to saturation of the hydrophilic sites and subsequent formation of clusters which results in lower H_2O/CH_4 adsorption selectivity. At 85 and 120 ºC, the H_2O/CH_4 adsorption selectivity decreased with increasing mole fraction of water in the gas phase which is due to the very small amount of methane adsorbed at higher temperatures. Methane not being adsorbed in the zeolite in detectable amounts at higher temperatures and higher mole fractions of water in the gas phase reduced the number of experimental data points for 85 and 120 ºC compared to 35 and 50 ºC. The H_2O/CO_2 adsorption selectivity as a function of the mole fraction of water in the gas phase at 35, 50, 85 and 120 ºC is shown in Figure 8. The selectivity decreased with increasing water content in the gas phase at all temperatures. Again, this can be explained by the formation of water clusters and the decreasing fraction of water

molecules being adsorbed when increasing the mole fraction of water in the gas phase as previously mentioned for the H_2O/CH_4 adsorption selectivity. Rege and Yang[14] studied binary adsorption of water and carbon dioxide in NaX zeolite at 22 ºC where the amount of water and carbon dioxide in the feed was a bit lower than in the present work. However, at the highest concentrations, 760 ppm and 3.59 % of water and carbon dioxide, respectively, they got a H_2O/CO_2 adsorption selectivity of 80. In the present work, a H_2O/CO_2 adsorption selectivity of 93 was determined for the highest amount of water in the gas phase. The slightly lower selectivity in the work of Rege and Yang, despite zeolite NaX being more hydrophilic, is probably a combined result of the differences in the total feed and the composition of the feed. Moreover, the selectivity in Figure 8 decreased with increasing water content and if one extrapolates the curve to the composition of Rege and Yang, the H_2O/CO_2 selectivity for the ZSM-5 film would probably be less than the selectivity of 80 determined from the work of Rege and Yang, as would be expected for high silica ZSM-5.

CONCLUSION

The binary adsorption of water/methane and water/carbon dioxide in a high silica zeolite Na-ZSM-5 film at various gas compositions and temperatures was studied using *in-situ* ATR-FTIR spectroscopy. Adsorbed concentrations were determined from the recorded infrared spectra showing that water is preferentially adsorbed compared to both methane and carbon dioxide and the presence of water had a lower effect on the amount of adsorbed carbon dioxide compared to methane. The adsorbed concentrations were compared to values predicted using the Ideal Adsorbed Solution Theory. The IAST was capable of predicting the binary adsorption of water and methane for the lowest temperatures studied in the present work while the predicted values deviated from the experimental data at the highest temperature studied. For the binary adsorption of water and carbon dioxide, the values predicted by the IAST followed the same trend as the experimental values. However, the IAST was not able to correctly predict the adsorption of water and carbon dioxide from binary mixtures. The deviation was assigned to the particular adsorption behavior of water in high silica MFI with cluster formation. The IAST is therefore not a reliable model for the prediction of binary mixtures of water and carbon dioxide. The H_2O/CH_4 adsorption selectivity decreased with increasing water content in the gas phase at low temperatures (35 and 50 ^oC), whereas the selectivity increased at higher temperatures (> 85 ^oC) . The H_2O/CO_2 adsorption selectivity decreased with increasing water content in the gas phase for all the studied temperatures. The decreasing selectivity for both the water/methane and the water/carbon dioxide mixtures can be explained by the formation of water clusters and the decreasing fraction of water molecules being adsorbed when increasing the mole fraction of water in the gas phase.

ACKNOWLEDGEMENT

The financial support from the Swedish Energy Agency and the Swedish Research Council under grant 621-2011-4060 is gratefully acknowledged. The Kempe foundation is acknowledged for funding of the spectroscopy lab.

Supporting information available: Heat of adsorption, saturation concentration and Langmuir adsorption coefficient for water, carbon dioxide and methane adsorbed in Na-ZSM-5 obtained in our previous work. This information is available free of charge via the Internet at http://pubs.acs.org.

REFERENCES

(1) Abdeshahian, P.; Dashti, M. G.; Kalil, M. S.; Yusoff, W. M. W. Production of Biofuel using Biomass as a Sustainable Biological Resource. *Biotechnology* **2010**, *9*, 274-282.

(2) Brown, R. C. In *Biorenewable resources : engineering new products from agriculture;* Iowa State Press: Ames, Iowa, 2003; .

(3) Cavenati, S.; Grande, C. A.; Rodrigues, A. E. Adsorption Equilibrium of Methane, Carbon Dioxide, and Nitrogen on Zeolite 13X at High Pressures. *J. Chem. Eng. Data* **2004**, *49*, 1095-1101.

(4) Busby, R. L. In *Natural gas in nontechnical language;* Busby, R. L., Ed.; Pennwell: Tulsa, Okla., 1999; .

(5) Baker, R. W. Future Directions of Membrane Gas Separation Technology. *Ind. Eng. Chem. Res.* **2002**, *41*, 1393-1411.

(6) Garcia-Perez, E.; Parra, J. B.; Ania, C. O.; Garcia-Sanchez, A.; van-Baten, J. M.; Krishna, R.; Dubbeldam, D.; Calero, S. A Computational Study of CO2, N-2, and CH4 Adsorption in Zeolites. *Adsorption* **2007**, *13*, 469-476.

(7) Krishna, R.; van-Baten, J. M. Segregation Effects in Adsorption of CO2-Containing Mixtures and their Consequences for Separation Selectivities in Cage-Type Zeolites. *Sep. Purif. Technol.* **2008**, *61*, 414-423.

(8) Lindmark, J.; Hedlund, J. Modification of MFI Membranes with Amine Groups for Enhanced CO(2) Selectivity. *J. Mater. Chem.* **2010**, *20*, 2219-2225.

(9) Krishna, R.; van Baten, J. M. Using Molecular Simulations for Screening of Zeolites for Separation of CO2/CH4 Mixtures. *Chem. Eng. J.* **2007**, *133*, 121-131.

(10) Harlick, P. J. E.; Tezel, F. H. Adsorption of Carbon Dioxide, Methane and Nitrogen: Pure and Binary Mixture Adsorption for ZSM-5 with SiO2/Al2O3 Ratio of 280. *Sep. Purif. Technol.* **2003**, *33*, 199-210.

(11) Li, S.; Falconer, J. L.; Noble, R. D. SAPO-34 Membranes for CO2/CH4 Separation. *J. Membr. Sci.* **2004**, *241*, 121-135.

(12) Mulgundmath, V. P.; Tezel, F. H.; Saatcioglu, T.; Golden, T. C. Adsorption and Separation of CO2/N2 and CO2/CH4 by 13X Zeolite. *Can. J. Chem. Eng.* **2012**, *90*, 730-738.

(13) Xu, X.; Zhao, X.; Sun, L.; Liu, X. Adsorption Separation of Carbon Dioxide, Methane, and Nitrogen on H Beta and Na-Exchanged Beta-Zeolite. *J. Nat. Gas Chem.* **2008**, *17*, 391-396.

(14) Rege, S. U.; Yang, R. T. A Novel FTIR Method for Studying Mixed Gas Adsorption at Low Concentrations: H2O and CO2 on NaX Zeolite and Gamma-Alumina. *Chem. Eng. Sci.* **2001**, *56*, 3781-3796.

(15) Brandani, F.; Ruthven, D. M. The Effect of Water on the Adsorption of CO_2 and C_3H_8 on Type X Zeolites. *Ind. Eng. Chem. Res.* **2004**, *43*, 8339-8344.

(16) Wang, Y.; LeVan, M. D. Adsorption Equilibrium of Binary Mixtures of Carbon Dioxide and Water Vapor on Zeolites 5A and 13X. *J. Chem. Eng. Data* **2010**, *55*, 3189-3195.

(17) Joos, L.; Swisher, J. A.; Smit, B. Molecular Simulation Study of the Competitive Adsorption of H_2O and CO_2 in Zeolite 13X. *Langmuir* **2013**, .

(18) Jentys, A.; Warecka, G.; Derewinski, M.; Lercher, J. Adsorption of Water on ZSM5 Zeolites. *J. Phys. Chem.* **1989**, *93*, 4837-4843.

(19) Ari, M. U.; Ahunbay, M. G.; Yurtsever, M.; Erdem-Senatalar, A. Molecular Dynamics Simulation of Water Diffusion in MFI-Type Zeolites. *J. Phys. Chem. B* **2009**, *113*, 8073-8079.

(20) Krishna, R.; van Baten, J. M. Hydrogen Bonding Effects in Adsorption of Water-Alcohol Mixtures in Zeolites and the Consequences for the Characteristics of the Maxwell-Stefan Diffusivities. *Langmuir* **2010**, *26*, 10854-10867.

(21) Trzpit, M.; Soulard, M.; Patarin, J.; Desbiens, N.; Cailliez, F.; Boutin, A.; Demachy, I.; Fuchs, A. H. The Effect of Local Defects on Water Adsorption in Silicalite-1 Zeolite: A Joint Experimental and Molecular Simulation Study. *Langmuir* **2007**, *23*, 10131-10139.

(22) Ahunbay, M. G. Monte Carlo Simulation of Water Adsorption in Hydrophobic MFI Zeolites with Hydrophilic Sites. *Langmuir* **2011**, *27*, 4986-4993.

(23) Desbiens, N.; Boutin, A.; Demachy, I. Water Condensation in Hydrophobic Silicalite-1 Zeolite: A Molecular Simulation Study. *J. Phys. Chem. B* **2005**, *109*, 24071-24076.

(24) Müller, E. A.; Hung, F. R.; Gubbins, K. E. Adsorption of Water Vapor-Methane Mixtures on Activated Carbons. *Langmuir* **2000**, *16*, 5418-5424.

(25) Grahn, M.; Holmgren, A.; Hedlund, J. Adsorption of N-Hexane and P-Xylene in Thin Silicalite-1 Films Studied by FTIR/ATR Spectroscopy. *J. Phys. Chem. C* **2008**, *112*, 7717-7724.

(26) Grahn, M.; Lobanova, A.; Holmgren, A.; Hedlund, J. Orientational Analysis of Adsorbates in Molecular Sieves by FTIR/ATR Spectroscopy. *Chem. Mater.* **2008**, *20*, 6270-6276.

(27) Ohlin, L.; Bazin, P.; Thibault-Starzyk, F.; Hedlund, J.; Grahn, M. Adsorption of CO_2, CH_4 and H_2O in zeolite ZSM-5 Zeolite Studied using in-situ ATR-FTIR Spectroscopy. *J. Phys. Chem. C* **2013**, *117*, 16972-16982.

(28) Ohlin, L.; Grahn, M. Detailed Investigation of the Binary Adsorption of Carbon Dioxide and Methane in Zeolite Na-ZSM-5 Studied using in Situ ATR-FTIR Spectroscopy. *J. Phys. Chem. C* **2014**, *118*, 6207-6213.

(29) Wang, Z.; Grahn, M.; Larsson, M. L.; Holmgren, A.; Sterte, J.; Hedlund, J. Zeolite Coated ATR Crystal Probes. *Sens. Actuators, B* **2006**, *115*, 685-690.

(30) Grahn, M.; Wang, Z.; Lidström-Larsson, M.; Holmgren, A.; Hedlund, J.; Sterte, J. Silicalite-1 Coated ATR Elements as Sensitive Chemical Sensor Probes. *Microporous Mesoporous Mater.* **2005**, *81*, 357-363.

(31) Tompkins, H. G. The Physical Basis for Analysis of the Depth of Absorbing Species using Internal Reflection Spectroscopy. *Appl. Spectrosc.* **1974**, *28*, 335-341.

(32) Mirabella, F. M., Ed.; In *Internal Reflection Spectroscopy : Theory and Applicatons;* Marcel Dekker, Inc.: New York, 1993; Vol. 15.

(33) Perdew, J. P.; Burke, K.; Ernzerhof, M. Generalized Gradient Approximation made Simple. *Phys. Rev. Lett.* **1996**, *77*, 3865.

(34) Grimme, S. Semiempirical GGA-Type Density Functional Constructed with a Long-Range Dispersion Correction. *J. Comput. Chem.* **2006**, *27*, 1787-1799.

(35) Grimme, S.; Antony, J.; Ehrlich, S.; Krieg, H. A Consistent and Accurate Ab Initio Parametrization of Density Functional Dispersion Correction (DFT-D) for the 94 Elements H-Pu. *J. Chem. Phys.* **2010**, *132*, 154104.

(36) Giannozzi, P., et al QUANTUM ESPRESSO: A Modular and Open-Source Software Project for Quantum Simulations of Materials. *J. Phys. : Condens. Matter* **2009**, *21*, 395502.

(37) http://www.quantum-espresso.org/pseudopotentials/ (accessed July, 2014).

(38) Myers, A. L.; Prausnitz, J. M. Thermodynamics of Mixed-Gas Adsorption. *AIChE J.* **1965**, *11*, 121-127.

(39) Ruthven, D. M. In *Principles of adsorption and adsorption processes;* Wiley-Interscience publication; Wiley: New York, 1984; .

(40) Sandström, L.; Lindmark, J.; Hedlund, J. Separation of Methanol and Ethanol from Synthesis Gas using MFI Membranes. *J. Membr. Sci.* **2010**, *360*, 265-275.

(41) Zou, X.; Bazin, P.; Zhang, F.; Zhu, G.; Valtchev, V.; Mintova, S. Ethanol Recovery from Water using Silicalite-1 Membrane: An Operando Infrared Spectroscopic Study. *ChemPlusChem* **2012**, *77*, 437-444.

(42) Scarano, D.; Bertarione, S.; Spoto, G.; Zecchina, A.; Arean, C. FTIR Spectroscopy of Hydrogen, Carbon Monoxide, and Methane Adsorbed and Co-Adsorbed on Zinc Oxide. *Thin Solid Films* **2001**, *400*, 50-55.

(43) Chen, L.; Lin, L.; Xu, Z.; Zhang, T.; Xin, Q.; Ying, P.; Li, G.; Li, C. Fourier Transform-Infrared Investigation of Adsorption of Methane and Carbon Monoxide on HZSM-5 and Mo/HZSM-5 Zeolites at Low Temperature. *J. Catal.* **1996**, *161*, 107-114.

(44) Wirawan, S. K.; Creaser, D. CO2 Adsorption on Silicalite-1 and Cation Exchanged ZSM-5 Zeolites using a Step Change Response Method. *Microporous Mesoporous Mater.* **2006**, *91*, 196-205.

Figure 1. Infrared spectra of water and methane for various compositions of the gas phase simultaneously adsorbed in Na-ZSM-5 at 35 °C. The total pressure was 1 atm where the partial pressure of water was 0, 378, 755, 1647 and 2105 Pa, starting from the bottom spectrum.

Figure 2. Adsorbed concentrations of water and methane as a function of the mole fraction of water in the gas phase at 35°C (□), 50°C (◊), 85°C (○) and 120°C (Δ). The filled markers are representing water and the open markers are representing methane. The lines are only a guide for the eyes.

Figure 3. Infrared spectra of water and carbon dioxide for various compositions of the gas phase simultaneously adsorbed in Na-ZSM-5 at 35 °C. The total pressure was 1 atm where the partial pressure of water was 0, 378, 755, 1647 and 2105 Pa, starting from the bottom spectrum.

Figure 4. Adsorbed concentrations of water and carbon dioxide as a function of the mole fraction of water in the gas phase at 35°C (□), 50°C (◊), 85°C (○) and 120°C (Δ). The filled markers are representing water and the open markers are representing carbon dioxide. The lines are only a guide for the eyes.

Figure 5. Experimentally determined adsorbed phase mole fraction of water (a) and methane (b) as a function of mole fraction of water in the gas phase and values predicted by the IAST at 35°C (□,–), 50°C (◊,---), 85°C (○,···) and 120°C (Δ,-·-). The markers are representing the experimental data and the lines represent values predicted using the IAST. The total pressure was 101.3 kPa.

Figure 6. Experimentally determined adsorbed phase mole fraction of water (a) and carbon dioxide (b) as a function of mole fraction of water in the gas phase and values predicted by the IAST at 35°C (□,–), 50°C (◊,---), 85°C (○,···) and 120°C (Δ,-·-). The markers are representing the

experimental data and the lines represent values predicted using the IAST. The total pressure was 101.3 kPa.

Figure 7. H_2O/CH_4 selectivity as a function of mole fraction of water in the gas phase at 35°C (□), 50°C (◊), 85°C (○) and 120°C (Δ) and a total pressure of 101.3 kPa

Figure 8. H_2O/CO_2 selectivity as a function of mole fraction of water in the gas phase at 35°C (□), 50°C (◊), 85°C (○) and 120°C (Δ) and a total pressure of 101.3 kPa.

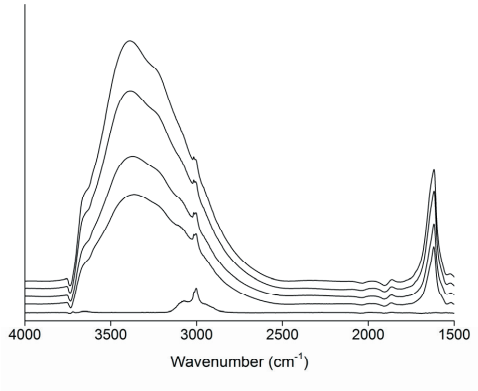

Figure 1

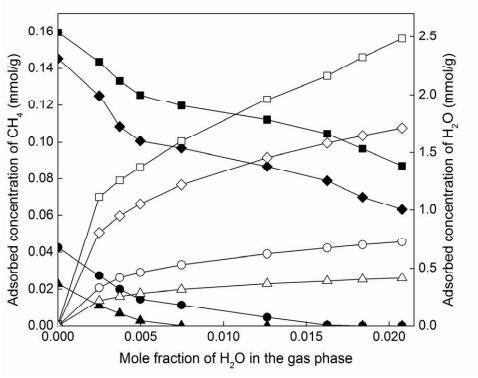

Figure 2

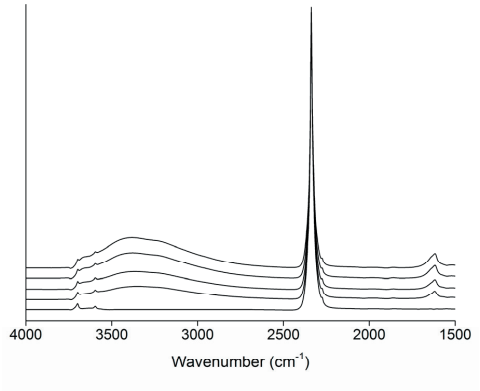

Figure 3

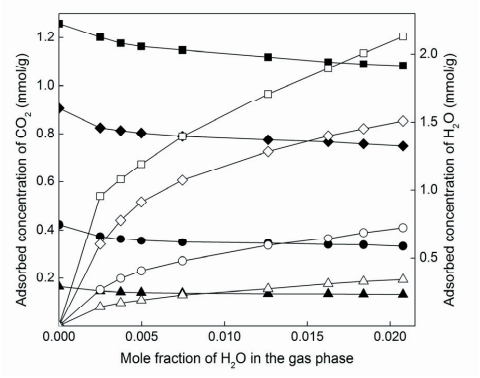

Figure 4

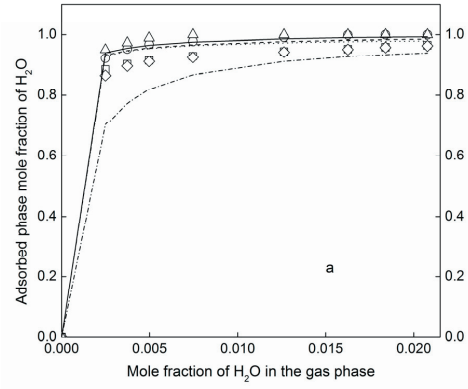

Figure 5a

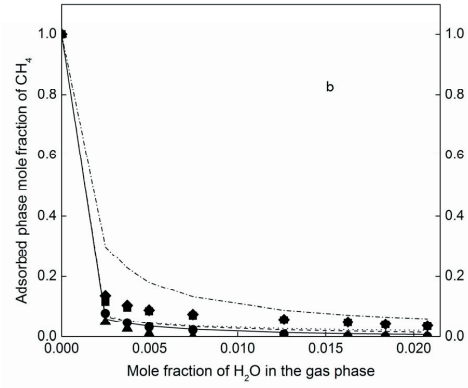

Figure 5b

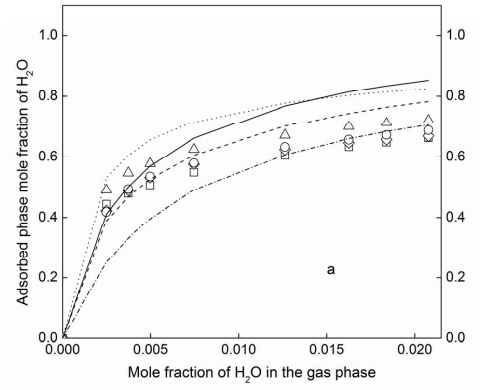

Figure 6a

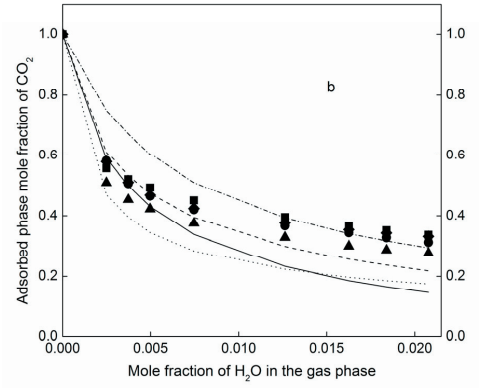

Figure 6b

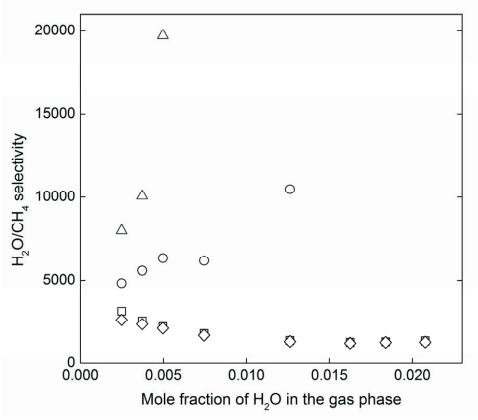

Figure 7

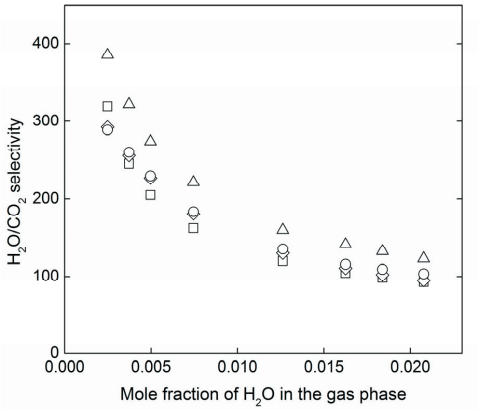

Figure 8

Effect of Water on the Adsorption of Methane and Carbon dioxide in Zeolite Na-ZSM-5 Studied Using in situ ATR-FTIR Spectroscopy

*Lindsay Ohlin[a], Vladimir Berezovsky[b], Sven Öberg[b], Amirfarrokh Farzaneh[a], Allan Holmgren[a] and Mattias Grahn[a]**

[a] Chemical Technology, Department of Civil, Environmental and Natural Resources Engineering, Luleå University of Technology, 971 87 Luleå, Sweden

[b] Applied physics, Department of Engineering Sciences and Mathematics, Luleå University of Technology, 971 87 Luleå, Sweden

* Corresponding author. Tel: +46 920 491928; e-mail address: mattias.grahn@ltu.se

The adsorbed concentrations of water, methane and carbon dioxide retrieved from binary mixtures in this work were compared to the adsorbed concentrations from single gas experiments in our previous work[1], see Table 1. The adsorbed concentrations were retrieved from infrared spectra at 35 °C using a total pressure of 101300 Pa. Experimental data from binary mixtures and from the single gas experiments were compared at the same partial pressure region. The Langmuir model was used to predict values for methane and carbon dioxide where no experimental data existed. The adsorbed concentration of water from single gas experiments is clearly higher compared to the adsorbed concentrations from the binary mixtures. The amount of water adsorbed in the zeolite is much lower in the H_2O/CO_2 mixture compared to the H_2O/CH_4 mixture indicating a much stronger competitive adsorption between water and carbon dioxide compared to water and methane, as may be expected. This is also confirmed when comparing the adsorbed concentrations between single gas experiments and binary mixtures for both methane and carbon dioxide.

To assess whether interactions between water and carbon dioxide molecules could affect the molar absorptivity when calculating the concentration of the adsorbed species, a limited number of DFT calculations were executed. Figure 1 represents simulated infrared spectra of free water and carbon dioxide molecules compared to simulated infrared spectra of a water molecule interacting with a carbon dioxide molecule. The interacting/free ratio is about the same for both water and carbon dioxide and the overall effect of the interaction between water and carbon dioxide on the concentration was small and was therefore neglected.

Table 1. Comparison of the adsorbed concentrations of water, methane and carbon dioxide in Na-ZSM-5 at 35 °C at a total pressure of 101300 Pa.

Adsorbate	Gas composition	Partial Pressure (Pa)	Adsorbed concentration (mmol/g)	Data	Reference
H_2O	single	2105	2.878	experimental	1
	H_2O/CH_4	2105	2.484	experimental	Present work
	H_2O/CO_2	2105	2.130	experimental	Present work
CH_4	single	96896	0.181	experimental	1
	single	99195	0.187	Langmuir	1
	single	101300	0.188	experimental	1
	H_2O/CH_4	99195	0.087	experimental	Present work
CO_2	single	11918	0.345	experimental	1
	single	99195	1.454	Langmuir	1
	single	101300	1.468	experimental	1
	H_2O/CO_2	99195	1.082	experimental	Present work

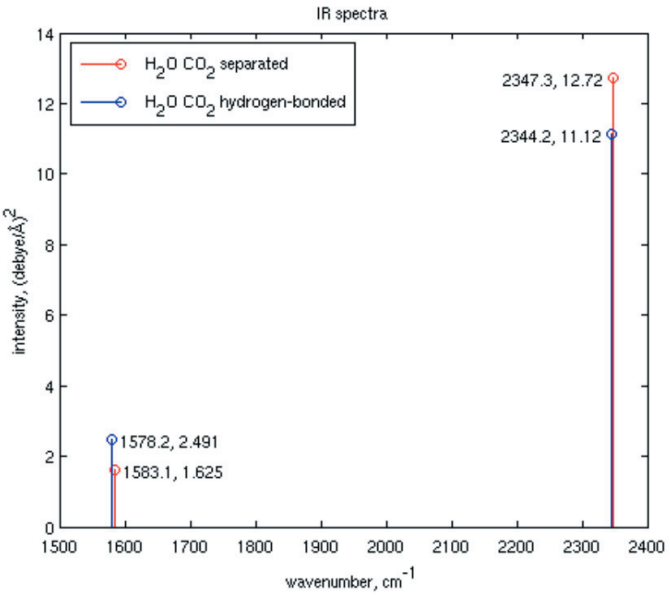

Figure 1. Simulated infrared spectra of water and carbon dioxide in free form and when interacting with each other.

References

(1) Ohlin, L.; Bazin, P.; Thibault-Starzyk, F.; Hedlund, J.; Grahn, M. Adsorption of CO_2, CH_4 and H_2O in zeolite ZSM-5 Zeolite Studied using in-situ ATR-FTIR Spectroscopy. *J. Phys. Chem. C* **2013**, *117*, 16972-16982.

Paper IV

Ternary adsorption of methane, water and carbon dioxide in zeolite Na-ZSM-5 studied using in situ ATR-FTIR spectroscopy

Lindsay Ohlin, Amirfarrokh Farzaneh, Allan Holmgren, Jonas Hedlund and Mattias Grahn

Manuscript

Ternary Adsorption of Methane, Water and Carbon dioxide in Zeolite Na-ZSM-5 Studied Using in situ ATR-FTIR Spectroscopy

*Lindsay Ohlin, Amirfarrokh Farzaneh, Allan Holmgren, Jonas Hedlund and Mattias Grahn**

Chemical Technology, Luleå University of Technology, 971 87 Luleå, Sweden

*Corresponding author. Tel: +46 920 491387, e-mail address: mattias.grahn@ltu.se

ABSTRACT

The main component in biogas and natural gas is methane. The gases also contain water and carbon dioxide and these components have to be removed in order to increase the calorific value of the gas. Membrane and adsorbent based technologies using zeolites are interesting alternatives for efficient separation of these components. To develop efficient processes, it is essential to know the adsorption properties of the zeolite. In the present work, adsorption from ternary mixtures (methane, water and carbon dioxide) in zeolite Na-ZSM-5 was studied using in-situ ATR (Attenuated Total Reflection) – FTIR (Fourier Transform Infrared) spectroscopy. Adsorbed concentrations were extracted from the infrared spectra and the observed loadings were compared to values predicted by the Ideal Adsorbed Solution Theory (IAST). However, the IAST could not fully capture the adsorption behavior of this ternary mixture, indicating that the adsorbed phase is not behaving as an ideal mixture. CO_2/CH_4 adsorption selectivities determined for ternary mixtures were compared to selectivities determined for binary mixtures in our previous work, indicating that the presence of water slightly improves the CO_2/CH_4 adsorption selectivity at lower temperatures. Further, the results show that ZSM-5 has a higher affinity for water and carbon dioxide compared to methane which implies that low alumina zeolite Na-ZSM-5 could be a promising membrane material for carbon dioxide and water separation from biogas.

Keywords: biogas, ternary adsorption, zeolite ZSM-5, IAST, selectivity

INTRODUCTION

Natural gas is a fossil fuel containing methane as the main components (80-95%) and various amounts of carbon dioxide, water and trace components.[1, 2] Even though natural gas is a fossil fuel, it is one of the most abundant assets in the world[3] and it is considered as helpful in the transition from fossil fuels to renewable fuels. Biogas is a renewable resource and an interesting alternative to fossil fuels. The gas is produced from anaerobic degradation of biomass where methane (about 60-70%) is the main component.[4, 5] The heat value of natural gas and biogas is reduced due to the presence of water and carbon dioxide. To upgrade biogas and natural gas and hence increase the heat value, amine absorption is commonly used today.[6] Adsorption and membrane based technologies where zeolite adsorbents/membranes are used is an interesting option for more energy efficient upgrading of both biogas and natural gas.[7, 8] For both adsorbent and membrane applications, detailed knowledge of the adsorption properties of methane, water and carbon dioxide in the zeolite is of great importance both for further development of the materials but also for optimizing the performance of the separation process. Single component adsorption experiments are commonly used as a start to determine the adsorption properties of zeolites. For example, Choudhary *et al*.[9], Sun *et al*.[10] and Dunne et al.[11, 12] used gravimetry to study single component adsorption of methane and carbon dioxide in MFI zeolites, whereas Bao *et al*.[13] used volumetric measurements. Jentys *et al.*[14] used transmission absorption infrared spectroscopy to study the adsorption of water in H-ZSM-5 and alkali metal exchanged ZSM-5 with a Si/Al ratio of 36. The largest fraction of water molecules was adsorbed on the cations whereas the interaction of water with the oxygen atoms in the zeolite structure was found to be negligible. At low equilibrium pressures, several water molecules were adsorbed on each cation in Na-ZSM-5 without lateral interactions. According to interpretation of the IR spectra, the

formation of water clusters was confirmed at higher pressures, where bands of OH-stretching vibrations associated with hydrogen-bonded water inside the clusters (perturbed water), and water at the boundary of the clusters (unperturbed water) were observed. Ari *et al.*[15] used molecular dynamics simulations to study the diffusion of water in MFI zeolites and reported formation of water clusters due to strong ion-dipole interactions when water molecules were located in the vicinity of the cation. Krishna and van Baten[16] studied the adsorption and diffusion of polar molecules such as water and alcohols using GCMC simulations, and reported that cluster formation of water occurred in MFI due to hydrogen bonding. Water clusters were also believed to be formed within defects containing silanol groups. Such defects are typically formed during synthesis at high pH, which is usually the case for zeolite MFI.[17] Multicomponent adsorption in zeolites is frequently non-ideal and a deviation from models assuming an ideal behavior, such as the extended Langmuir model or the Ideal adsorbed solution theory (IAST), is therefore expected. These models are popular because they only require single component adsorption data as input and can be used to illustrate deviations from ideality. Consequently, it is of interest to study multicomponent adsorption and to assess whether these models are suitable for predicting the multicomponent adsorption behavior or if more sophisticated models ought to be used. Despite the practical importance of the effect of intermolecular interactions within multicomponent mixtures, experimental data on multicomponent adsorption is scarce. For the methane/carbon dioxide system, experimental data on co-adsorption primarily exists for other zeolite frameworks than MFI, although various concentration pulse methods have been used to study this binary adsorption in MFI.[18-20] More commonly, the behavior of binary mixtures of methane and carbon dioxide in MFI zeolite has been studied using molecular dynamic simulations and Grand Canonical Monte Carlo (GCMC) simulations.[21-23] For binary adsorption

of mixtures containing water, there are some data available in the literature concerning water and carbon dioxide mixtures. Data of binary adsorption of water and methane, on the other hand, is scarce. For binary adsorption of water and carbon dioxide, Rege and Yang[24] studied adsorption in NaX zeolite and on γ-alumina using Fourier-transform infrared (FTIR) spectroscopy, whereas Brandani and Ruthven[25] used the zero length column (ZLC) method to study the binary adsorption of these gases in different type of X zeolites. Furthermore, Wang and LeVan[26] studied adsorption in zeolites 5A and 13X using a volumetric apparatus and Joos *et al.*[27] used GCMC simulations to study the competitive adsorption of water and carbon dioxide in zeolite 13X. However, to the best of our knowledge, there is only one report on binary adsorption of water and methane in MFI zeolite.[28] We have previously reported experimental data from single gas[29] adsorption of methane, carbon dioxide and water as well as binary adsorption of methane/carbon dioxide[30], water/methane[28] and water/carbon dioxide[28] mixtures in Na-ZSM-5 zeolite using ATR-FTIR (attenuated total reflection – Fourier transform infrared) spectroscopy. Studies of adsorption from mixtures containing all three components are of great importance as ternary mixtures have a higher resemblance to real biogas. However, in general, literature regarding adsorption of ternary mixtures is very scarce.

In this paper we present experimental data from ternary adsorption mixtures including three of the main components, i.e. methane, carbon dioxide and water, in natural gas and biogas for the first time.

EXPERIMENTAL

Synthesis and characterization

A trapezoidal ZnS crystal (Spectral systems, 50 x 20 x 2 mm, 45° cut edges) was used as a support when growing the ZSM-5 zeolite film (Si/Al = 130, Na/Al = 1) using a seeding method. The sample preparation and characterization has previously been described in detail,[29, 31] hence the procedure will only be briefly presented here. The ZnS crystal was thoroughly cleaned in acetone, ethanol and distilled water using an ultrasonic bath prior to seeding. The surface was rendered positively charged by immersing the ZnS crystal in a cationic polymer solution. After rinsing with ammonia solution, a monolayer of silicalite-1 seed crystals was deposited on the surface by immersing the ZnS crystal in a seed suspension. To grow the seed crystals into a continuous zeolite film, the seeded ZnS crystal was kept in a synthesis solution under reflux at 100 °C for 48 h. The zeolite film was then carefully rinsed, dried overnight and finally calcined at 500 °C.

Scanning electron microscopy (SEM) and X-ray diffraction (XRD) were used to determine the thickness and morphology of the film and to verify the zeolite phase formed.

Adsorption experiments

After synthesis, the zeolite coated ZnS crystal was mounted into a flow cell which was connected to a gas delivery system. In order to remove any pre-adsorbed species, the zeolite film was dried under a flow of helium (AGA, 99.999 %) by heating the cell to 300 °C for four hours. Prior to measurements, a background spectrum of the dried film was recorded under a flow of helium at the temperature at which the adsorption experiment was to be performed. The ternary adsorption experiments using mixtures of water (distilled water), methane (AGA, 99.9995 %) and carbon dioxide (AGA, 99.995 %) were performed by stepwise increasing the partial pressure

of methane and water while decreasing the partial pressure of carbon dioxide at a total pressure of 1 atm. A stream of methane gas was passed through a saturator filled with distilled water in order to saturate the gas with water vapor. The temperature of the saturator was controlled in order to reach a specific partial pressure of water in the gas phase. The stream of methane gas containing water vapor was mixed with a stream of carbon dioxide gas, and the stream was fed to the flow cell. Spectra were recorded every 5 minutes for each composition of the gas phase until equilibrium was reached. A more detailed description of the equipment can be found elsewhere.[29, 32] Infrared spectra were recorded using a Bruker IFS 66v/S FTIR spectrometer equipped with a deuterated triglycine sulphate (DTGS) detector by averaging 256 scans at a resolution of 4 cm^{-1}.

Theory

In transmission experiments, the adsorbed concentration is determined using the well-known Lambert-Beers law, however, this relationship is not directly applicable to the ATR technique due to the geometry of the experimental set-up and the exponential decay of the electric field penetrating outside the surface of the ATR crystal. Fortunately, expressions for determining the adsorbed concentrations from ATR experiments have been derived by Tompkins[33] and Mirabella[34]. Adsorbed concentrations were calculated from the infrared spectra using equation 1

$$\frac{A}{N} = \frac{n_{21} E_0^2 d_p C}{2\cos\theta} \varepsilon \left(1 - e^{-\frac{2d_a}{d_p}} \right) \qquad (1)$$

where A is the integrated absorbance of a characteristic band in the infrared spectrum, N is the number of reflections inside the ATR element, n_{21} is the ratio of the refractive indices of the denser (ZnS element) and the rarer (zeolite film) medium, E_0 is the amplitude of the electric field at the ATR element/zeolite film interface, d_p is the penetration depth, C is the concentration of

the adsorbate in the zeolite, θ is the angle of incidence, ε is the molar absorptivity and d_a is the thickness of the zeolite film. The penetration depth, d_p, is a rough measure of the distance outside the ZnS crystal that is probed by the electromagnetic field originating from the infrared beam and is given by equation 2

$$d_p = \frac{\lambda_1}{2\pi(\sin^2\theta - n_{21}^2)^{1/2}} \qquad (2)$$

where λ_1 is the wavelength of the infrared radiation inside the ATR crystal. Details of how to calculate the adsorbed concentrations in the zeolite film have been described in detail in our previous work.[29] Myers and Prausnitz[35] proposed that the IAST provides a link between single component and multicomponent adsorption. Because of this convenient link, together with the fact that for many systems it works well, it has gained popularity as a simple means for predicting multicomponent adsorption in zeolites.[18-21, 24, 26] In this work, the IAST was used to predict the adsorbed concentrations of water, methane and carbon dioxide in ternary mixtures for various compositions of the gas phase and the predicted values were compared to the adsorbed concentrations determined experimentally. The single component adsorption data required was taken from our previous study[29] using the same zeolite film. Saturation loadings and Langmuir parameters used are presented in table 1 in the supporting information. The adsorption selectivity[36] is an important parameter to indicate the potential of an adsorbent or membrane to selectively separate molecules from each other and was determined by

$$\alpha_{i/j} = \frac{X_i / X_j}{Y_i / Y_j} \qquad (3)$$

where *i* and *j* represents gas components, *X* is the mole fraction in the adsorbed phase and *Y* is the mole fraction of the gas phase at equilibrium.

RESULTS AND DISCUSSION

Film characterization

SEM images reported in our previous work[29] showed that the zeolite film had a thickness of about 550 nm, consisting of well-intergrown crystals forming a continuous film. The XRD analysis of the zeolite film showed that the film consists of randomly oriented ZSM-5 crystals.[29] Both the SEM images and the XRD pattern were very similar to previous reports on zeolite coated ATR elements.[31, 37] The Si/Al and Na/Al ratios of crystals prepared from a synthesis solution with the same composition as that used for growth of the zeolite film were determined to 130 and 1, respectively, using Inductively Coupled Plasma Mass Spectrometry (ICP-MS).

Adsorption experiments

Infrared spectra of water, methane and carbon dioxide adsorbed from ternary mixtures of various compositions of the gas phase at 35 °C are presented in Figure 1. The broad band in the 3750-2500 cm^{-1} region is assigned to the O-H stretching vibration of adsorbed water whereas the band at ca. 1617 cm^{-1} is assigned to the bending vibration of adsorbed water.[38] The broad band is associated with hydrogen bonded water indicating the formation of water clusters and only a very small amount of water (if any) interacts with the defect free parts of the pores, which is in agreement with the work of Jentys *et al.*[14] Bands in the 3050-2950 cm^{-1} region are assigned to the C-H stretching vibration of adsorbed methane,[39, 40] where two bands can be observed at 3016 cm^{-1} and 3005 cm^{-1}. The most prominent band in the spectra is found at 2338 cm^{-1} and is assigned to the asymmetric stretching vibration of physisorbed carbon dioxide.[24] The top spectrum in Figure 1 was recorded at the lowest amount of water (0.03 mole %) in the gas phase with methane and carbon dioxide concentrations of 16.66 and 83.31 mole %, respectively. At this gas phase composition, the amount of adsorbed methane in the zeolite film is very low,

whereas the amount of adsorbed carbon dioxide is very high, which can be explained by the difference in the partial pressure of the gases but also by the stronger affinity of carbon dioxide compared to methane. The Langmuir adsorption coefficients reported in our previous work[29], and presented in table 1 in the supporting information, reveals that the Langmuir adsorption coefficients for carbon dioxide is about 10 times higher than the corresponding coefficients for methane. In the experiments carried out in the present work, the total pressure was always 1 atm, and as the partial pressures of water and methane were increased, the partial pressure of carbon dioxide was decreased. Hence, the bottom spectrum was recorded at the highest amount of water (0.63%) and methane (82.81%) and the lowest amount of carbon dioxide (16.56%) in the gas phase. With increasing concentration of water and methane in the gas phase, the intensities of the bands assigned to water and methane increased while the intensity of the band assigned to carbon dioxide decreased, as expected. Spectra of adsorbed water, methane and carbon dioxide from ternary mixtures recorded at higher temperatures (50, 85 and 120 ºC) were similar in appearance, but with lower intensity, as expected from the reduced adsorption at higher temperatures. Integration of the bands for methane (3016 cm^{-1} and 3005), carbon dioxide (2338 cm^{-1}) and water (1617 cm^{-1}) was performed to determine the adsorbed concentrations of each species using the calculations presented in detail in our previous work.[29] The retrieved adsorbed concentrations plotted against the mole fraction of water in the gas phase are presented in Figure 2 for water (a), methane (b) and carbon dioxide (c). Figure 2 shows that the amount of adsorbed water and methane increased with increasing mole fraction of water (and methane) in the gas phase whereas the amount of adsorbed carbon dioxide decreased (due to the amount of carbon dioxide was decreased in the gas phase as the amount of water and methane was increased). At the highest mole fraction of water in the gas phase at 35 ºC, where the partial pressure of methane

and carbon dioxide was 131 and 26 times higher, respectively, than that of water, the adsorbed concentration of water is 1.92 mmol/g while the adsorbed concentration of methane and carbon dioxide is 0.11 mmol/g and 0.37 mmol/g, respectively. This clearly indicates that water is preferentially adsorbed in the zeolite compared to both methane and carbon dioxide, as expected due to the more negative heat of adsorption and larger Langmuir adsorption coefficient values for water compared to both methane and carbon dioxide. Values for the heat of adsorption and Langmuir adsorption coefficient are presented in table 1 in the supporting information. Water and carbon dioxide are first adsorbed on vacant high affinity sites, i.e. polar sites associated with sodium ions or defects in the form of silanol groups. In addition, carbon dioxide adsorbs on other sites on the defect free parts of the pore walls[41], i.e. essentially silicalite-1 walls considering the low aluminum content (Si/Al=130) of this zeolite. As discussed earlier, water on the other hand seems to form clusters on the polar sites and very little water (if any) seem to interact with the defect free parts of the pores. In fact, CBMC simulations on water adsorption in defect free silicalite-1 show that substantial partial pressure, in the order of as much as 90-130 MPa, of water is needed for water to adsorb in the defect free parts of the pores.[17] Recently, Trzpit *et al*.[17] and Zhang *et al*.[42] studied adsorption of water in silicalite-1 samples prepared by both conventional synthesis at high pH and essentially defect free crystals prepared by the fluoride route[43]. In concert with the modeling results, significantly less water adsorbed in the essentially defect free samples. Adsorbed concentrations of carbon dioxide (a) and methane (b), from binary mixtures reported in our previous work[30] and from ternary mixtures (also including water in the gas phase) reported in this work, as a function of the mole fraction of carbon dioxide in the gas phase are shown in Figure 3. At lower temperatures (35 and 50 ºC), the adsorbed concentrations of carbon dioxide and methane show a decrease for ternary mixtures compared to binary

mixtures. This was expected since water has a much higher affinity for the zeolite compared to both carbon dioxide and methane at lower temperatures, see table 1 in the supporting information, and hence the effect of water is greater compared to higher temperatures. At higher temperatures (85 and 120 ºC), the adsorption of carbon dioxide and methane seem to be unaffected by the presence of water and no significant change in the adsorbed concentrations is found. This may be an effect of the low loadings at higher temperatures for both carbon dioxide and methane, due to adsorption being an exothermic reaction. For example, the highest loadings of carbon dioxide observed at 85 and 120°C were only 0.42 and 0.18 mmol/g, respectively. This corresponds to about 8.1 and 3.5 % of the total capacity, respectively.[44] At these low loadings one can expect that the competition is not noticeable because of the high abundance of vacant sites. Moreover, water has a higher affinity for the zeolite compared to both carbon dioxide and methane also at higher temperatures; however, the difference in affinity is much smaller at higher temperatures compare to lower temperatures, see table 1 in the supporting information. Hence, the presence of water has a greater effect on the adsorption of carbon dioxide and methane at lower temperatures compared to higher temperatures. In general, water has a stronger effect on the adsorption of methane compared to carbon dioxide as seen in our previous work.[28]

Comparison between experimentally determined adsorbed concentrations and values predicted by the IAST

The IAST was used for predicting the amount of adsorbed water, methane and carbon dioxide from ternary gas mixtures. This model requires input in the form of single component parameters from a suitable adsorption model. In this work, we used the Langmuir parameters (saturation concentration, q_{sat}, and Langmuir adsorption coefficients, b) determined from single component adsorption measurements performed in our previous work[29]. Figure 4 shows the adsorbed phase

mole fractions of water (a), methane (b) and carbon dioxide (c) as a function of the mole fraction of water in the gas phase, where values predicted by the IAST (solid lines) are compared to the experimental data (markers) obtained in the present work. For methane, the values predicted by the IAST agree reasonably well with the experimental data, which is in agreement with our previous work.[28-30] Values predicted by the IAST deviate slightly from the experimental values at 120 ^{o}C, which could be an effect of the low amount of adsorbed methane at this temperature. For water and carbon dioxide, the values predicted by the IAST follows the same trend as the experimental values, but the fit is poor. This indicates that dual-site Langmuir model in combination with IAST does not describe the system sufficiently well, or alternatively, that the system is non-ideal. Non-ideal adsorption behavior has previously been reported in the literature for binary adsorption of water and carbon dioxide in zeolite NaX, 5A, 13X and Na-ZSM-5. [24, 26, 28] Previous investigations have also shown that the IAST may not predict the adsorbed concentrations very well for mixtures containing water. Rege and Yang[24] studied the binary adsorption of water and carbon dioxide in the zeolites NaX and 13X while Wang and LeVan[26] studied the same binary adsorption in zeolite 5A. Both studies showed that the IAST could not fully capture the adsorption behavior of carbon dioxide and water in these polar zeolites. The more advanced RAST (Real adsorbed solution theory) showed somewhat better performance for predicting the adsorbed loadings, albeit it could still not fully capture the adsorption behavior.[24] In the present work, the discrepancy between the experimental data of water and carbon dioxide and values predicted by the IAST seem to be related to the formation of water clusters at polar sites. Developing an adsorption model taking into account the possible formation of clusters may give better agreement between experimental data and model predictions which may thus be a way forward.

Selectivity

The CO_2/CH_4 adsorption selectivities determined for adsorption from ternary mixtures are presented in Figure 5. It is clear that the selectivity is increasing with increasing mole fraction of carbon dioxide in the gas phase, which is in agreement with results from our group, as well as other groups, reported in the literature.[8, 21, 30] In the present work, the highest CO_2/CH_4 adsorption selectivity for an equimolar mixture of carbon dioxide and methane in a ternary gas mixture (49.9 % methane, 49.9% carbon dioxide and 0.2 % water) was 17.6 at 35 °C and a total pressure of 101.3 kPa. In our previous work, we reported a CO_2/CH_4 adsorption selectivity value of 15.4 for an equimolar binary gas mixture of carbon dioxide and methane at the same temperature and pressure, indicating a more efficient separation of carbon dioxide from methane in the presence of a small amount of water. Li and Tezel[18] reported a separation factor of 7 for an equimolar binary gas mixture of carbon dioxide and methane at 40 °C in silicalite-1. Krishna and van Baten[8] reported an adsorption selectivity of 2.2 for silicalite-1 and 13 for Na-ZSM-5 (Si/Al = 23) at 27 °C at a pressure of 0.1 MPa. The higher selectivity for both the ternary and binary mixtures, presented in the present and in our previous work, indicates a more efficient separation of carbon dioxide from methane using the zeolite studied in our work. For a gas composition of 66.6 % methane, 33.3 % carbon dioxide and 0.1 % water, similar to the composition of biogas and some natural gas sources, the CO_2/CH_4 adsorption selectivity was determined to 18.3 at 35 °C. In our previous work,[30] the corresponding value for dry gas (with a molar composition of 65% methane and 35 % carbon dioxide) was 16.9. The slightly higher CO_2/CH_4 selectivity for the ternary mixture can be explained by the higher affinity of water and carbon dioxide in comparison with methane, see table 1 in the supporting information, where methane have difficulties competing with both water and carbon dioxide for the adsorption sites, or

alternatively, some interaction between adsorbed water and adsorbed carbon dioxide might occur. Figures 6a and b show the effect of water on the CO_2/CH_4 adsorption selectivities at low and high temperatures, respectively. At low temperatures the CO_2/CH_4 adsorption selectivity is slightly improved as water is added to the system, whereas the effect is small at the higher temperatures. This is probably due to the adsorbed loading of methane being more affected by the introduction of water than carbon dioxide at low temperatures. This is shown in Figure 3a and b, where the introduction of a small partial pressure of water will decrease the adsorption of both carbon dioxide and methane at lower temperatures due to competitive adsorption. The decrease in the adsorbed concentration when water is added to the gas is larger for methane than for carbon dioxide. Again, this reflects the higher affinity of water for the zeolite at low temperatures compared to high temperatures, leading to a greater effect on the adsorption of methane and carbon dioxide at lower temperatures. At the higher temperatures, the CO_2/CH_4 selectivity for the ternary mixtures is similar compared to the CO_2/CH_4 selectivity for binary mixtures, see Figure 6b. Hence, the presence of water slightly improves the CO_2/CH_4 adsorption selectivity at lower temperatures. The H_2O/CH_4 and the H_2O/CO_2 selectivities as a function of the mole fraction of water in the gas phase are presented in Figure 7a and 7b, respectively. It is clear that these selectivities are strongly dependent on the mole fraction of water in the gas phase and are decreasing with increasing mole fraction of water. As discussed above, water and carbon dioxide molecules will first adsorb on polar high energy sites associated with hydrophilic silanol groups and sites related to the sodium/aluminum content of the zeolite framework. At low mole fractions of water in the gas phase, water molecules are primarily adsorbed on these high energy sites.[14, 17] Carbon dioxide molecules will also be adsorbed on these sites, but since water has a higher affinity ($b=7.90 \times 10^{-2}$ 1/Pa) compared to carbon dioxide ($b=6.33 \times 10^{-4}$ 1/Pa), water will

be preferably adsorbed and therefore the H_2O/CO_2 selectivity will be highest at low mole fractions of water in gas phase where adsorption predominantly occur at the high energy sites. At higher partial pressure of water, water will form clusters at the high affinity sites with little competition from carbon dioxide which is adsorbing on the more hydrophobic parts of the pores.[14, 41] Since methane has a lower affinity compared to both water and carbon dioxide, the H_2O/CH_4 selectivity will also decrease as the mole fraction of water in the gas phase is increasing. The H_2O/CH_4 selectivity reaches much higher values compared the H_2O/ CO_2 selectivity which reflects the higher affinity of carbon dioxide for the zeolite compared to methane. Rege and Yang[24] studied the binary adsorption of water and carbon dioxide in zeolite NaX at 22 ºC. Using the experimental data provided by Rege and Yang and equation 2 in the present work, a H_2O/CO_2 adsorption selectivity of 80 can be determined for the highest pressure of water and carbon dioxide. In the present work, a H_2O/CO_2 adsorption selectivity of 135 at 35 ºC was determined for the highest amount of water in the gas phase. The lower selectivity of Rege and Yang reflects the lower partial pressures of water and carbon dioxide used compared to the pressures used in the present work.

CONCLUSION

In-situ ATR-FTIR spectroscopy was used to study the adsorption of methane, water and carbon dioxide in Na-ZSM-5 from ternary mixtures at different gas compositions and temperatures. The concentrations of the adsorbed components were calculated from infrared spectra and the values obtained were compared to values predicted using the IAST. Even though the experimental data and the predicted values followed the same trend, the IAST was not fully capable of predicting the adsorbed amounts of water and carbon dioxide from the ternary mixtures indicating a non-ideal behavior for the mixtures studied. On the other hand, the predicted values for methane were in reasonably good agreement with the experimental data. The CO_2/CH_4 selectivity was shown to increase with increasing mole fraction of carbon dioxide in the gas phase, whilst the H_2O/CH_4 and the H_2O/ CO_2 selectivity decreased with an increasing mole fraction of water in the gas phase, reflecting adsorption on sites with different adsorption energies. At low temperatures, the CO_2/CH_4 adsorption selectivity was slightly higher for the ternary mixtures also containing water as compared to the dry binary mixtures.

ACKNOWLEDGMENT

The financial support from The Swedish Energy Agency and the Swedish Research Council under grant 621-2011-4060 is gratefully acknowledged. The Kempe foundation is acknowledged for funding of the spectroscopy lab.

Supporting information available: Heat of adsorption, saturation concentration and Langmuir adsorption coefficient for water, carbon dioxide and methane adsorbed in Na-ZSM-5 obtained in our previous work. This information is available free of charge via the Internet at http://pubs.acs.org.

References

(1) Busby, R. L. In *Natural gas in nontechnical language;* Busby, R. L., Ed.; Pennwell: Tulsa, Okla., 1999; .

(2) Cavenati, S.; Grande, C. A.; Rodrigues, A. E. Adsorption Equilibrium of Methane, Carbon Dioxide, and Nitrogen on Zeolite 13X at High Pressures. *J. Chem. Eng. Data* **2004**, *49*, 1095-1101.

(3) Bechtold, R. L. In *Alternative fuels guidebook : properties, storage, dispensing and vehicle facility modifications;* Society of Automotive Engineers, cop.: Warrendale, Pa., 1997; .

(4) Abdeshahian, P.; Dashti, M. G.; Kalil, M. S.; Yusoff, W. M. W. Production of Biofuel using Biomass as a Sustainable Biological Resource. *Biotechnology* **2010**, *9*, 274-282.

(5) Brown, R. C. In *Biorenewable resources : engineering new products from agriculture;* Iowa State Press: Ames, Iowa, 2003; .

(6) Baker, R. W. Future Directions of Membrane Gas Separation Technology. *Ind. Eng. Chem. Res.* **2002**, *41*, 1393-1411.

(7) D'Alessandro, D. M.; Smit, B.; Long, J. R. Carbon Dioxide Capture: Prospects for New Materials. *Angew. Chem. , Int. Ed.* **2010**, *49*, 6058-6082.

(8) Krishna, R.; van Baten, J. M. In Silico Screening of Zeolite Membranes for CO2 Capture. *J. Membr. Sci.* **2010**, *360*, 323-333.

(9) Choudhary, V. R.; Mayadevi, S. Adsorption of Methane, Ethane, Ethylene, and Carbon Dioxide on Silicalite-I. *Zeolites* **1996**, *17*, 501-507.

(10) Sun, M. S.; Shah, D. B.; Xu, H. H.; Talu, O. Adsorption Equilibria of C-1 to C-4 Alkanes, CO2, and SF6 on Silicalite. *J. Phys. Chem. B* **1998**, *102*, 1466-1473.

(11) Dunne, J. A.; Mariwala, R.; Rao, M.; Sircar, S.; Gorte, R. J.; Myers, A. L. Calorimetric Heats of Adsorption and Adsorption Isotherms .1. O-2, N-2, Ar, CO2, CH4, C2H6 and SF6 on Silicalite. *Langmuir* **1996**, *12*, 5888-5895.

(12) Dunne, J. A.; Rao, M.; Sircar, S.; Gorte, R. J.; Myers, A. L. Calorimetric Heats of Adsorption and Adsorption Isotherms .2. O-2, N-2, Ar, CO2, CH4, C2H6, and SF6 on NaX, H-ZSM-5, and Na-ZSM-5 Zeolites. *Langmuir* **1996**, *12*, 5896-5904.

(13) Bao, Z.; Yu, L.; Dou, T.; Gong, Y.; Zhang, Q.; Ren, Q.; Lu, X.; Deng, S. Adsorption Equilibria of CO(2), CH(4), N(2), O(2), and Ar on High Silica Zeolites. *J. Chem. Eng. Data* **2011**, *56*, 4017-4023.

(14) Jentys, A.; Warecka, G.; Derewinski, M.; Lercher, J. Adsorption of Water on ZSM5 Zeolites. *J. Phys. Chem.* **1989**, *93*, 4837-4843.

(15) Ari, M. U.; Ahunbay, M. G.; Yurtsever, M.; Erdem-Senatalar, A. Molecular Dynamics Simulation of Water Diffusion in MFI-Type Zeolites. *J. Phys. Chem. B* **2009**, *113*, 8073-8079.

(16) Krishna, R.; van Baten, J. M. Hydrogen Bonding Effects in Adsorption of Water-Alcohol Mixtures in Zeolites and the Consequences for the Characteristics of the Maxwell-Stefan Diffusivities. *Langmuir* **2010**, *26*, 10854-10867.

(17) Trzpit, M.; Soulard, M.; Patarin, J.; Desbiens, N.; Cailliez, F.; Boutin, A.; Demachy, I.; Fuchs, A. H. The Effect of Local Defects on Water Adsorption in Silicalite-1 Zeolite: A Joint Experimental and Molecular Simulation Study. *Langmuir* **2007**, *23*, 10131-10139.

(18) Li, P.; Tezel, F. H. Pure and Binary Adsorption Equilibria of Methane and Carbon Dioxide on Silicalite. *Sep. Sci. Technol.* **2007**, *42*, 3131-3153.

(19) Harlick, P. J. E.; Tezel, F. H. Adsorption of Carbon Dioxide, Methane, and Nitrogen: Pure and Binary Mixture Adsorption by ZSM-5 with SiO2/Al2O3 Ratio of 30. *Sep. Sci. Technol.* **2002**, *37*, 33-60.

(20) Harlick, P. J. E.; Tezel, F. H. Adsorption of Carbon Dioxide, Methane and Nitrogen: Pure and Binary Mixture Adsorption for ZSM-5 with SiO2/Al2O3 Ratio of 280. *Sep. Purif. Technol.* **2003**, *33*, 199-210.

(21) Krishna, R.; van Baten, J. M. Using Molecular Simulations for Screening of Zeolites for Separation of CO2/CH4 Mixtures. *Chem. Eng. J.* **2007**, *133*, 121-131.

(22) Krishna, R.; van Baten, J. M.; Garcia-Perez, E.; Calero, S. Diffusion of CH4 and CO2 in MFI, CHA and DDR Zeolites. *Chem. Phys. Lett.* **2006**, *429*, 219-224.

(23) Krishna, R.; van Baten, J. M.; Garcia-Perez, E.; Calero, S. Incorporating the Loading Dependence of the Maxwell-Stefan Diffusivity in the Modeling of CH4 and CO2 Permeation Across Zeolite Membranes. *Ind. Eng. Chem. Res.* **2007**, *46*, 2974-2986.

(24) Rege, S. U.; Yang, R. T. A Novel FTIR Method for Studying Mixed Gas Adsorption at Low Concentrations: H2O and CO2 on NaX Zeolite and Gamma-Alumina. *Chem. Eng. Sci.* **2001**, *56*, 3781-3796.

(25) Brandani, F.; Ruthven, D. M. The Effect of Water on the Adsorption of CO_2 and C_3H_8 on Type X Zeolites. *Ind. Eng. Chem. Res.* **2004**, *43*, 8339-8344.

(26) Wang, Y.; LeVan, M. D. Adsorption Equilibrium of Binary Mixtures of Carbon Dioxide and Water Vapor on Zeolites 5A and 13X. *J. Chem. Eng. Data* **2010**, *55*, 3189-3195.

(27) Joos, L.; Swisher, J. A.; Smit, B. Molecular Simulation Study of the Competitive Adsorption of H_2O and CO_2 in Zeolite 13X. *Langmuir* **2013**, .

(28) Ohlin, L.; Grahn, M. Effect of Water on the Adsorption of Methane and Carbon Dioxide in Zeolite Na-ZSM-5 Studied using in-Situ ATR-FTIR Spectroscopy. *J. Phys. Chem. C* **To be submitted**, .

(29) Ohlin, L.; Bazin, P.; Thibault-Starzyk, F.; Hedlund, J.; Grahn, M. Adsorption of CO_2, CH_4 and H_2O in zeolite ZSM-5 Zeolite Studied using in-situ ATR-FTIR Spectroscopy. *J. Phys. Chem. C* **2013**, *117*, 16972-16982.

(30) Ohlin, L.; Grahn, M. Detailed Investigation of the Binary Adsorption of Carbon Dioxide and Methane in Zeolite Na-ZSM-5 Studied using in Situ ATR-FTIR Spectroscopy. *J. Phys. Chem. C* **2014**, *118*, 6207-6213.

(31) Wang, Z.; Grahn, M.; Larsson, M. L.; Holmgren, A.; Sterte, J.; Hedlund, J. Zeolite Coated ATR Crystal Probes. *Sens. Actuators, B* **2006**, *115*, 685-690.

(32) Grahn, M.; Wang, Z.; Lidström-Larsson, M.; Holmgren, A.; Hedlund, J.; Sterte, J. Silicalite-1 Coated ATR Elements as Sensitive Chemical Sensor Probes. *Microporous Mesoporous Mater.* **2005**, *81*, 357-363.

(33) Tompkins, H. G. The Physical Basis for Analysis of the Depth of Absorbing Species using Internal Reflection Spectroscopy. *Appl. Spectrosc.* **1974**, *28*, 335-341.

(34) Mirabella, F. M., Ed.; In *Internal Reflection Spectroscopy : Theory and Applicatons;* Marcel Dekker, Inc.: New York, 1993; Vol. 15.

(35) Myers, A. L.; Prausnitz, J. M. Thermodynamics of Mixed-Gas Adsorption. *AIChE J.* **1965**, *11*, 121-127.

(36) Ruthven, D. M. In *Principles of adsorption and adsorption processes;* Wiley-Interscience publication; Wiley: New York, 1984; .

(37) Grahn, M.; Holmgren, A.; Hedlund, J. Adsorption of N-Hexane and P-Xylene in Thin Silicalite-1 Films Studied by FTIR/ATR Spectroscopy. *J. Phys. Chem. C* **2008**, *112*, 7717-7724.

(38) Zou, X.; Bazin, P.; Zhang, F.; Zhu, G.; Valtchev, V.; Mintova, S. Ethanol Recovery from Water using Silicalite-1 Membrane: An Operando Infrared Spectroscopic Study. *ChemPlusChem* **2012**, *77*, 437-444.

(39) Scarano, D.; Bertarione, S.; Spoto, G.; Zecchina, A.; Arean, C. FTIR Spectroscopy of Hydrogen, Carbon Monoxide, and Methane Adsorbed and Co-Adsorbed on Zinc Oxide. *Thin Solid Films* **2001**, *400*, 50-55.

(40) Chen, L.; Lin, L.; Xu, Z.; Zhang, T.; Xin, Q.; Ying, P.; Li, G.; Li, C. Fourier Transform-Infrared Investigation of Adsorption of Methane and Carbon Monoxide on HZSM-5 and Mo/HZSM-5 Zeolites at Low Temperature. *J. Catal.* **1996**, *161*, 107-114.

(41) Wirawan, S. K.; Creaser, D. CO2 Adsorption on Silicalite-1 and Cation Exchanged ZSM-5 Zeolites using a Step Change Response Method. *Microporous Mesoporous Mater.* **2006**, *91*, 196-205.

(42) Zhang, K.; Lively, R. P.; Noel, J. D.; Dose, M. E.; McCool, B. A.; Chance, R. R.; Koros, W. J. Adsorption of Water and Ethanol in MFI-Type Zeolites. *Langmuir* **2012**, *28*, 8664-8673.

(43) Dose, M. E.; Zhang, K.; Thompson, J. A.; Leisen, J.; Chance, R. R.; Koros, W. J.; McCool, B. A.; Lively, R. P. Effect of Crystal Size on Framework Defects and Water Uptake in Fluoride Mediated Silicalite-1. *Chem. Mater.* , , 4368-4376.

(44) Krishna, R.; van Baten, J. M. Investigating the Influence of Diffusional Coupling on Mixture Permeation Across Porous Membranes. *J. Membr. Sci.* **2013**, *430*, 113-128.

Figure 1. Infrared spectra of adsorbed water, methane and carbon dioxide from ternary mixtures of various compositions in the gas phase in zeolite Na-ZSM-5 at 35 °C. The total pressure was 101.3 kPa where the composition of water in the gas phase was 0.03, 0.05, 0.10, 0.23, 0.41, 0.54 and 0.63 kPa, starting from the top spectrum.

Figure 2. Adsorbed concentrations of water (a), methane (b) and carbon dioxide (c) as a function of the mole fraction of water in the gas phase at 35°C (□), 50°C (◊), 85°C (○) and 120°C (Δ). The lines are only a guide for the eyes.

Figure 3. Adsorbed concentrations of carbon dioxide (a) and methane (b), from binary mixtures (filled markers) reported in our previous work[30] compared to ternary mixtures (open markers) reported in this work, as a function of the mole fraction of carbon dioxide in the gas phase at 35°C (□), 50°C (◊), 85°C (○) and 120°C (Δ). The lines are only a guide for the eyes.

Figure 4. Adsorbed phase mole fraction of water (a), methane (b) and carbon dioxide (c) as a function of the mole fraction of water in the gas phase at 35°C (□,–), 50°C (◊,---), 85°C (○,···) and 120°C (Δ,-·-). The markers are representing the experimental data and the solid lines represents values predicted using the IAST. The total pressure was 101.3 kPa.

Figure 5. CO_2/CH_4 selectivity from ternary mixtures as a function of mole fraction of carbon dioxide in the gas phase at 35°C (□), 50°C (◊), 85°C (○) and 120°C (Δ) using a total pressure of 101.3 kPa.

Figure 6. CO_2/CH_4 selectivity from ternary mixtures and binary mixtures as a function of mole fraction of carbon dioxide in the gas phase using a total pressure of 101.3 kPa. Figure a show the selectivity at low temperatures, 35 (□) and 50°C (◊), and figure b show the selectivity at high

temperatures, 85 (○) and 120°C (Δ). Open markers represent data from ternary mixtures while filled markers represent data from binary mixtures.

Figure 7. H_2O/CH_4 selectivity (a) and H_2O/ CO_2 selectivity (b) as a function of mole fraction of water in the gas phase at 35°C (□), 50°C (◊), 85°C (○) and 120°C (Δ) using a total pressure of 101.3 kPa.

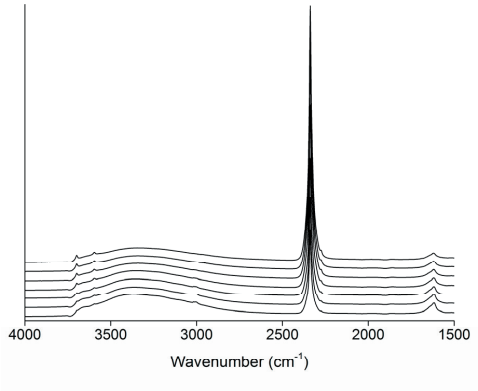

Figure 1

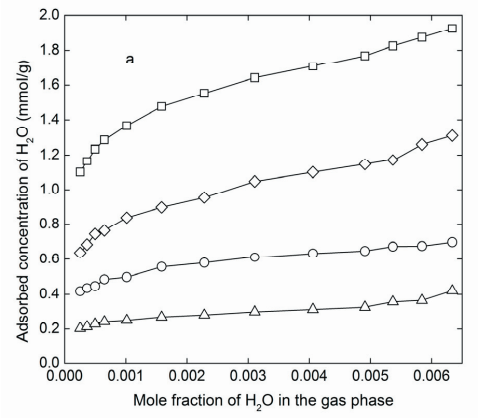

Figure 2a

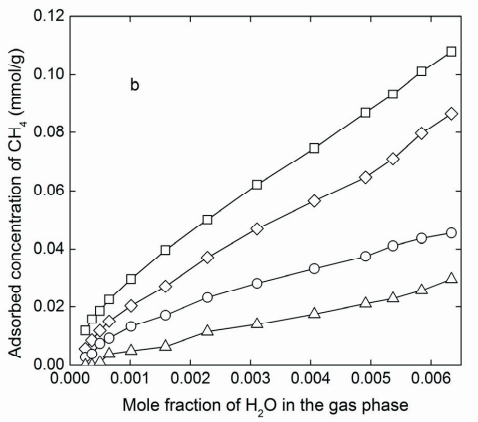

Figure 2b

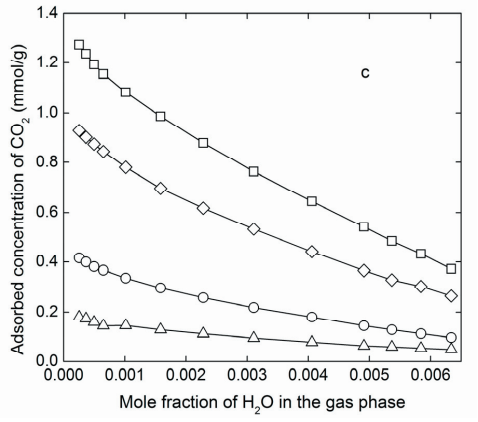

Figure 2c

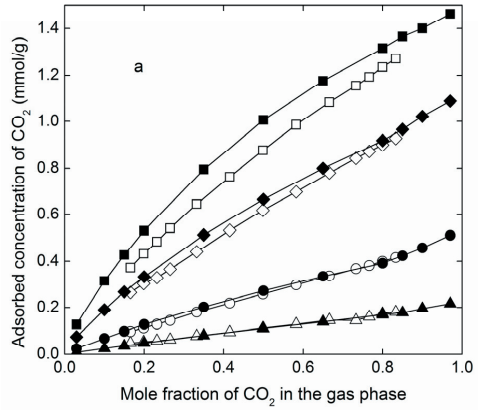

Figure 3a

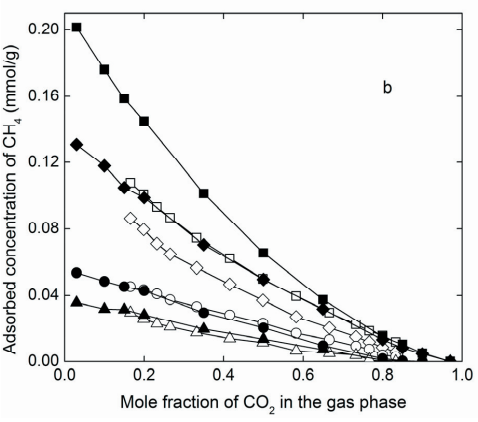

Figure 3b

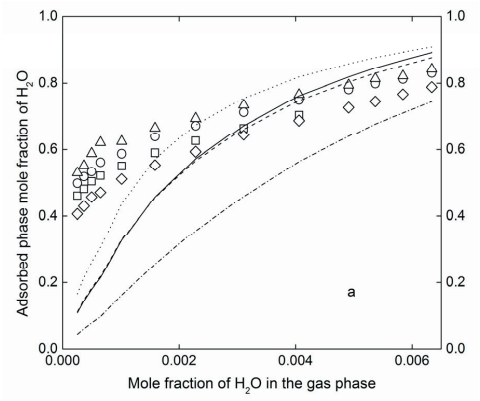

Figure 4a

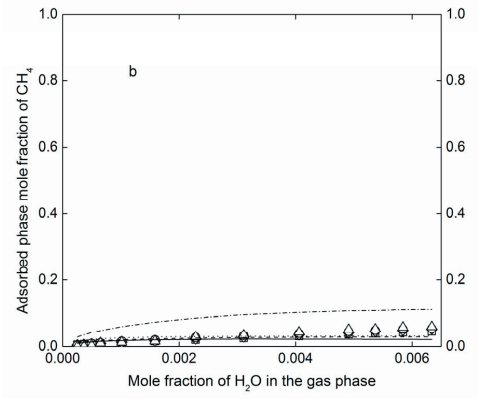

Figure 4b

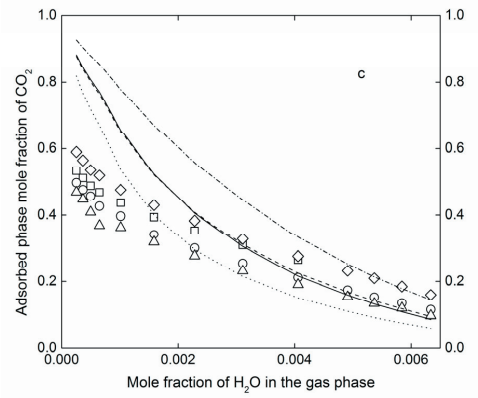

Figure 4c

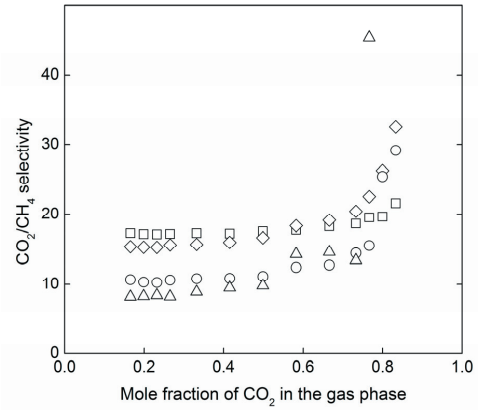

Figure 5

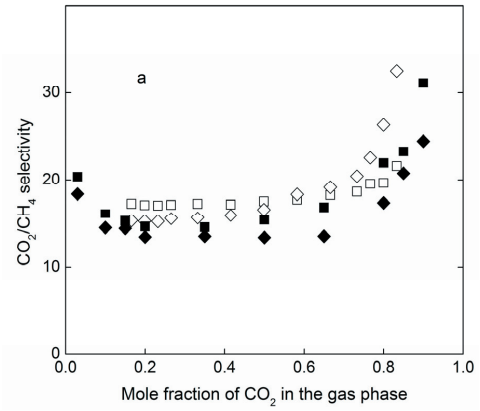

Figure 6a

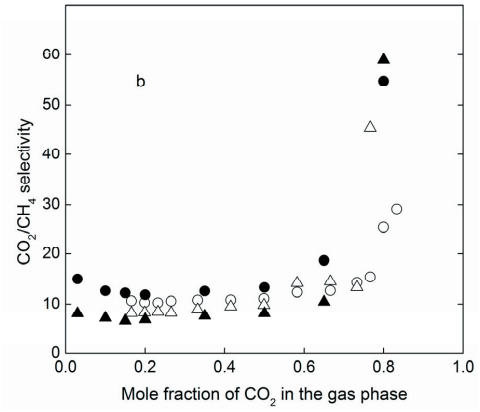

Figure 6b

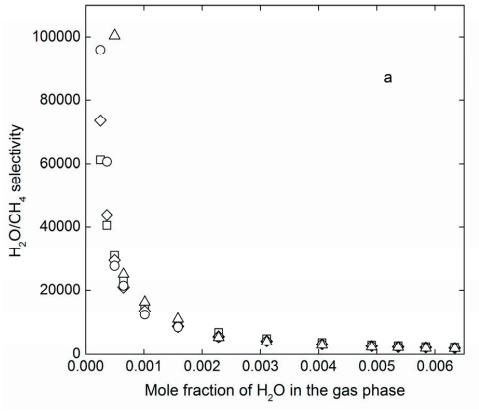

Figure 7a

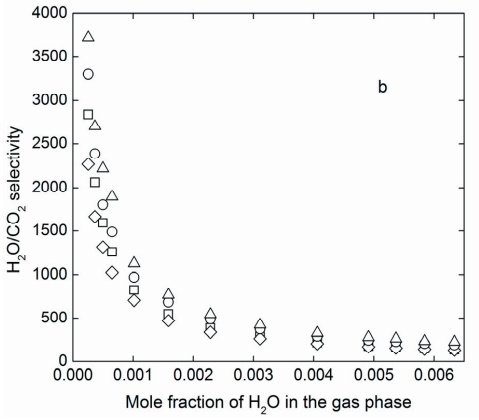

Figure 7b

Ternary Adsorption of Methane, Water and Carbon dioxide in Zeolite Na-ZSM-5 Studied Using in situ ATR-FTIR Spectroscopy

*Lindsay Ohlin, Amirfarrokh Farzaneh, Allan Holmgren, Jonas Hedlund and Mattias Grahn**

Chemical Technology, Luleå University of Technology, 971 87 Luleå, Sweden

* Corresponding author. Tel: +46 920 491928; e-mail address: mattias.grahn@ltu.se

The Ideal Adsorbed Solution Theory (IAST) was proposed by Myers and Prausnitz[1] to provide a link between single and multicomponent adsorption. In our previous work[2] on the single component adsorption of methane, water and carbon dioxide, saturation loadings and Langmuir adsorption coefficients were determined, which are presented in table 1. In this work, adsorbed concentrations of methane, water and carbon dioxide from ternary mixtures were predicted using the IAST and hence the required data from the single component experiments. The adsorbed concentrations predicted by the IAST were compared to the values determined experimentally. Furthermore, the temperature dependence of the Langmuir adsorption coefficients were also used to determine the heat of adsorption.

Table 1. Heat of adsorption (ΔH, kJ/mol), saturation concentration (q_{sat}, mmol/g) and Langmuir adsorption coefficient (b, Pa^{-1}) for water, carbon dioxide and methane adsorbed in Na-ZSM-5.

Adsorbate	ΔH (kJ/mol)	Temp. (°C)	q_1 (mmol/g)	b_1 (1/Pa)	q_2 (mmol/g)	b_2 (1/Pa)
H_2O	-72 (site 1)	35	5.34	$3.75 \cdot 10^{-4}$	0.50	$7.90 \cdot 10^{-2}$
	-58 (site 2)	50	5.34	$1.10 \cdot 10^{-4}$	0.50	$2.80 \cdot 10^{-2}$
		85	5.34	$1.10 \cdot 10^{-5}$	0.50	$8.10 \cdot 10^{-3}$
		120	5.34	$8.00 \cdot 10^{-7}$	0.50	$4.63 \cdot 10^{-4}$
CO_2	-37 (site 1)	35	2.78	$1.04 \cdot 10^{-5}$	0.04	$6.33 \cdot 10^{-4}$
	-54 (site 2)	50	2.78	$5.03 \cdot 10^{-6}$	0.04	$2.47 \cdot 10^{-4}$
		85	2.78	$1.24 \cdot 10^{-6}$	0.04	$1.83 \cdot 10^{-5}$
		120	2.78	$4.44 \cdot 10^{-7}$	0.04	$8.31 \cdot 10^{-6}$
CH_4	-23	35	2	$1.04 \cdot 10^{-6}$	-	-
		50	2	$5.53 \cdot 10^{-7}$	-	-
		85	2	$2.38 \cdot 10^{-7}$	-	-
		120	2	$1.18 \cdot 10^{-7}$	-	-

REFERENCES

(1) Myers, A. L.; Prausnitz, J. M. Thermodynamics of Mixed-Gas Adsorption. *AIChE J.* **1965**, *11*, 121-127.

(2) Ohlin, L.; Bazin, P.; Thibault-Starzyk, F.; Hedlund, J.; Grahn, M. Adsorption of CO_2, CH_4 and H_2O in zeolite ZSM-5 Zeolite Studied using in-situ ATR-FTIR Spectroscopy. *J. Phys. Chem. C* **2013**, *117*, 16972-16982.

Paper V

Adsorption of water and butanol in silicalite-1 film studied with in situ attenuated total reflectance-fourier transform infrared spectroscopy

Amirfarrokh Farzaneh, Ming Zhou, Elisaveta Potapova, Zoltán Bacsik, Lindsay Ohlin, Allan Holmgren, Jonas Hedlund, Mattias Grahn

Langmuir

Langmuir

Article

pubs.acs.org/Langmuir

Adsorption of Water and Butanol in Silicalite-1 Film Studied with *in Situ* Attenuated Total Reflectance–Fourier Transform Infrared Spectroscopy

Amirfarrokh Farzaneh,[†] Ming Zhou,[†] Elisaveta Potapova,[†] Zoltán Bacsik,[‡] Lindsay Ohlin,[†] Allan Holmgren,[†] Jonas Hedlund,[†] and Mattias Grahn*[,†]

[†]Chemical Technology, Luleå University of Technology, SE-971 87 Luleå, Sweden

[‡]Department of Material and Environmental Chemistry, Stockholm University, SE-106 91 Stockholm, Sweden

ABSTRACT: Biobutanol produced by, e.g., acetone–butanol–ethanol (ABE) fermentation is a promising alternative to petroleum-based chemicals as, e.g., solvent and fuel. Recovery of butanol from dilute fermentation broths by hydrophobic membranes and adsorbents has been identified as a promising route. In this work, the adsorption of water and butanol vapor in a silicalite-1 film was studied using *in situ* attenuated total reflectance–Fourier transform infrared (ATR–FTIR) spectroscopy to better understand the adsorption properties of silicalite-1 membranes and adsorbents. Single-component adsorption isotherms were determined in the temperature range of 35–120 °C, and the Langmuir model was successfully fitted to the experimental data. The adsorption of butanol is very favorable compared to that of water. When the silicalite-1 film was exposed to a butanol/water vapor mixture with 15 mol % butanol (which is the vapor composition of an aqueous solution containing 2 wt % butanol, a typical concentration in an ABE fermentation broth, i.e., the composition of the gas obtained from gas stripping of an ABE broth) at 35 °C, the adsorption selectivity toward butanol was as high as 107. These results confirm that silicalite-1 quite selectively adsorbs hydrocarbons from vapor mixtures. To the best of our knowledge, this is the first comprehensive study on the adsorption of water and butanol in silicalite-1 from vapor phase.

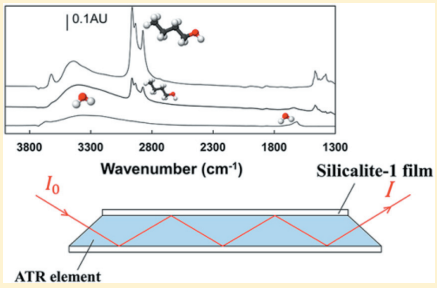

INTRODUCTION

With the depleting reservoirs of fossil fuels, increasing environmental concerns for flue gas emissions from fossil fuel combustion, and growing world population, the need for new sustainable fuels is higher than ever.[1] Alcohols are important substitutes for the traditional petroleum-based fuels because they can be produced from renewable feedstocks via, for instance, fermentation.[2] Ethanol is already used extensively in the world as fuel in Otto engines,[3] albeit typically as blended in gasoline in varying proportions. 1-Butanol (further referred to as butanol) has great potential as biofuel for Otto engines because of its high octane number of 95 as well as a higher specific energy value than that of ethanol, and in addition, it shows low corrosivity and suitable volatility.[4] Butanol can be produced from sugars by a fermentive process, called acetone–butanol–ethanol (ABE) fermentation, using, e.g., a Clostridia strain of bacteria. The fermentation broth typically contains acetone, butanol, and ethanol in the ratio 3:6:1, where the maximum concentration of butanol is roughly 2 wt % set by the bacteria.[5] At this low concentration of butanol, the energy required to recover butanol by distillation is higher than the energy content of the product itself.[6] Therefore, an efficient separation method for the recovery of butanol from a dilute aqueous solution is a prerequisite for this process to be competitive. The situation can be improved using a so-called gas-stripping ABE fermentation process. Gas stripping is one of the processes that can be a simple process for recovery of liquid fuels, such as butanol. In this process, gas can be sparged through the fermenter and butanol (with a higher concentration compared to the fermentation broth) can be condensed and recovered from the condenser.[7]

Adsorption and membrane separation processes are in general considered as energy-efficient separation processes compared to thermally driven processes, such as distillation, and have also been identified as promising for efficient recovery of biobutanol from ABE fermentation broths.[8] Because of the great potential of butanol, there has recently been an increased interest in developing suitable adsorbents for butanol recovery, with some of the most studied materials including zeolite,[9] activated carbon,[10,11] and polymeric resins.[12,13] Silicalite-1 is the pure silica analogue of the zeolite ZSM-5.[14,15] The absence of aluminum in the crystal makes the material more hydrophobic than ZSM-5.[16] Because of its hydrophobic character, organic compounds, such as methanol, ethanol, acetone, propanol, and

Received: February 6, 2015
Revised: April 13, 2015
Published: April 14, 2015

DOI: 10.1021/acs.langmuir.5b00489
Langmuir 2015, 31, 4887–4894

butanol, are preferentially adsorbed over water from aqueous solutions. Several groups have studied the adsorption of butanol and other components present in the ABE fermentation broth in silicalite-1[17−19] and low-aluminum ZSM-5[2,20,21] from aqueous solutions. Adsorption on hydrophobic adsorbents, such as silicalite-1,[17,18,20,21] was suggested as a promising technique for recovery of butanol from fermentation broth compared to pervaporation or liquid−liquid extraction. For example, Stoeger et al.[22] studied bioalcohol recovery potential of a pure silica MFI membrane and reported a separation factor of 21 and total flux of 0.11 kg m^{-2} h^{-1} for butanol extraction from an aqueous mixture. Our group has previously investigated the recovery of butanol from dilute aqueous solutions with both adsorbents and membranes. Faisal et al.[23] (also previously Oudshoorn et al.[9]) investigated the recovery of butanol and butyric acid from model and real fermentation broths using high-silica MFI, and it was shown that other species present in the broth, e.g., acetone, ethanol, and acetic acid, only had a minor effect on the amount of butanol or butyric acid adsorbed. The Langmuir isotherm model fitted the experimental data for butanol adsorption in MFI zeolite, and a maximum loading of 1.6 mmol/g was reported for butanol adsorption at room temperature. Zhou et al.[24] evaluated MFI membranes for separation of butanol and water by vapor permeation and reported very high permeance of butanol (11×10^{-7} mol m^{-2} s^{-1} Pa^{-1}), with a butanol/water selectivity of 19. Korelskiy et al.[25] reported very high fluxes (up to 4 kg m^{-2} h^{-1}) in separation of butanol and water by pervaporation using a hydrophobic MFI membrane with a Si/Al ratio of 139. The aim of the current work was to measure adsorption isotherms of butanol and water in a silicalite-1 film from vapor phase using *in situ* attenuated total reflectance−Fourier transform infrared (ATR−FTIR) spectroscopy. Adsorption data for this system from the vapor phase is scarce but is of great value for understanding the performance of silicalite-1 membranes for pervaporation and vapor permeation processes and also the performance of silicalite-1 adsorbents in gas-phase separation processes. The data could aid the design of a process for separation of butanol from the vapor emanating from a gas stripping of an ABE broth or from a vaporized broth. The ATR−FTIR technique used in this work was developed within the group and has previously been used for studying the adsorption of hydrocarbons (methane, *n*-hexane, and *p*-xylene) and light gases (carbon dioxide and water vapor) in silicalite-1 and ZSM-5 films.[26−29]

EXPERIMENTAL SECTION

Film Synthesis and General Characterization. Thin silicalite-1 films were grown on both sides of a ZnS ATR crystal (with the dimension of 50 × 20 × 2 mm and 45° cut edges, Crystran, Ltd.) using a seeding method. This method has been developed in our group, and details of the procedure can be found elsewhere.[30−32] However, the method will be briefly explained here. Silicalite-1 seed crystals were synthesized from a mixture of tetraethoxysilane (TEOS, 99%, Merck), tetrapropylammonium hydroxide (TPAOH, AppliChem, 40 wt % aqueous solution), and water by hydrolysis for 1 day, followed by hydrothermal treatment at 130 °C for 9 h under constant stirring. The molar composition of the synthesis mixture was 1.00 TEOS/0.200 TPAOH/100 H_2O. The synthesized crystals were separated from the supernatant by repetitive centrifugation, and after each step, the crystals were redispersed in doubly distilled water.[30]

To facilitate the attachment of the seeds to the ATR crystal, both sides of the ATR crystal were coated by a thin layer of cellulosic polymer [hydroxypropylcellulose (HPC), Sigma-Aldrich, 99%] using a spin coater (2% HPC dissolved in ethanol solution, and the spin coating was conducted at 3000 rpm for 15 s).[31] After drying at 105 °C for 1 h, a monolayer of silicalite-1 crystals was assembled on the ATR crystal by rubbing the powder of seeds onto both surfaces.[32] The seeded ATR crystal was calcined at 500 °C for 2 h with a heating and cooling rate of 0.8 °C/min to remove the polymer layer between the silicalite seeds and the ATR crystal. Thereafter, the seeded ATR crystal was kept for 5 h in a synthesis solution, which was prehydrolyzed for 12 h on a shaker, with a molar composition of 1.00 TEOS/0.0500 TPAOH/165 H_2O in an autoclave at 150 °C to grow the seed crystals into a continuous silicalite-1 film. After synthesis, the film was thoroughly rinsed with a 0.1 M ammonia solution and dried at 50 °C overnight. The film was subsequently calcined at 500 °C for 2 h with a heating and cooling rate of 0.8 °C/min to remove the template molecules from the pores of the zeolite.

For the characterization of the film, scanning electron microscopy (SEM) images were recorded using a Magellan 400 (FEI Company, Eindhoven, Netherlands) microscope, and X-ray diffraction (XRD) patterns were recorded using a PANalytical Empyrean instrument, equipped with a PIXcel3D detector and a Cu LFF HR X-ray tube.

***In Situ* ATR−FTIR Experiments.** The ATR−FTIR spectra were recorded on a Bruker IFS66v/S FTIR spectrometer equipped with a deuterated triglycine sulfate (DTGS) detector. Each spectrum was obtained by averaging 256 scans at a resolution of 4 cm^{-1}. The ATR crystal was mounted in a steel flow cell connected to a gas delivery system, which has been described in detail previously.[33] Prior to the adsorption experiment, the silicalite-1-film-coated ATR crystal was mounted in the cell and dried under a constant flow rate of helium at 300 °C for 4 h. The heating and cooling rates were 0.9 °C/min. A background spectrum of the dried film was recorded under helium flow at the desired experimental temperature prior to the adsorption measurements. After the background was recorded, the adsorption experiment was carried out by introducing butanol or water to the helium flow and recording spectra at equilibrium. The helium carrier gas was fed to two saturators connected in series and filled with either water or butanol or a butanol/water mixture. The temperature of the second saturator was always lower than that of the first saturator, and the cooling was controlled by a cooling jacket connected to a circuit of glycol. The saturated helium stream was thereafter diluted with an appropriate amount of helium to arrive at the desired partial pressure. The total pressure was 1 atm in all measurements. In an ATR experiment, the Beer−Lambert law is not directly applicable because of the experimental conditions; however, Mirabella et al.[34] and Tompkins et al.[35] have shown that the concentration of components adsorbed in a film deposited on an ATR crystal can be determined from eq 1

$$\frac{A}{N} = \frac{n_{21} E_0^{\,2} \varepsilon}{\cos\theta} \int_0^\infty C(z)^{-2z/d_p}\, \mathrm{d}_z \tag{1}$$

where A represents the integrated absorbance of a characteristic absorption band in the infrared (IR) spectrum, N is the number of reflections (20) inside the ATR element between the gaskets sealing of the cell, and n_{21} is the ratio of the refractive indices of the ZnS ATR crystal and silicalite-1 film. The refractive index of ZnS is ca. 2.25, whereas Tsapatsis and Nair[36] reported the refractive index of empty MFI zeolite films in the IR region of 3000−1500 cm^{-1}. As water or butanol adsorbs in the film, the refractive index of the film will change, and to compensate for this, it was assumed that the refractive index of the film changed linearly with adsorbed loading. Further, E_0 is the amplitude of the electric field at the film−ATR crystal interface,[26,29] and ε is the molar absorptivity, which was determined for water by Ohlin et al.[28] for a high-silica (Si/Al = 130) film. θ is the angle of incidence (45°), and $C(z)$ is the concentration of an adsorbate in the film. Further, d_p is the penetration depth, which is defined as the distance required for the electric field amplitude to fall to e^{-1} of its value at the surface and is calculated using eq 2.

$$d_p = \frac{\lambda_1}{2\pi(\sin^2\theta - n_{21}^{\,2})^{1/2}} \tag{2}$$

DOI: 10.1021/acs.langmuir.5b00489
Langmuir 2015, 31, 4887−4894

In this equation, λ_1 is the wavelength of the IR radiation in the ATR element. After integrating eq 1 over the film thickness, assuming a homogeneous concentration of the adsorbate in the film at equilibrium, and neglecting the absorbance from the adsorbate in the bulk gas outside the film, a reasonable assumption as shown previously[26] (eq 3) is obtained.

$$\frac{A}{N} = \frac{n_{21}E_0^{\,2}d_pC}{2\cos\theta}\varepsilon(1 - e^{-2d_a/d_p}) \quad (3)$$

Here, d_a is the thickness of the silicalite film.

To use the Beer–Lambert law for the data obtained from ATR–FTIR, "effective thickness" (d_e) was introduced as

$$d_e = \frac{n_{21}E_0^{\,2}d_p}{2\cos\theta} \quad (4)$$

which is the distance required to reach the same absorbance in a transmission experiment as in an ATR experiment, and it was described in detail previously.[26,34]

The butanol/water selectivity of the silicalite-1 film was also determined by exposing the film to a gas mixture with a molar composition of 15% butanol and 85% water at 35 °C. The adsorption selectivity was calculated using eq 5

$$\alpha_{BuOH/H_2O} = \frac{X_{BuOH}/X_{H_2O}}{Y_{BuOH}/Y_{H_2O}} \quad (5)$$

where X is the mole fraction of an adsorbate in the film and Y is the mole fraction of an adsorbate in the feed.

Adsorption of Butanol in Silicalite-1 Powder. The adsorption isotherm of butanol from the vapor phase in silicalite-1 powder at 35 °C were determined using an ASAP 2020 gas adsorption instrument (Micromeritics, Norcross, GA). Prior to the adsorption measurements, the sample was dried under dynamic vacuum conditions (<0.1 mPa) at 300 °C for 4 h with heating and cooling rates of 1 °C/min. The temperature was controlled by immersing the sample in a Dewar flask coupled to a refrigerating and heating circulator (Julabo, Germany).

Because the molar absorptivity for butanol adsorbed in silicalite-1 is not yet reported, it was assumed that the silicalite-1 film had the same saturation capacity for butanol as the silicalite-1 powder.[37] Hammond et al.[38] compared the adsorption behavior of a MFI membrane to that of a MFI powder and drew the conclusion that the adsorption behavior for the two samples was very similar and that the adsorption behavior of the membrane could safely be approximated to that of the corresponding powder. Moreover, because the saturation loading of butanol in MFI is dictated by how many molecules may fit per unit cell, it that should be very similar for both powder and films. Strain in the zeolite film may possibly affect the pore volume.[39,40] However, considering that the kinetic diameter of 1-butanol (4.4 Å) is considerably smaller than the pore diameter of MFI (5.5 Å), strain is unlikely to affect the saturation loading, and even if the saturation capacity was reduced by strain by reducing the pore volume, the same should apply to water, leading to only a minor effect on the adsorption selectivity. The maximum absorbance determined for butanol from IR spectra of the butanol-loaded silicalite-1 film was assumed to correspond to the maximum adsorbed loading of butanol determined by the volumetric adsorption measurements on the silicalite-1 powder. It should be noted that the saturation capacity of the powder was determined below the mesoporous region (P/P_0 = 0.15) to avoid contribution from any butanol capillary condensating between the powder grains.

RESULT AND DISCUSSION

Film Characterization. Panels a and b of Figure 1 show SEM images of the surface of an ATR crystal coated with a monolayer of silicalite-1 seeds. A closely packed and uniformly b-oriented layer of silicalite-1 seeds covered the ATR crystal, and no polymer layer was present between the layer of the seeds and the ATR element after calcination. Top- and side-view SEM images of the silicalite-1 film after synthesis are shown in panels c and d of Figure 1. These images show that the seed crystals grew uniformly without secondary nucleation and formed a dense layer of b-oriented crystals with a thickness of approximately 750 nm. After a thorough examination by SEM, neither cracks nor pinholes could be observed.

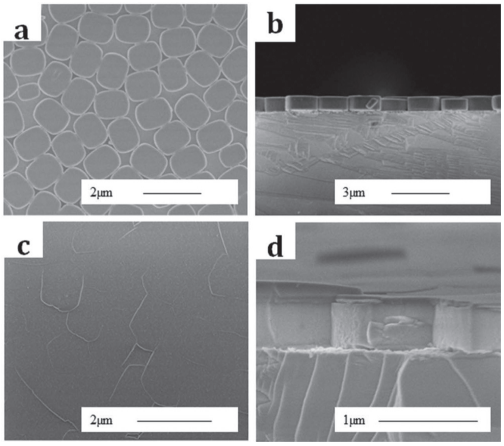

Figure 1. (a and c) Top-view and (b and d) side-view SEM images of the (a and b) silicalite-1 seed layer and (c and d) grown film.

Figure 2 shows an XRD pattern of an ATR crystal coated by a silicalite-1 film after growth in the synthesis solution. The pattern shows that the film consists of b-oriented crystals as merely reflections from (0 k 0) planes observed. This is in agreement with the SEM observations, showing that the seed crystals were b-oriented and that these crystals grew to a uniform film without any secondary nucleation. Weaker reflections emanating from the ZnS support are observed at 2θ of 28.5° and 47.5° in the pattern as well. These results are in very good agreement with previous findings.[30,41]

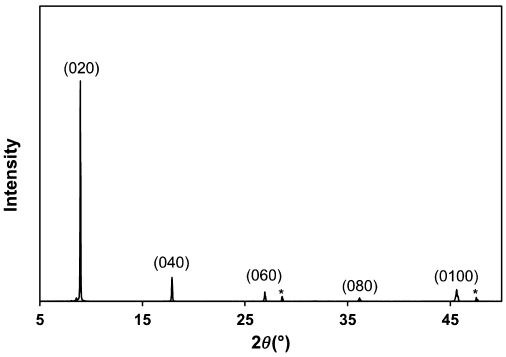

Figure 2. XRD pattern of a silicalite-1 film synthesized on a ZnS crystal in the 2θ range of 5–50°. The indexed reflections emanate from the film comprised of b-oriented crystals, and the reflections labeled "∗" represent the ZnS crystal.

ATR–FTIR Adsorption Experiments. *Water.* Figure 3 shows IR spectra of water adsorbed in the silicalite-1 film at 35

DOI: 10.1021/acs.langmuir.5b00489
Langmuir 2015, 31, 4887–4894

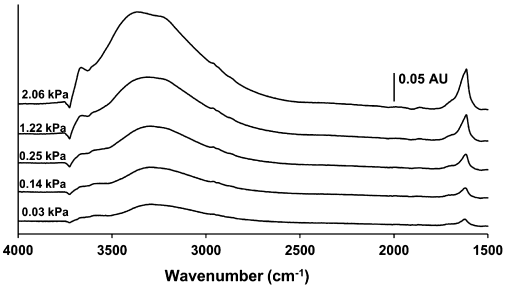

Figure 3. IR spectra of water adsorbed in silicalite-1 at 35 °C at different partial pressures.

°C and various partial pressures. Two main bands assigned to adsorbed water appear in the spectra. The broad band in the range of 3700−2700 cm^{-1} originates from the O−H stretching vibration modes (asymmetric and symmetric) in adsorbed water, and the band at ca. 1620 cm^{-1} is assigned to the bending vibration of water.[42,43] The peak value of the bending vibration band was observed at a lower wavenumber than the same vibration mode in bulk water (ca. 1650 cm^{-1}), which indicates that the interaction between water molecules and the zeolite surface was weaker than the interaction between water molecules in liquid water. Further, a negative band was observed at 3730 cm^{-1}, which was previously assigned to the O−H stretching vibration of free silanol groups.[44] When water adsorbs on the silanol groups, the intensity of this band decreased and a downshifted broader band appears for H-bonded silanol groups (partially overlapped by the OH bands of water). As expected, the intensity of the bands assigned to adsorbed water increases with increasing partial pressure in the feed, showing that the amount of adsorbed water increases with an increasing partial pressure in the feed. The spectra are typical for water adsorbed in zeolite and very similar to the spectra reported previously by, e.g., Ohlin et al.,[28] Jentys et al.,[44] and Rege et al.[45]

The amount of water adsorbed in the zeolite at different partial pressures of water was determined from the recorded IR spectra by integrating the area of the O−H band at 1620 cm^{-1} and calculating the corresponding loadings using eq 3. Ohlin et al.[28] determined the molar absorptivity (ε) for the same band of water adsorbed in the ZSM-5 to 0.654 cm/μmol using a method for combined analysis by gravimetry and infrared spectroscopy (AGIR).[46] This value was assumed to be valid in this work, and this assumption should be reasonable because the ZSM-5 film used by Ohlin et al.[28] had a very low aluminum content (Si/Al = 130) and should, therefore, show similar properties to the silicalite-1 film used in this work.

Figure 4 shows the adsorption isotherms of water in silicalite-1 derived from the IR spectra and using eq 3. Only isotherms recorded at 35, 50, and 85 °C are shown because no signal from adsorbed water was observed at 120 °C. The isotherms at lower temperatures show a steep increase in loading at low partial pressures, corresponding to adsorption of water on the high-energy sites, but at higher partial pressures, the slope of the isotherms is decreased and the maximum loading is not reached at any of the temperatures at the conditions (e.g., partial pressure of water in the gas phase) studied in this work. As expected, the amount adsorbed decreased rapidly with increasing temperature and the adsorption isotherm recorded

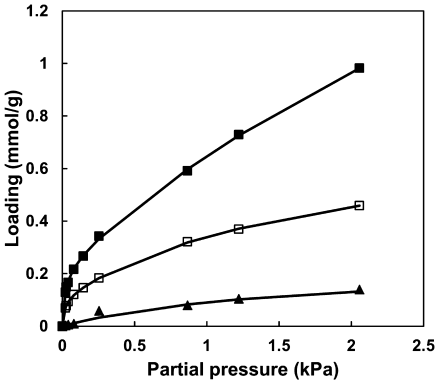

Figure 4. Adsorption isotherms for water in the silicalite-1 film determined at (■) 35 °C, (□) 50 °C, and (▲) 85 °C. Symbols present the experimental data, and solid lines represent the dual-site Langmuir model fitted to the experimental data.

at 85 °C shows little adsorption. The dual-site Langmuir model (eq 6) was fitted to the experimental data

$$q_{tot} = q_1 \frac{b_1 p}{1 + b_1 p} + q_2 \frac{b_2 p}{1 + b_2 p} \quad (6)$$

where q_1 and q_2 are the saturation loadings of the sites (mmol/g), p is the partial pressure of adsorbate in the gas phase (kPa), and b_1 and b_2 are the Langmuir adsorption coefficients (kPa^{-1}) for each site. The fitted parameters determined in the present work are shown in Table 1. The fitted data at 35 and 50 °C

Table 1. Saturation Loadings (q_{sat}, mmol/g) and Langmuir Adsorption Parameters (b_i, kPa^{-1}) for Water and Butanol in Silicalite-1

adsorbate	temperature (°C)	q_1 (mmol/g)	b_1 (kPa^{-1})	q_2 (mmol/g)	b_2 (kPa^{-1})
water	35	0.23	48.38	2.96	0.17
	50	0.23	12.14	2.96	0.04
	85	0.23	3.43		
butanol	35	1.8	860		
	50	1.8	267		
	85	1.8	15.6		
	120	1.8	2.6		

show a site with the maximum loading of 2.96 mmol/g and very low affinities (see Table 1). Therefore, it was assumed that water molecules cannot adsorb at that site at 85 °C, and the Langmuir data were fitted to a maximum loading of 0.23 mmol/g at 85 °C.

The fitted saturation loading ($q_1 + q_2$) of 3.2 mmol/g in the present work is close to the saturation loadings reported previously for water adsorbed in silicalite-1 and ZSM-5 with a high Si/Al ratio.[47,48] For example, Zhang et al.[49] reported maximum loadings of water in silicalite-1, NH_4-ZSM5, and H-ZSM5 zeolites with Si/Al of 140 ranging between 2 and 3 mmol/g. Our values of b_1 and b_2 for silicalite-1 at 35, 50, and 85 °C are lower than those reported by Ohlin et al.[28] for Na-ZSM-5 zeolite with a Si/Al ratio of 130, which shows that silicalite-1 has lower affinity for water, i.e., is less hydrophilic compared to Na-ZSM-5.

DOI: 10.1021/acs.langmuir.5b00489
Langmuir 2015, 31, 4887−4894

Table 2. Heat of Adsorption for Butanol and Water in This Work and from Literature Data

adsorbate	adsorbent	ΔH_{ads} (kJ/mol)	reference
water	silicalite-1	−79 (site 1)	this work
		−46 (site 2)	
	Na-ZSM-5	−72 (site 1)	Ohlin et al.[28]
		−58 (site 2)	
	silicalite-1	−68	Bolis et al.[48]
	silicalite-1	−46	Zhang et al.[49]
	H-ZSM-5	−75	Olson et al.[47]
butanol	silicalite-1	−69	this work
	ZIF-8	−40	Zhang et al.[53]
		−50	Einicke et al.[54]
	silicalite-1 (for butane isomers)	−56	Zhu et al.[55]

The Langmuir parameters are related to the heat of adsorption (ΔH_{ads}), reflecting the affinity of the adsorbate for the adsorbent surface. The limiting heat of adsorption was determined using the van't Hoff equation from the linear region of the isotherms

$$\ln b = -\frac{\Delta H_{ads}}{RT} + \frac{\Delta S_{ads}}{R} \quad (7)$$

where ΔS_{ads} is the entropy change upon the adsorption, R is the gas constant, and T is the absolute temperature. Table 2 shows the values for heat of adsorption for water determined in the present work together with the values previously reported in the literature. The values of −79 and −46 kJ/mol for sites 1 and 2, respectively, obtained in the present work are comparable to previously reported results. Bolis et al.[41] and Zhang et al.[42] reported values of heat of adsorption in silicalite-1 to −68 and −46 kJ/mol, respectively. Olson et al.[40] reported the heat of adsorption for water in H-ZSM-5 with a Si/Al ratio of 38 to −113 kJ/mol. Ohlin et al.[27] used the same experimental setup as used in the present work and determined the heat of adsorption for water in Na-ZSM-5 with a Si/Al ratio of 130 to −72 and −58 kJ/mol for the two sites, respectively. These latter results are quite close to the results obtained in the present work.

Butanol. Figure 5 shows IR spectra of butanol adsorbed in the silicalite-1 film at 35 °C with different partial pressures of butanol in the feed. The intensity of the bands increase with increasing partial pressures, indicating increased adsorption with increasing partial pressure of butanol in the feed. The spectra recorded during butanol adsorption contain the characteristic CH_3 and CH_2 stretching vibration bands at 3000−2800 cm^{-1} originating from butanol adsorbed in silicalite-1 film.[50,51] The bands at 1380 and 1465 cm^{-1} were assigned to the CH_3 and CH_2 bending vibrations. The broad band in the range of 3700−2700 cm^{-1} originates from the O−H stretching vibration in adsorbed butanol. A negative band at 3730 cm^{-1} is associated with the decreasing amount of free silanol groups because they interact with butanol adsorbed.

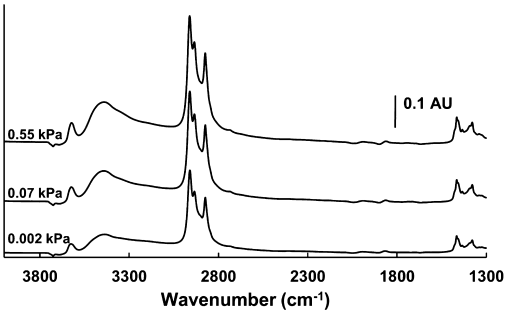

Figure 5. IR spectra of butanol adsorbed in silicalite-1 at 35 °C at different partial pressures.

Figure 6 shows the adsorption isotherms of butanol in silicalite-1 in the temperature range of 35−120 °C extracted from the IR spectra together with the fitted single-site Langmuir adsorption model (eq 8).

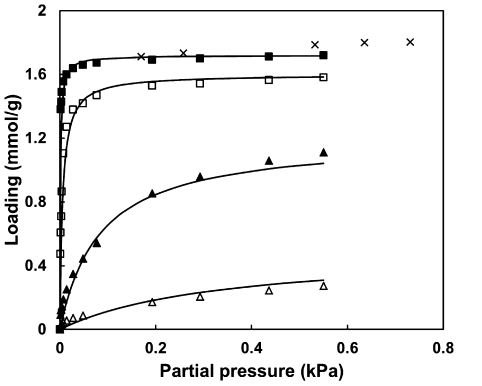

Figure 6. Adsorption isotherms for butanol in silicalite-1 film at (■) 35 °C, (□) 50 °C, (▲) 85 °C, and (△) 120 °C, obtained from FTIR experiments and in silicalite-1 powder at 35 °C (×) obtained from volumetric measurements. Symbols present the experimental data, and solid lines represent the single-site Langmuir model fitted to the experimental data.

$$q = q_m \frac{bp}{1 + bp} \quad (8)$$

The isotherms are typical for adsorption in microporous materials and are very similar to previous reported isotherms of butanol in silicalite-1.[9,20,52] The Langmuir data were fitted to a maximum loading of 1.7 mmol/g, which is the plateau value for the isotherm at 35 °C in Figure 6. This value for maximum loading was obtained from the isotherms determined for silicalite-1 powder at 35 °C using the volumetric gas adsorption technique (also presented in Figure 6). The isotherm obtained

DOI: 10.1021/acs.langmuir.5b00489
Langmuir 2015, 31, 4887−4894

from the volumetric gas adsorption measurement (×) shows that the loading of butanol in silicalite-1 was increasing slowly at high pressures, resulting in adsorbed loadings higher than 1.7 mmol/g at partial pressures closer to the saturated vapor pressure of butanol at 35 °C (P^* = 1.8 kPa). This is probably due to capillary condensation in the voids between the crystals of the silicalite-1 powder.

In general, the single-site Langmuir adsorption model fits the data well; however, for the two highest temperatures, there is some discrepancy between the model and experimental data, probably because of the presence of a few high-energy adsorption sites as evident by the sharp increase in loadings at low pressures also at these high temperatures. The fitted parameters are listed in Table 2 together with values previously reported in the literature. According to the previous studies,[2,5,9,19,21,23] the maximum loadings of butanol in silicalite-1 and MFI zeolites are reported in the range of 0.7−2.5 mmol/g. The inconsistency is probably due to the different experimental conditions and samples used. However, most of the values reported are in the range of 1.3−2 mmol/g. As shown in Figure 6, the maximum loading according to the present work was 1.7 mmol/g (determined using a volumetric gas adsorption analyzer), which is in the range of the literature data.

The heat of adsorption was determined to be −69 kJ/mol using the van't Hoff equation (eq 7) from all four temperatures. The fit was very good, with a R^2 value of 0.998.

There are only few reports on the heat of adsorption for butanol in hydrophobic adsorbents in the literature. However, the heat of adsorption calculated in the present work is in good agreement with the previous findings reported by Einicke et al.[54] and Zhang et al.[53] (−49.6 and −40 kJ/mol, respectively). Several papers reported the heat of adsorption of butane (which should have a reasonable similar adsorption behavior as butanol in hydrophobic adsorbents) in silicalite-1 in the range from −50 to −60 kJ/mol,[55−58] which is also in a good agreement with the present work.

Adsorption of Butanol and Water from a Binary Mixture. By considering the single-component adsorption results, it would be expected that butanol would be preferentially adsorbed in silicalite-1 from a butanol/water vapor mixture. A number of experiments were carried out with simultaneous adsorption of water and butanol at 35 °C with partial pressures in the feed of 2.04 and 0.35 kPa for water and butanol (with a molar composition of 15% butanol), respectively. The partial pressures of water and butanol vapor in the feed gas were obtained by passing the carrier gas (helium) to saturators filled with a dilute butanol/water mixture containing 2 wt % butanol, i.e., a typical concentration in an ABE fermentation broth. In other words, these conditions simulate a gas-stripping ABE fermentation process.[21,52] Figure 7 shows IR spectra recorded of the butanol and water adsorbed simultaneously in the silicalite-1 film at 35 °C as well as reference spectra of water and butanol adsorbed from the single-component measurements for visualization of the difference between single-component and binary mixture adsorption. The reference spectra were recorded at the partial pressures close to those in the mixture, viz., 2.06 kPa for water and 0.05 kPa for butanol. Both the characteristic band of water at 1620 cm^{-1} and the band assigned to butanol at 1465 cm^{-1} are visible and clearly separated in the spectrum recorded for the binary mixture. The bands assigned to water are significantly smaller than the bands in the reference spectrum, whereas the difference is much smaller in the case of butanol. This observation clearly shows that the silicalite-1 film is selective toward butanol. The adsorption selectivity, as determined by extracting the adsorbed concentrations from the spectrum using eqs 3 and 4, was $\alpha_{BuOH/water}$ = 107, showing that the film is highly butanol-selective at these conditions. By increasing the partial pressure of butanol in the feed, butanol/water selectivity was measured also at feed compositions, 2.03 kPa water and 0.57 kPa butanol and 1.80 kPa water and 0.70 kPa butanol, which resulted in selectivities of 84 and 62, respectively. The lower selectivities at higher feed pressures may be expected, because silicalite-1 was already saturated by butanol at low partial pressures. Unfortunately, only a few reports exist in the literature on the adsorption selectivity for adsorption of a butanol/water vapor mixture in zeolites. However, Zhang et al.[59] reported butanol adsorption selectivity in the range of 12−60 and 15−80 (at different mole fractions of butanol in the liquid phase) for ZIF-8 and ZIF-71 zeolitic imidazolates, respectively. The high butanol selectivity obtained in the present work indicates that recovery of butanol from the vapor phase from a gas-stripping ABE fermentation process may be an interesting option.

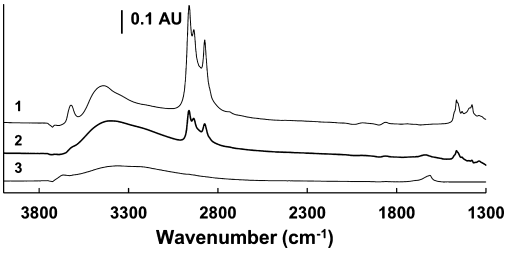

Figure 7. IR spectrum of butanol and water adsorbed in silicalite-1 film at 35 °C for a binary mixture of butanol and water with a mole fraction of 0.15 for butanol in the vapor phase (2), together with the spectra of pure butanol (1) and water (3) at partial pressures of 0.05 and 2.06 kPa, respectively.

■ CONCLUSION

The adsorption of butanol and water in silicalite-1 was studied and quantitatively determined at four different temperatures using ATR−FTIR spectroscopy. The adsorption was typical for microporous materials, and the Langmuir model was found to fit well to the experimental data. The Langmuir parameters, heats of adsorption, and maximum loadings determined were in a good agreement with previously reported data. The saturation concentration of butanol in silicalite-1 powder was measured using a volumetric gas adsorption technique, and the amount of butanol and water adsorbed in the silicalite-1 film were determined from IR spectra. Moreover, it was shown that the silicalite-1 film was butanol-selective with an adsorption selectivity of 107 at 35 °C when adsorbed from a binary vapor mixture with the molar composition of 15% butanol and 85% water. The results indicate that a silicalite-1 adsorbent or membrane may effectively separate butanol from the vapor obtained in an ABE fermentation gas-stripping process.

■ AUTHOR INFORMATION

Corresponding Author

*E-mail: mattias.grahn@ltu.se.

DOI: 10.1021/acs.langmuir.5b00489
Langmuir 2015, 31, 4887−4894

Notes

The authors declare no competing financial interest.

■ ACKNOWLEDGMENTS

The authors acknowledge the Swedish Research Council (VR, under Grant 621-2011-4060) for financially supporting this work.

■ REFERENCES

(1) Yuan, J. S.; Tiller, K. H.; Al-Ahmad, H.; Stewart, N. R.; Stewart, C. N., Jr. Plants to power: Bioenergy to fuel the future. *Trends Plant Sci.* **2008**, *13*, 421−429.

(2) Saravanan, V.; Waijers, D.; Ziari, M.; Noordermeer, M. Recovery of 1-butanol from aqueous solutions using zeolite ZSM-5 with a high Si/Al ratio; suitability of a column process for industrial applications. *Biochem. Eng. J.* **2010**, *49*, 33−39.

(3) Demirbas, A. *Biodiesel*; Springer: New York, 2008.

(4) Crabbe, E.; Nolasco-Hipolito, C.; Kobayashi, G.; Sonomoto, K.; Ishizaki, A. Biodiesel production from crude palm oil and evaluation of butanol extraction and fuel properties. *Process Biochem.* **2001**, *37*, 65−71.

(5) Qureshi, N.; Hughes, S.; Maddox, I.; Cotta, M. Energy-efficient recovery of butanol from model solutions and fermentation broth by adsorption. *Bioprocess Biosyst. Eng.* **2005**, *27*, 215−222.

(6) García, V.; Päkkilä, J.; Ojamo, H.; Muurinen, E.; Keiski, R. L. Challenges in biobutanol production: How to improve the efficiency? *Renewable Sustainable Energy Rev.* **2011**, *15*, 964−980.

(7) Ezeji, T.; Qureshi, N.; Blaschek, H. Acetone butanol ethanol (ABE) production from concentrated substrate: Reduction in substrate inhibition by fed-batch technique and product inhibition by gas stripping. *Appl. Microbiol. Biotechnol.* **2004**, *63*, 653−658.

(8) Liu, F.; Liu, L.; Feng, X. Separation of acetone−butanol−ethanol (ABE) from dilute aqueous solutions by pervaporation. *Sep. Purif. Technol.* **2005**, *42*, 273−282.

(9) Oudshoorn, A.; van der Wielen, L. A. M.; Straathof, A. J. Adsorption equilibria of bio-based butanol solutions using zeolite. *Biochem. Eng. J.* **2009**, *48*, 99−103.

(10) Nielsen, L.; Larsson, M.; Holst, O.; Mattiasson, B. Adsorbents for extractive bioconversion applied to the acetone−butanol fermentation. *Appl. Microbiol. Biotechnol.* **1988**, *28*, 335−339.

(11) Giusti, D.; Conway, R.; Lawson, C. Activated carbon adsorption of petrochemicals. *J.—Water Pollut. Control Fed.* **1974**, 947−965.

(12) Nielsen, D. R.; Prather, K. J. *In situ* product recovery of *n*-butanol using polymeric resins. *Biotechnol. Bioeng.* **2009**, *102*, 811−821.

(13) Lin, X.; Wu, J.; Fan, J.; Qian, W.; Zhou, X.; Qian, C.; Jin, X.; Wang, L.; Bai, J.; Ying, H. Adsorption of butanol from aqueous solution onto a new type of macroporous adsorption resin: Studies of adsorption isotherms and kinetics simulation. *J. Chem. Technol. Biotechnol.* **2012**, *87*, 924−931.

(14) Szostak, R.; Nair, V.; Thomas, T. L. Incorporation and stability of iron in molecular-sieve structures. Ferrisilicate analogues of zeolite ZSM-5. *J. Chem. Soc., Faraday Trans. 1* **1987**, *83*, 487−494.

(15) Wang, Z.; Larsson, M. L.; Grahn, M.; Holmgren, A.; Hedlund, J. Zeolite coated ATR crystals for new applications in FTIR−ATR spectroscopy. *Chem. Commun. (Cambridge, U. K.)* **2004**, 2888−2889.

(16) Stelzer, J.; Paulus, M.; Hunger, M.; Weitkamp, J. Hydrophobic properties of all-silica zeolite beta. *Microporous Mesoporous Mater.* **1998**, *22*, 1−8.

(17) Huang, J.; Meagher, M. Pervaporative recovery of *n*-butanol from aqueous solutions and ABE fermentation broth using thin-film silicalite-filled silicone composite membranes. *J. Membr. Sci.* **2001**, *192*, 231−242.

(18) Qureshi, N.; Meagher, M.; Huang, J.; Hutkins, R. Acetone butanol ethanol (ABE) recovery by pervaporation using silicalite−silicone composite membrane from fed-batch reactor of *Clostridium acetobutylicum*. *J. Membr. Sci.* **2001**, *187*, 93−102.

(19) Zhou, H.; Su, Y.; Chen, X.; Wan, Y. Separation of acetone, butanol and ethanol (ABE) from dilute aqueous solutions by silicalite-1/PDMS hybrid pervaporation membranes. *Sep. Purif. Technol.* **2011**, *79*, 375−384.

(20) Masuda, T.; Otani, S.; Tsuji, T.; Kitamura, M.; Mukai, S. R. Preparation of hydrophilic and acid-proof silicalite-1 zeolite membrane and its application to selective separation of water from water solutions of concentrated acetic acid by pervaporation. *Sep. Purif. Technol.* **2003**, *32*, 181−189.

(21) Qureshi, N.; Meagher, M.; Hutkins, R. Recovery of butanol from model solutions and fermentation broth using a silicalite/silicone membrane. *J. Membr. Sci.* **1999**, *158*, 115−125.

(22) Stoeger, J. A.; Choi, J.; Tsapatsis, M. Rapid thermal processing and separation performance of columnar MFI membranes on porous stainless steel tubes. *Energy Environ. Sci.* **2011**, *4*, 3479−3486.

(23) Faisal, A.; Zarebska, A.; Saremi, P.; Korelskiy, D.; Ohlin, L.; Rova, U.; Hedlund, J.; Grahn, M. MFI zeolite as adsorbent for selective recovery of hydrocarbons from ABE fermentation broths. *Adsorption* **2014**, *20*, 465−470.

(24) Zhou, H.; Korelskiy, D.; Sjöberg, E.; Hedlund, J. Ultrathin hydrophobic MFI membranes. *Microporous Mesoporous Mater.* **2013**, *192*, 76−81.

(25) Korelskiy, D.; Leppäjärvi, T.; Zhou, H.; Grahn, M.; Tanskanen, J.; Hedlund, J. High flux MFI membranes for pervaporation. *J. Membr. Sci.* **2013**, *427*, 381−389.

(26) Grahn, M.; Holmgren, A.; Hedlund, J. Adsorption of *n*-hexane and *p*-xylene in thin silicalite-1 films studied by FTIR/ATR spectroscopy. *J. Phys. Chem. C* **2008**, *112*, 7717−7724.

(27) Ohlin, L.; Grahn, M. Detailed investigation of the binary adsorption of carbon dioxide and methane in zeolite Na-ZSM-5 studied using *in situ* ATR−FTIR spectroscopy. *J. Phys. Chem. C* **2014**, *118*, 6207−6213.

(28) Ohlin, L.; Bazin, P.; Thibault-Starzyk, F.; Hedlund, J.; Grahn, M. Adsorption of CO2, CH4, and H2O in Zeolite ZSM-5 Studied Using In Situ ATR-FTIR Spectroscopy. *J. Phys. Chem. C* **2013**, *117*, 16972−16982.

(29) Grahn, M.; Lobanova, A.; Holmgren, A.; Hedlund, J. Orientational analysis of adsorbates in molecular sieves by FTIR/ATR spectroscopy. *Chem. Mater.* **2008**, *20*, 6270−6276.

(30) Zhou, M.; Korelskiy, D.; Ye, P.; Grahn, M.; Hedlund, J. A uniformly oriented MFI membrane for improved CO_2 separation. *Angew. Chem., Int. Ed.* **2014**, *53*, 3492−3495.

(31) Zhou, M.; Grahn, M.; Zhou, H.; Holmgren, A.; Hedlund, J. The facile assembly of nanocrystals by optimizing humidity. *Chem. Commun.* **2014**, *50*, 14261−14264.

(32) Li, X.; Peng, Y.; Wang, Z.; Yan, Y. Synthesis of highly b-oriented zeolite MFI films by suppressing twin crystal growth during the secondary growth. *CrystEngComm* **2011**, *13*, 3657−3660.

(33) Grahn, M.; Wang, Z.; Lidström-Larsson, M.; Holmgren, A.; Hedlund, J.; Sterte, J. Silicalite-1 coated ATR elements as sensitive chemical sensor probes. *Microporous Mesoporous Mater.* **2005**, *81*, 357−363.

(34) Mirabella, F. M. *Internal Reflection Spectroscopy: Theory and Applications*; CRC Press: Boca Raton, FL, 1992; Vol. *15*.

(35) Tompkins, H. G. The physical basis for analysis of the depth of absorbing species using internal reflection spectroscopy. *Appl. Spectrosc.* **1974**, *28*, 335−341.

(36) Nair, S.; Tsapatsis, M. Infrared reflectance measurements of zeolite film thickness, refractive index and other characteristics. *Microporous Mesoporous Mater.* **2003**, *58*, 81−89.

(37) Bowen, T. C.; Noble, R. D.; Falconer, J. L. Fundamentals and applications of pervaporation through zeolite membranes. *J. Membr. Sci.* **2004**, *245*, 1−33.

(38) Hammond, K. D.; Hong, M.; Tompsett, G. A.; Auerbach, S. M.; Falconer, J. L.; Conner, W. C. High-resolution physical adsorption on supported borosilicate MFI zeolite membranes: Comparison with powdered samples. *J. Membr. Sci.* **2008**, *325*, 413−419.

DOI: 10.1021/acs.langmuir.5b00489
Langmuir 2015, 31, 4887−4894

(39) Jeong, H.; Lai, Z.; Tsapatsis, M.; Hanson, J. C. Strain of MFI crystals in membranes: An *in situ* synchrotron X-ray study. *Microporous Mesoporous Mater.* **2005**, *84*, 332−337.
(40) Lassinantti, M.; Jareman, F.; Hedlund, J.; Creaser, D.; Sterte, J. Preparation and evaluation of thin ZSM-5 membranes synthesized in the absence of organic template molecules. *Catal. Today* **2001**, *67*, 109−119.
(41) Zhou, M.; Liu, X.; Zhang, B.; Zhu, H. Assembly of oriented zeolite monolayers and thin films on polymeric surfaces via hydrogen bonding. *Langmuir* **2008**, *24*, 11942−11946.
(42) Krishna, R.; van Baten, J. M. Highlighting pitfalls in the Maxwell−Stefan modeling of water−alcohol mixture permeation across pervaporation membranes. *J. Membr. Sci.* **2010**, *360*, 476−482.
(43) Jentys, A.; Warecka, G.; Derewinski, M.; Lercher, J. A. Adsorption of water on ZSM 5 zeolites. *J. Phys. Chem.* **1989**, *93*, 4837−4843.
(44) Jentys, A.; Tanaka, H.; Lercher, J. Surface processes during sorption of aromatic molecules on medium pore zeolites. *J. Phys. Chem. B* **2005**, *109*, 2254−2261.
(45) Rege, S. U.; Yang, R. T. A novel FTIR method for studying mixed gas adsorption at low concentrations: H_2O and CO_2 on NaX zeolite and γ-alumina. *Chem. Eng. Sci.* **2001**, *56*, 3781−3796.
(46) Bazin, P.; Alenda, A.; Thibault-Starzyk, F. Interaction of water and ammonium in NaHY zeolite as detected by combined IR and gravimetric analysis (AGIR). *Dalton Trans.* **2010**, *39*, 8432−8436.
(47) Olson, D.; Haag, W.; Borghard, W. Use of water as a probe of zeolitic properties: Interaction of water with HZSM-5. *Microporous Mesoporous Mater.* **2000**, *35*, 435−446.
(48) Bolis, V.; Busco, C.; Ugliengo, P. Thermodynamic study of water adsorption in high-silica zeolites. *J. Phys. Chem. B* **2006**, *110*, 14849−14859.
(49) Zhang, K.; Lively, R. P.; Noel, J. D.; Dose, M. E.; McCool, B. A.; Chance, R. R.; Koros, W. J. Adsorption of water and ethanol in MFI-type zeolites. *Langmuir* **2012**, *28*, 8664−8673.
(50) Yee, G. G.; Fulton, J. L.; Smith, R. D. Fourier transform infrared spectroscopy of molecular interactions of heptafluoro-1-butanol or 1-butanol in supercritical carbon dioxide and supercritical ethane. *J. Phys. Chem.* **1992**, *96*, 6172−6181.
(51) Lin-Vien, D.; Colthup, N. B.; Fateley, W. G.; Grasselli, J. G. *The Handbook of Infrared and Raman Characteristic Frequencies of Organic Molecules*; Elsevier: Amsterdam, Netherlands, 1991.
(52) Oudshoorn, A.; van der Wielen, L. A. M.; Straathof, A. J. Assessment of options for selective 1-butanol recovery from aqueous solution. *Ind. Eng. Chem. Res.* **2009**, *48*, 7325−7336.
(53) Zhang, K.; Zhang, L.; Jiang, J. Adsorption of C_1−C_4 alcohols in zeolitic imidazolate framework-8: Effects of force fields, atomic charges, and framework flexibility. *J. Phys. Chem. C* **2013**, *117*, 25628−25635.
(54) Einicke, W.; Messow, U.; Schöllner, R. Liquid-phase adsorption of *n*-alcohol/water mixtuers on zeolite NaZSM-5. *J. Colloid Interface Sci.* **1988**, *122*, 280−282.
(55) Zhu, W.; Van de Graaf, J.; Van den Broeke, L.; Kapteijn, F.; Moulijn, J. TEOM: A unique technique for measuring adsorption properties. Light alkanes in silicalite-1. *Ind. Eng. Chem. Res.* **1998**, *37*, 1934−1942.
(56) Sun, M. S.; Shah, D.; Xu, H. H.; Talu, O. Adsorption equilibria of C_1 to C_4 alkanes, CO_2, and SF_6 on silicalite. *J. Phys. Chem. B* **1998**, *102*, 1466−1473.
(57) Zhu, W.; Kapteijn, F.; Moulijn, J. Adsorption of light alkanes on silicalite-1: Reconciliation of experimental data and molecular simulations. *Phys. Chem. Chem. Phys.* **2000**, *2*, 1989−1995.
(58) Vlugt, T.; Krishna, R.; Smit, B. Molecular simulations of adsorption isotherms for linear and branched alkanes and their mixtures in silicalite. *J. Phys. Chem. B* **1999**, *103*, 1102−1118.
(59) Zhang, K.; Lively, R. P.; Dose, M. E.; Brown, A. J.; Zhang, C.; Chung, J.; Nair, S.; Koros, W. J.; Chance, R. R. Alcohol and water adsorption in zeolitic imidazolate frameworks. *Chem. Commun.* **2013**, *49*, 3245−3247.

DOI: 10.1021/acs.langmuir.5b00489
Langmuir 2015, 31, 4887−4894